Order Number 9315502

High-resolution robot tracking and direction finding for space station environment

Shahrabi, Kamal, Ph.D.

City University of New York, 1993

U·M·I
300 N. Zeeb Rd.
Ann Arbor, MI 48106

HIGH RESOLUTION ROBOT TRACKING AND DIRECTION FINDING FOR SPACE STATION ENVIRONMENT

by

KAMAL SHAHRABI

A Dissertation submitted to the Graduate Faculty in Engineering in partial fulfillment of the requirements for the degree of Doctor of Philosophy, The City University of New York.

1993

This manuscript has been read and accepted for the Graduate Faculty in Engineering in satisfaction of the dissertation requirement for the degree of Doctor of Philosophy.

1/16/93
Date

Chair of Examining Committee

1/20/93
Date

Executive Officer

Dr. Joseph Barba

Dr. Radomir Bozovic

Dr. Svetislav Maric

Dr. Tarek Saadawi
Supervisory Committee

The City University of New York

ABSTRACT

HIGH RESOLUTION ROBOTS TRACKING AND LOCATION FINDING FOR SPACE STATION ENVIRONMENT

by

Kamal Shahrabi

Advisor: Dr. Donald L. Schilling

In the past few years the problem of location finding and tracking of an extra-vehicular robots in Space Station environment, and the related problem of estimating the parameters of signals in noise have attracted considerable interest. Conventional direction finding, tracking and locating techniques such as *Maximum Likelihood (ML), MUltiple Signal Characterization (MUSIC),* ..... etc. are proving inadequate to support the full and effective utilization of robotics in a Space Station environment.

The scope of this work is to provide a new and more efficient signal processing technique for a Space Station robotic tracking system which overcomes existing technical

limitations such as radio transmission multipath, station reflections, the number of robots, Space Station environment, stringent resolution requirements and Space Station architecture. In general, this work contains block level design and study of a communication system for a Space Station involving *spread spectrum* and digital processing of signal techniques that achieves a Space Station robotic tracking implementation. This report contains an extensive analysis of the system performance from the following points of view:

1. Utilization of a chirp signal, which in conjunction with a polling procedure, allows for individual robot identification, location and tracking.
2. Estimate the number of antennae
3. Determine the location of the antennae on the Space Station
4. Generate a detailed block diagram design
5. Perform an overall system analysis that considers the effects of signal multipath

ACKNOWLEDGMENTS

A number of people have contributed in many ways to the completion of this research and it is a pleasure to acknowledge them. I am particularly indebted to Professor Donald L. Schilling for his inspired teaching, generous counsel, constant encouragement and marvelous capacity for broad subtle concepts which greatly contributed to the preparation of this work.

I am grateful for the generous assistance provided by Emanuel Kanterakis at SCS Telecom, Inc. I also wish to express my appreciation to Reza Aghazadehalavi for his critical comments and constructive suggestions. Thanks are also due to Shiju Abraham who edited the successive drafts of the manuscript.

And not least, grateful thanks are due to my wife, Zahra, and my children, Neda, and Sarah, especially Zahra, who have encouraged me not only in completing of this work, but throughout my career. Also, I am thankful to my father, Jalal, for his advocation, influence and the endless support. They all made many sacrifices which are much appreciated.

Finaly, I am also most grateful to my other professional associates who made this study possible.

TABLE OF CONTENTS

LISTS OF TABLES

Chapter One

Chapter Three

LISTS OF FIGURES

Figures:

Chapter One

Chapter Two

Chapter Three

Chapter Four

Chapter Five

Appendix A

CHAPTER ONE

OVERVIEW & CONTRIBUTIONS

1.0 INTRODUCTION

In order to effectively communicate with an extra-vehicular robot, the robot location should be known at all times. Currently, designers of communication systems are working on the development of systems and devices which can continuously monitor the location and status of an extra-vehicular robots in a Space Station environment. The problem of particular interest here is to implement a high resolution Space Station robotic tracking systems.

Location finding is the process of estimating the time difference of arrival (TDOA), frequency difference of arrival (FDOA), angle of arrival, signal strength, carrier frequency and distance of propagating signals from an object to a receiver, that is, to perform high-resolution direction finding. The term direction finding refers to the

process of estimating the directions of arrival (DOA) of propagating signals as they impinge upon a man-made receivers.See Figure 1.1.

A location finding system is a collection of electronic or electromechanical devices which are used to acquire information about the direction of signal's arrival and their distance in order to determine the location of the transmitting source. It should be noted that a location finding (LF) system must interface with some other electronic systems such as computer, radio communication systems and some type of display. A variety of potential applications for location finding systems exist. Some of these applications are listed in Table 1.1.

Table 1.1: Some applications of Location Finding.

RADAR SYSTEMS (AIR TRAFFIC CONTROL)
POLICE
MOBILE COMMUNICATION SYSTEMS
PUBLIC TRANSPORTATION
RADIO ASTRONOMY
SIGNAL EXTRACTION
GEOPHYSICS (SEISMOLOGY)

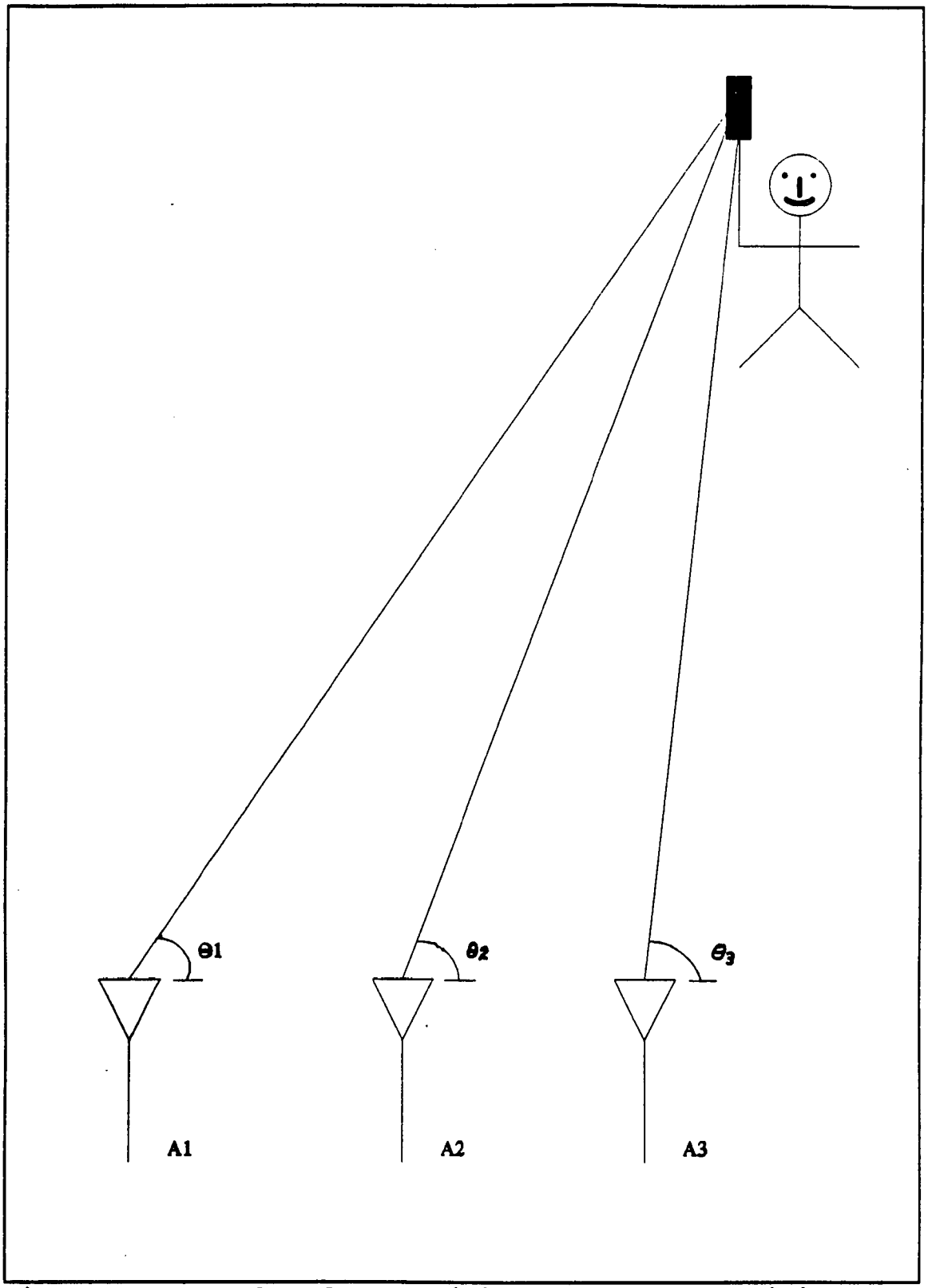

Figure 1.1 Example of a receiving plane wave arriving from angle θ

The locating and tracking of an extra-vehicular robot in Space Station environment is complicated by radio transmission multipath and reflections, the number of robots, Space Station architecture, resolution requirements, and antennae shielding due to the geometry. The scope of this work is to analyze and implement a new, more efficient signal processing technique for a Space Station robotic tracking system which overcomes existing technical limitations. The system must be capable of locating and tracking a single robot at a time anywhere around the Space Station in a few fraction of seconds.

1.1 AN OVERVIEW OF A LOCATION FINDING SYSTEM

The basic approach used in locating an extra-vehicular robot is direct measurements on radio signals traveling between the robot and a number (at least three) of fixed receiving antennae. In this method the distance between the robot and at least three receiving antennae is measured by determining the signal travel time (τ) from the antennae to the robot and back to the antennae. From this information one may solve for the distance (D) between the robot and antennae. Given the three distances D_1, D_2, and D_3, the robot is then located at the intersection of three circles of radius D_1, D_2, and D_3 centered on antennae 1, 2, and 3 respectively, as shown in Figure 1.2. This technique requires that the robot be equipped with a transmitter and receiver which would retransmit a signal at some fixed time increment after reception of a signal from the main control station.

The transmitted signal is usually an electromagnetic signal. The signal can be

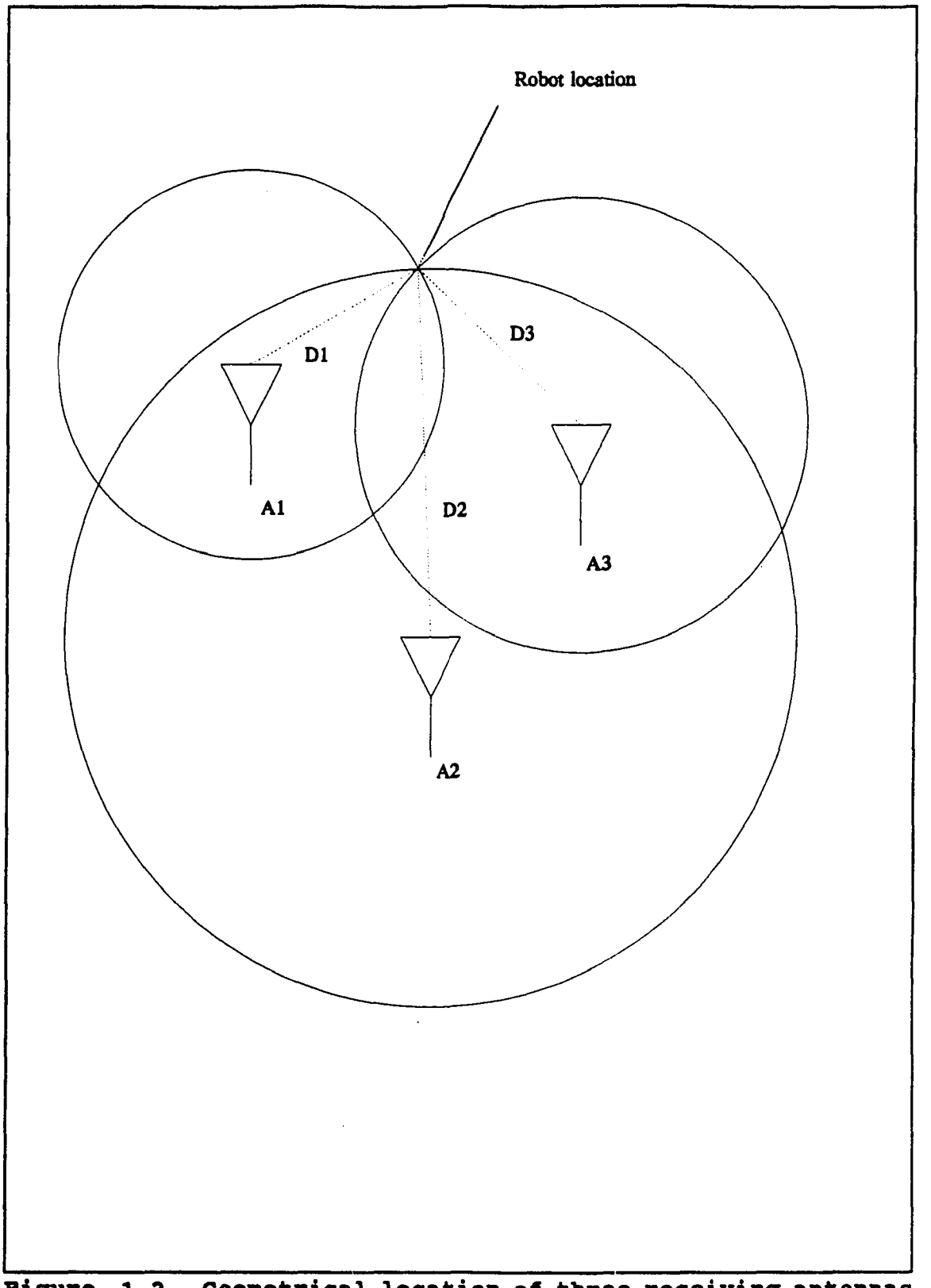

Figure 1.2 Geometrical location of three receiving antennas and a robot.

described by a carrier sine wave at frequency f_c with modulation of one or more of its parameters. Such a signal S(t) can be denoted by

$$S(t) = A \cos(\omega_c t + \varphi) \tag{1.1}$$

The relationship between the distance D and signal travel time τ can be defined by

$$D = \frac{1}{2}\tau C \tag{1.2}$$

where C is the velocity of propagation. The propagation velocity is the speed of light (C=2.997925 x 10^{10} cm/s) if the signal propagates in vacuum. The factor 1/2 is the result of the round trip travel time. Figure 1.3 shows a simple block diagram of a robot location finding system.

1.2 SYSTEM DESCRIPTION

In order to perform high resolution three dimensional locating and tracking of extra-vehicular robots in the Space Station environment the system must be able to:

1. Identify the direct path signal from robot
2. Discriminate the multipath signal components
3. Measure propagation time delays in the order of a few nanoseconds

In addition, the system must be simple, low cost, lightweight, have low power requirements and flexible enough to perform different tasks.

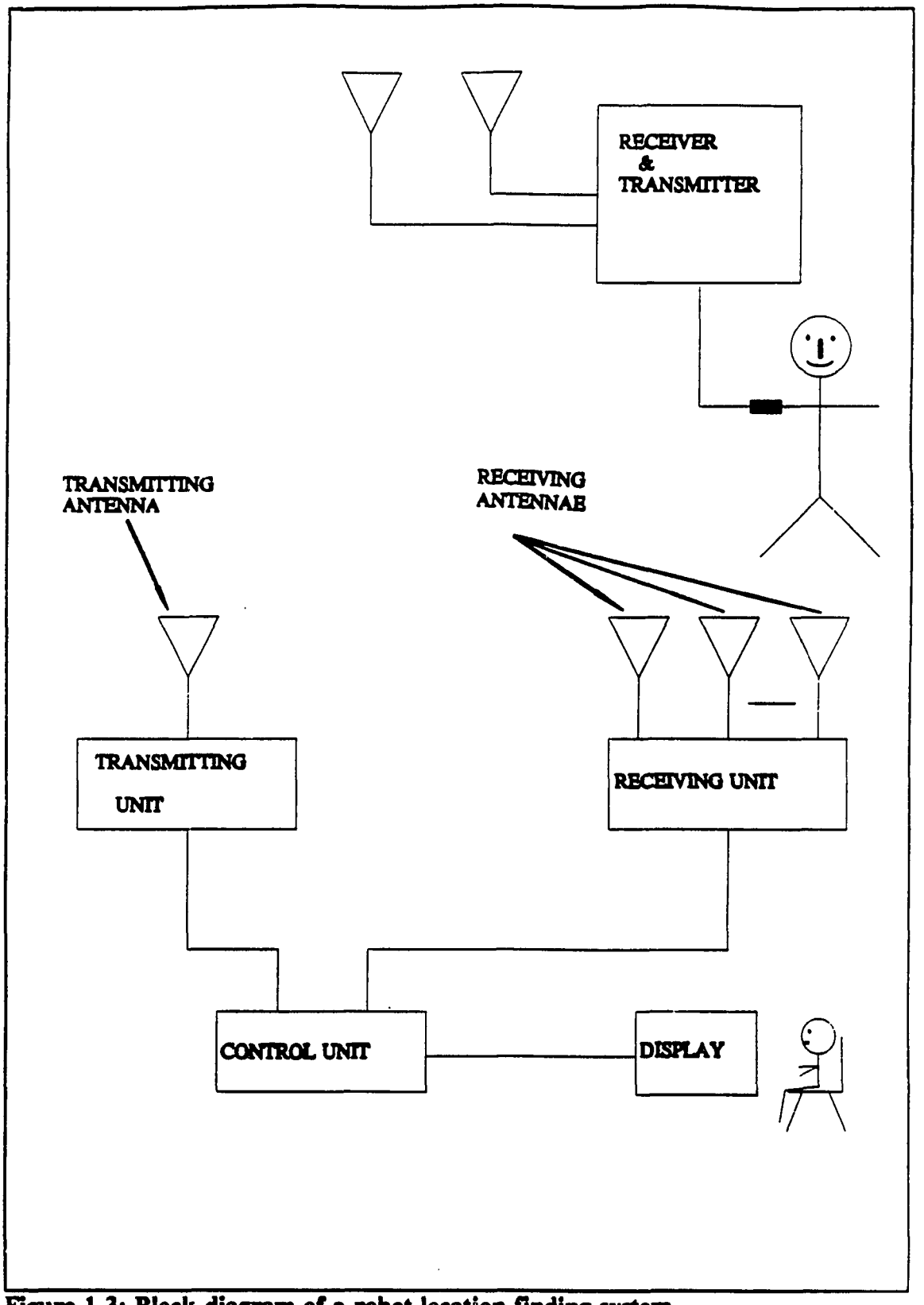

Figure 1.3: Block diagram of a robot location finding system.

1.2.1 SYSTEM REQUIREMENTS

In the simplest form of trilateration, the distance between the extra-vehicular robot and at least three receiving antennae is measured by determining the propagation delays of a signal emanating from the robot to the receiving antennae. This requires that the robot be equipped with one receiving and one transmitting antenna connected to a small repeater which would rebroadcast the signal at some fixed time increment following receipt of the incoming signal. The minimum system requirement for estimating the propagation delays of a signal is one transmitter with transmitting antennae and three receivers with receiving antennae. Due to the architecture of the Space Station the number of transmitting and receiving antennae will be larger than the number of receiving and the transmitting units. The transmitting antennae are connected to the transmitter via a multiplexer and the receiving units are connected to the receiving antennae which are located on the Space Station via a demultiplexer.

1.2.2 SYSTEM ALGORITHM

To find the location of an extra-vehicular robot the system must be capable to generate three independent variables that ultimately converge at a point in space. The basic algorithm for the system design is accomplished in the following manner:

1. Transmit a wake-up call tone (to select a particular robot)

2. A Chirp signal (S(t)) will be transmitted if the response to the tone signal is positive

$$S(t) = A \cos(\omega_c t + \frac{1}{2}\mu t^2) \tag{1.3}$$

3. Received Chirp signals ($r_i(t)$) from the three receiving antennae will be correlated with the one transmitted. The received signals at antennae 1, 2, and 3, respectively, are as follows

$$r_1(t) = B_1 \cos(\omega_c (t - \tau_1) + \frac{1}{2}\mu_1(t - \tau_1)^2 + \phi_1) \tag{1.4}$$

$$r_2(t) = B_2 \cos(\omega_c (t - \tau_2) + \frac{1}{2}\mu_2(t - \tau_2)^2 + \phi_2) \tag{1.5}$$

$$r_3(t) = B_3 \cos(\omega_c (t - \tau_3) + \frac{1}{2}\mu_3(t - \tau_3)^2 + \phi_3) \tag{1.6}$$

Where τ_1, τ_2, and τ_3 are the propagation delays of a signal from the robot to the receiving antennae placed at different locations on the Space Station.

4. The value of these correlations will be sent to the central processing unit for computing the location of the robot.

5. The system will display the robot coordinates and proceed to locate other robots or keep track of the same robot.

The transmitter unit consists of a Chirp signal generator, a tone generator, a multiplexer, a transmitting filter, and transmitting antennae. The tone generator is used to generate the address of any robot. The tone generator and the Chirp signal generator are connected to the transmitting filter through a switch. During the addressing period, the tone generator is connected, while the Chirp signal generator is connected during the location finding. The block diagram of the transmitting unit is shown in Figure 1.4.

As shown in Figure 1.5 the receiving unit consists of receiving antennae, receiving filter, demultiplexer, tone detector, and a power measurement circuit. The receiving antennae are connected to the receiving filter via a demultiplexer The output of each receiving filter is geared to a subsystem which consists of a tone detector and a power measurement circuit. The function of these subsystems are to supply the controller with information about the presence of an addressed robot and the background noise. If the robot is present then the signal is transferred to the dechirping circuit, otherwise the receiver signal is disregarded (for that particular antenna).

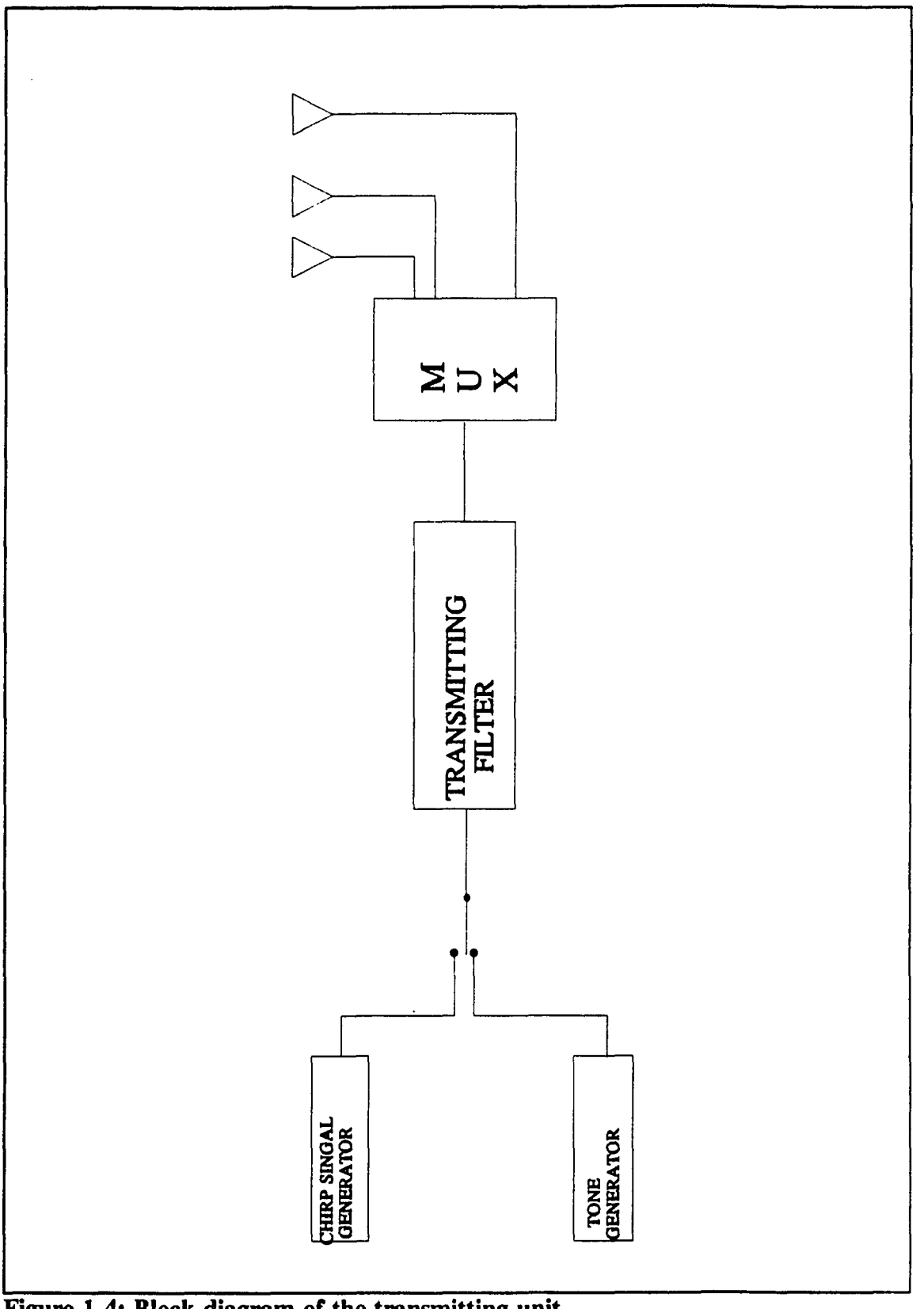

Figure 1.4: Block diagram of the transmitting unit.

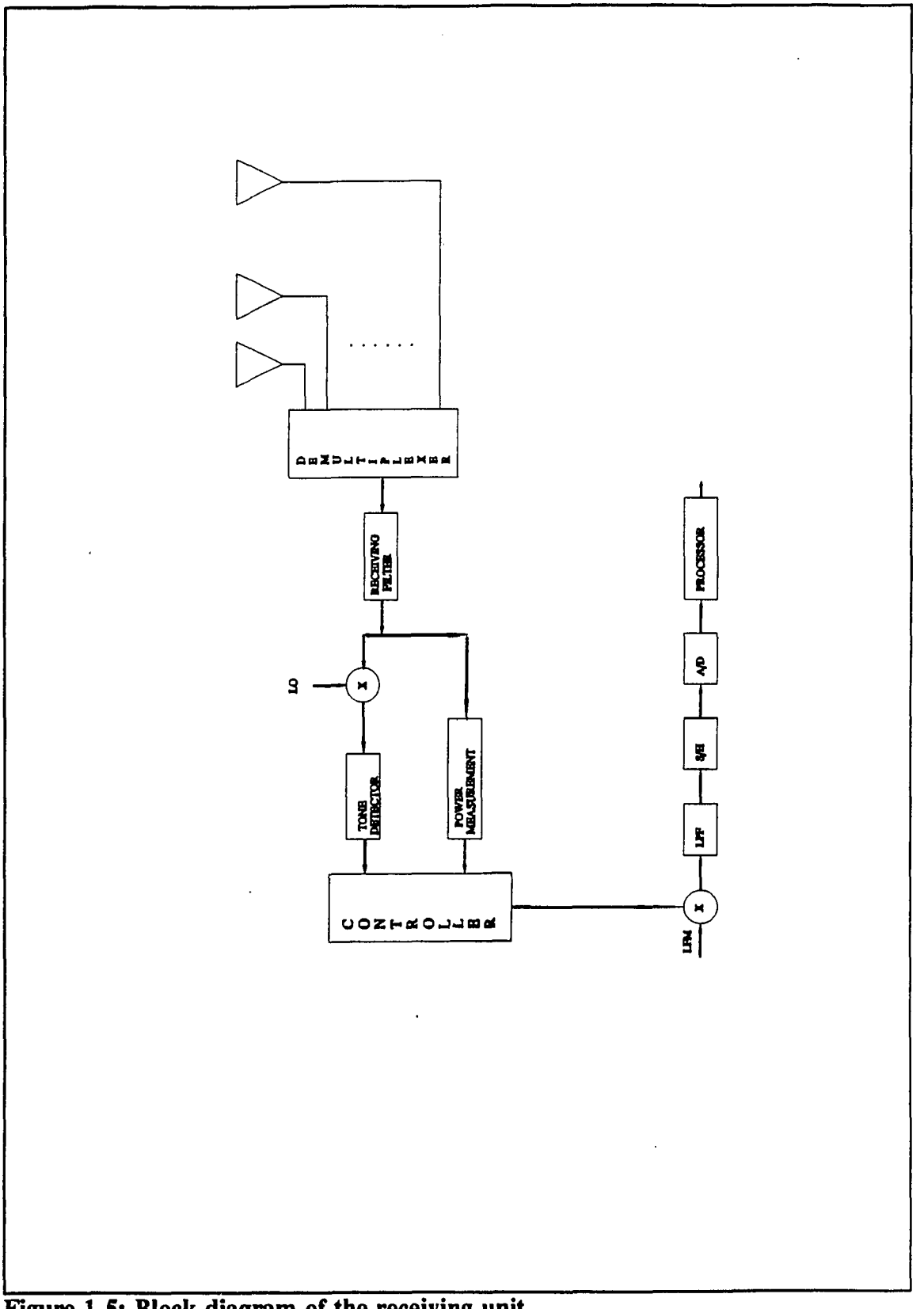

Figure 1.5: Block diagram of the receiving unit.

The dechirping circuit will perform the correlation between the received signals and the transmitted signal. The correlation operation is performed as follows:

1. All received signals are multiplied by the transmitted Chirp signal. Thus, S(t), r(t), and X(t) are the transmitted signal (Figure 1.6),received signal (Figure 1.7), and the product of the received and transmitted signal (Figure 1.8) respectively.

$$S(t) = A \cos\left(\omega_c t + \frac{1}{2}\mu t^2\right) \tag{1.7}$$

$$r(t) = B \cos\left(\omega_c(t + \tau) + \frac{1}{2}\mu(t + \tau)^2 + \phi\right) \tag{1.8}$$

$$X(t) = S(t) \times r(t) \tag{1.9}$$

2. Remove the quadratic dependence of X(t). (See Figure 1.9.)

3. Each output signal is sampled and digitized by an A/D converter.

4. Each output is separately Fourier transformed in order to determine the delays for the received waveforms. (See Figure 1.10)

5. The distances traveled by the received signals can be determined from Equation 1.2. Finally, the robot is located at the intersection of the three spheres of radius D_i centered on antenna i as shown in Figure 1.11.

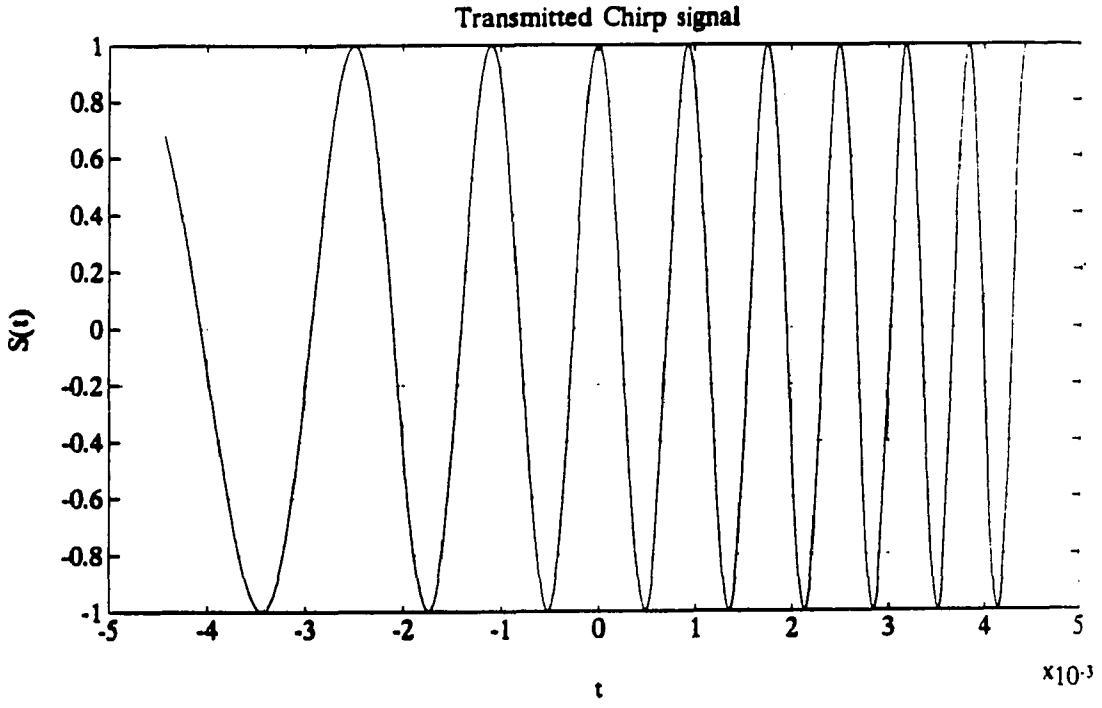

Figure 1.6: Transmitted chirp signal.

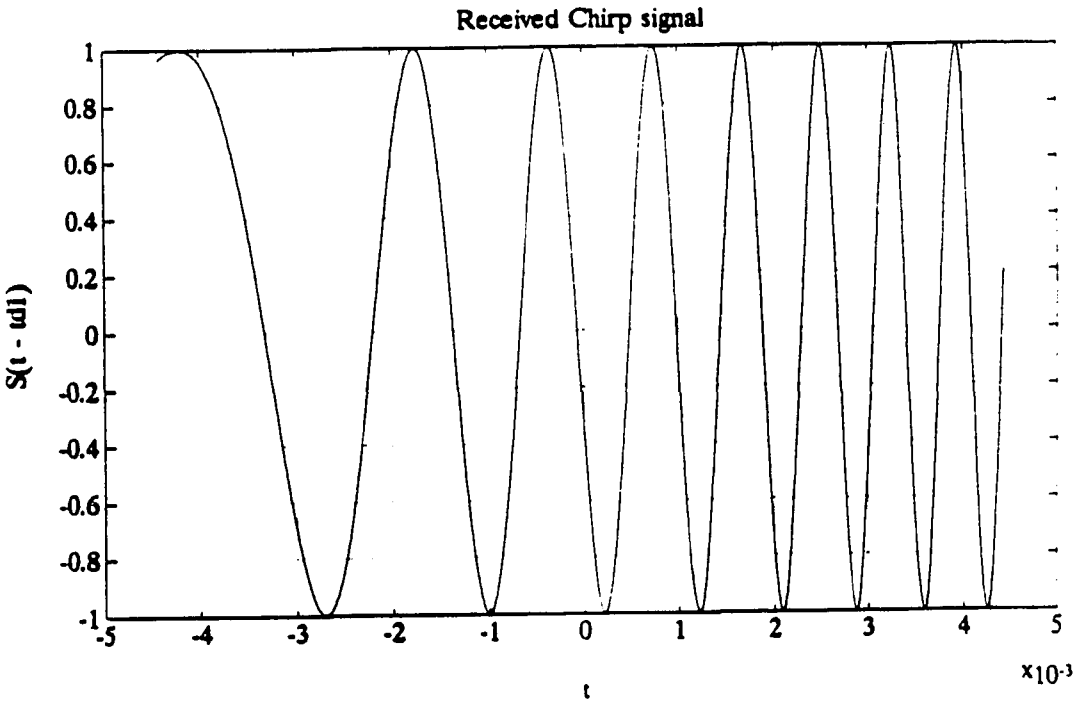

Figure 1.7: Received chirp signal.

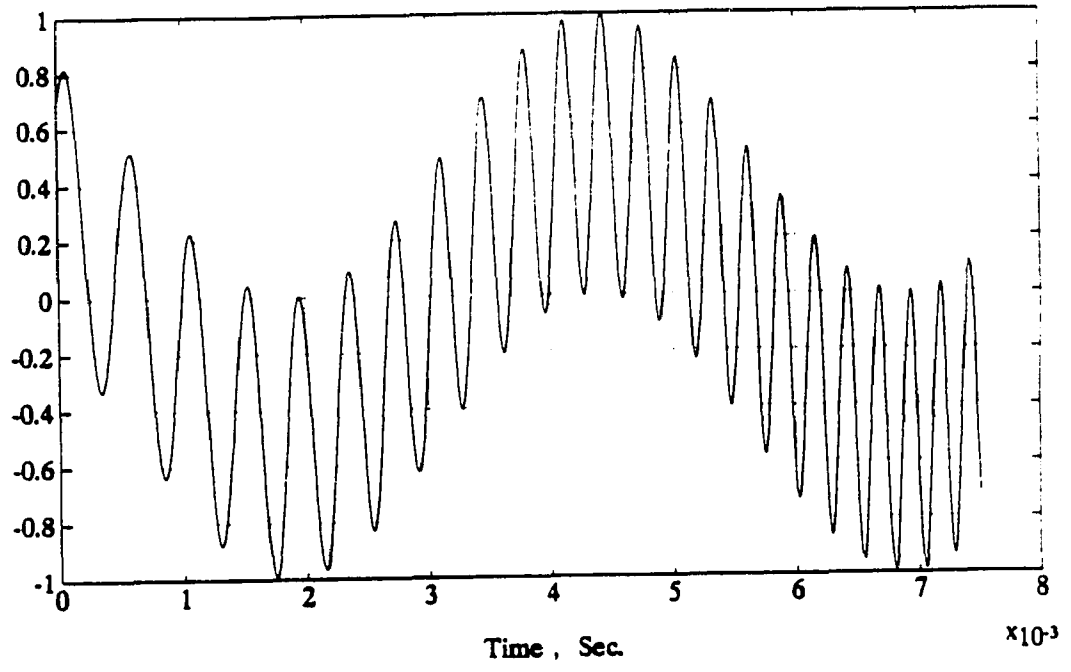

Figure 1.8: Product of the received and transmitted signal.

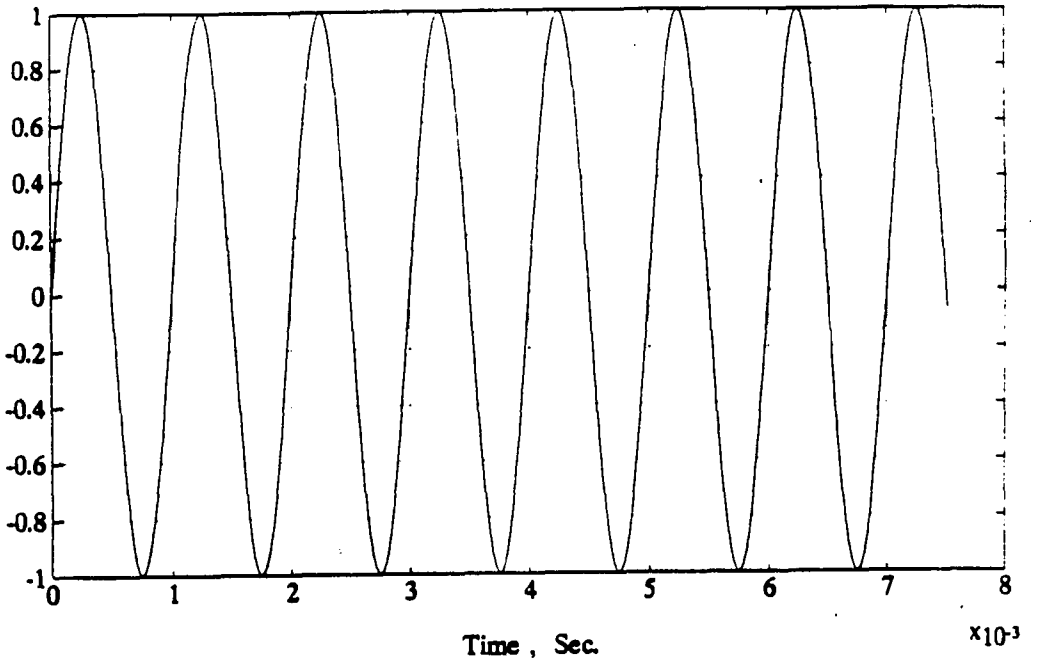

Figure 1.9: The dechirped waveform.

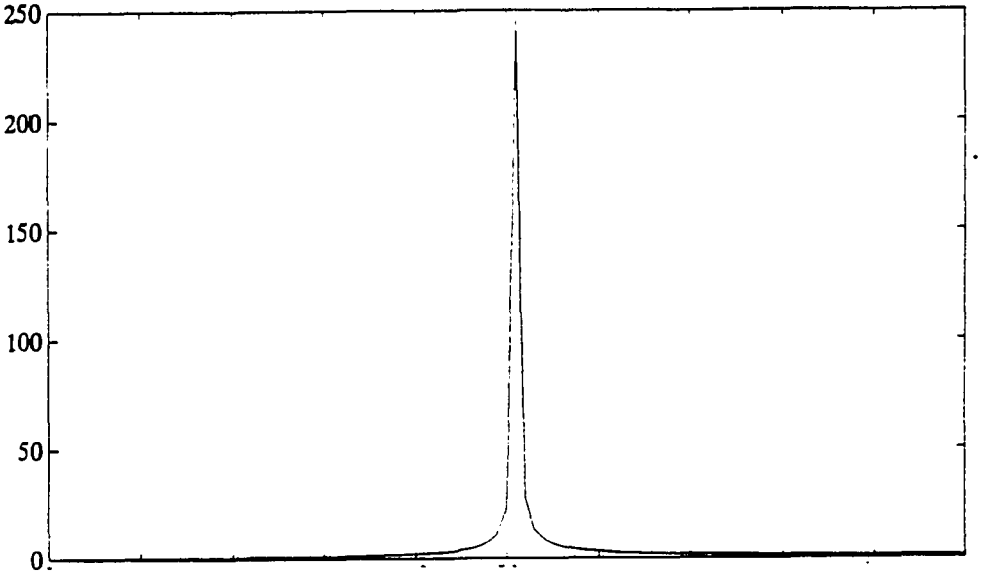

Figure 1.10: Fourier transform of the output signal.

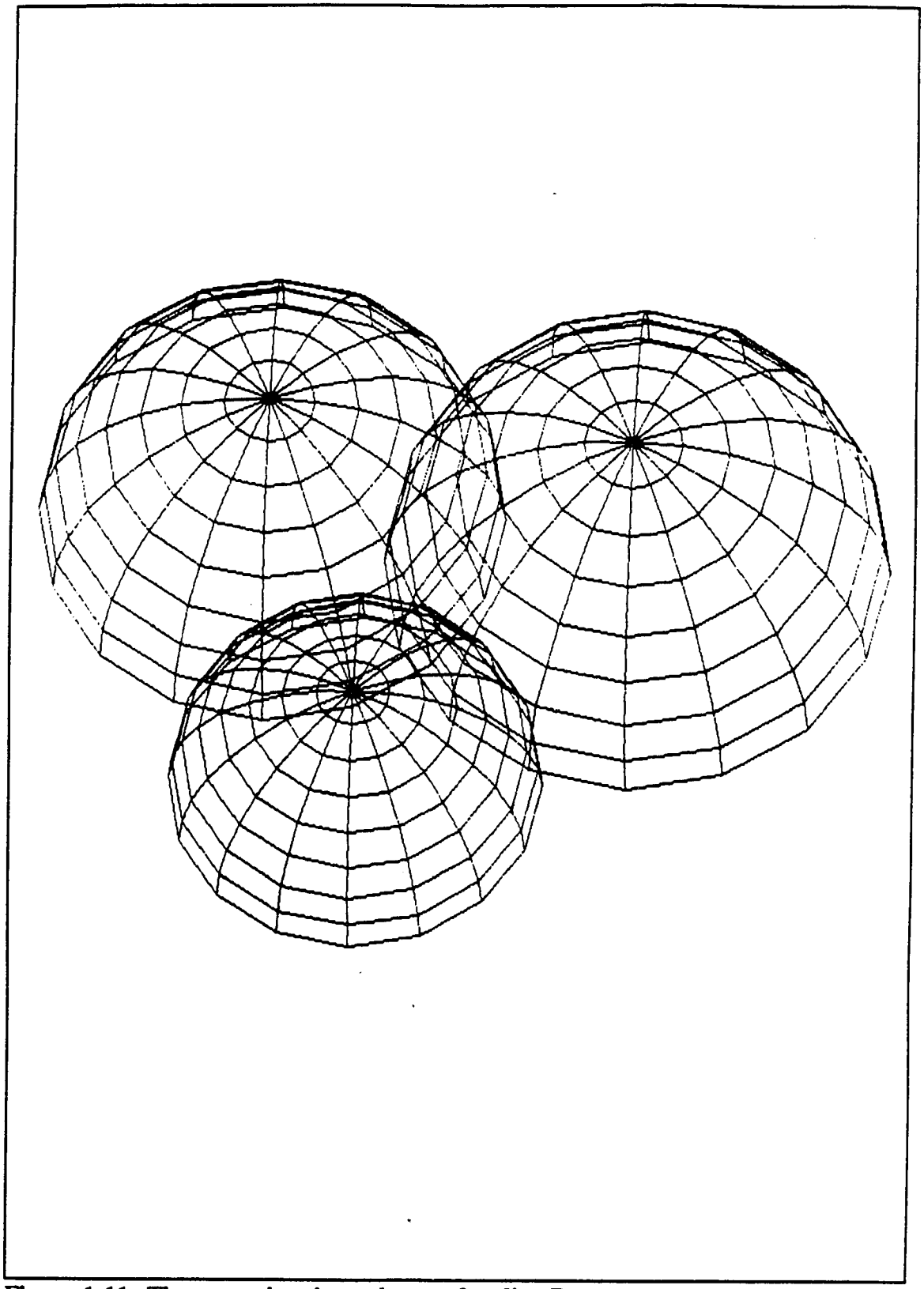

Figure 1.11: Three overlapping spheres of radius D_i.

Further description of each unit with the specific function and required parameters of the signals are given in Chapter 4 and 5.

1.3 OBJECTIVE

The objective to be accomplished is:

Perform the mathematical analysis, computer simulation and block level design of the location finding system, which is able to:

1. Discriminate the multipath signal components

2. Identify the direct path signal from robot

3. Measure propagation time delays in the order of a nanoseconds

4. Determine the minimum number of required transmitting and receiving antennae

CHAPTER TWO

BASIC ESTIMATION THEORY

2.0 INTRODUCTION

Assigning a value to an unknown parameter based on noise- corrupted observations involving some function of the parameter is called stochastic estimation. The value which is assigned to the unknown parameter is known as the estimate and the analyzes of the observations yielding the estimate is called the estimator. Regardless of the result of the estimation the function which assigns an estimate is called estimator. Hence, the estimation is optimal if the assignment of estimate is in accordance with minimization of some estimation criterion.

In this chapter some basic aspects of the parameter estimation will be considered. First the *Maximum Likelihood Estimation (MLE)* theory is developed which can be used to estimate non-random parameters. Then the procedure which commonly is used to estimate random parameters will be discussed (*Bayes Estimation*). In Bayes estimation, the minimization of the risk, which is a function of the error between the estimate and true value, is discussed.

In section 2.3 some criteria for a good estimator will be discussed. Finally this chapter will be concluded with a section about *Cramer-Rao Bound (CRB)* which is an alternate way to measure the error variance. Throughout this chapter, the noise is assumed to have known statistical properties.

2.1 PARAMETER ESTIMATION

Lets assume that the receiver has made a decision whether the information that is present at the receiver is the signal plus noise or just the noise. The goal is to estimate some unknown parameters associated with the signal based on a finite number of samples of the received signal.

Let $Y_1, Y_2, \ldots . Y_N$ be N samples and $y_1, y_2, \ldots . y_n$ be the corresponding sample values of $Y_1, Y_2, \ldots . Y_N.$, where $Y_1, Y_2, \ldots . Y_N$ are N independent, random signals, and identically distributed with some probability density function (PDF) depending on an

unknown parameter θ. If $g(Y_1, Y_2, \ldots . Y_N)$[1] is a function of the samples used to estimate the value of θ, we call $g(Y_1, Y_2, \ldots . Y_N)$ an estimator of θ and can be shown by

$$\hat{\theta} = g(Y_1, Y_2, \ldots . Y_N) \tag{2.1}$$

and $E[\hat{\theta}]$ denotes the mean of $\hat{\theta}$:

$$E[\hat{\theta}] = E[g(Y_1, Y_2, \ldots . Y_N)] \tag{2.2}$$

The procedures commonly used to estimate random and non-random parameters are known as *Bayes* estimation and *Maximum Likelihood* Estimation (MLE) respectively.

2.1.1 MAXIMUM LIKELIHOOD ESTIMATION (MLE)

Let Y be a random variable and $Y_1, Y_2, \ldots, Y_N$ be N independent and identically distributed samples of Y, with sample values $y_1, y_2, \ldots, y_n$. If the PDF of the random variable Y is $f_Y(y \mid \theta)$ then the *likelihood function*, $L(\theta)$, is

$$L(\theta) = f_{Y_1, \ldots . Y_N}(y_1, \ldots . y_n \mid \theta) \tag{2.3}$$

$$L(\theta) = \prod_{n=1}^{N} f_{Y_N}(y_n \mid \theta) . \tag{2.4}$$

Note that θ is the unknown parameter which we wish to estimate. To maximize the

---

[1]The $g(Y_1, Y_2, \ldots . Y_N)$ is called a statistic and is a random variable.

likelihood function $L(\theta)$, it is sufficient to maximize its log, since logarithmic functions are monotonic. Maximization of $\text{Log}[L(\theta)]$ is done by taking its partial derivative with respect to the parameter that is being maximized and then setting it equal to zero. This is known as the *likelihood equation*. Thus,

$$\frac{\partial}{\partial\theta} Ln\ f_Y(y \mid \theta) = 0 \tag{2.5}$$

Sometimes it is required to estimate more than one parameter. In such a case θ is a vector, Θ, given by

$$\Theta = \begin{bmatrix} \theta_1 \\ \theta_2 \\ \vdots \\ \theta_k \end{bmatrix} \tag{2.6}$$

Then, the likelihood function and the likelihood equation become

$$L(\Theta) = f_Y(y_1,\ y_2,\ \cdots y_N \mid \theta_1,\ \theta_2,\ \cdots \theta_k) \tag{2.7}$$

$$\frac{\partial}{\partial\,\Theta}\ Ln\ f_Y(y_1, y_2 \cdots y_N \mid \theta_1, \theta_2 \cdots \theta_k) = 0 \tag{2.8}$$

respectively.

2.2 BAYES ESTIMATION

An estimate is a function of the received observations which is chosen so as to minimize the expected value, risk function R, of the cost function $C(\tilde{\theta})$. The cost is a function of the estimation error $\tilde{\theta}$, i.e., a non-negative real valued function of the two random variables θ (true value) and $\hat{\theta}$ (estimated value). Thus,

$$\tilde{\theta} = \theta - \hat{\theta} \tag{2.9}$$

An estimator which minimizes the risk function, R,

$$R = E[C(\tilde{\theta})] \tag{2.10}$$

in order to obtain an optimum estimate of θ is known as a *Bayes Estimator.*

The estimate of θ is dependent upon the cost function assignment. The most often used cost assignments which are a function of the estimation error, $\tilde{\theta}$, are

1. $$C(\tilde{\theta}) = \tilde{\theta}^2 \tag{2.11}$$

2. $$C(\tilde{\theta}) = |\tilde{\theta}| \tag{2.12}$$

3. $$C(\tilde{\theta}) = \begin{cases} 0 & , \quad \tilde{\theta} < \frac{\varepsilon}{2} \\ \frac{1}{\varepsilon} & , \quad \tilde{\theta} \geq \frac{\varepsilon}{2} \end{cases} \tag{2.13}$$

The above functions are known as *squared error, absolute value of error, and uniform* cost functions respectively. Figure 2.1 illustrates these cost functions.

Lets $C(\tilde{\theta})$ be the cost function and θ be the unknown parameter, i.e., continuous random variable with power density function $f_\theta(\theta)$. Then the Bayes risk, R, of EQ. (2.9) becomes

$$R = E[C(\tilde{\theta})] = E[C(\theta - \hat{\theta})] \tag{2.14}$$

$$R = \int_{-\infty}^{\infty}\int_{-\infty}^{\infty} C(\theta - \hat{\theta})\, f_{\theta,Y}(\theta, y)\; dy\; d\theta \tag{2.15}$$

where $f_{\theta,Y}(\theta,y)$ is the joint density function of θ and Y. Thus,

$$Y = \begin{bmatrix} Y_1 \\ Y_2 \\ \vdots \\ Y_k \end{bmatrix} \tag{2.16}$$

where $Y_1, Y_2, \ldots . Y_K$ are K observation of the random variable Y.

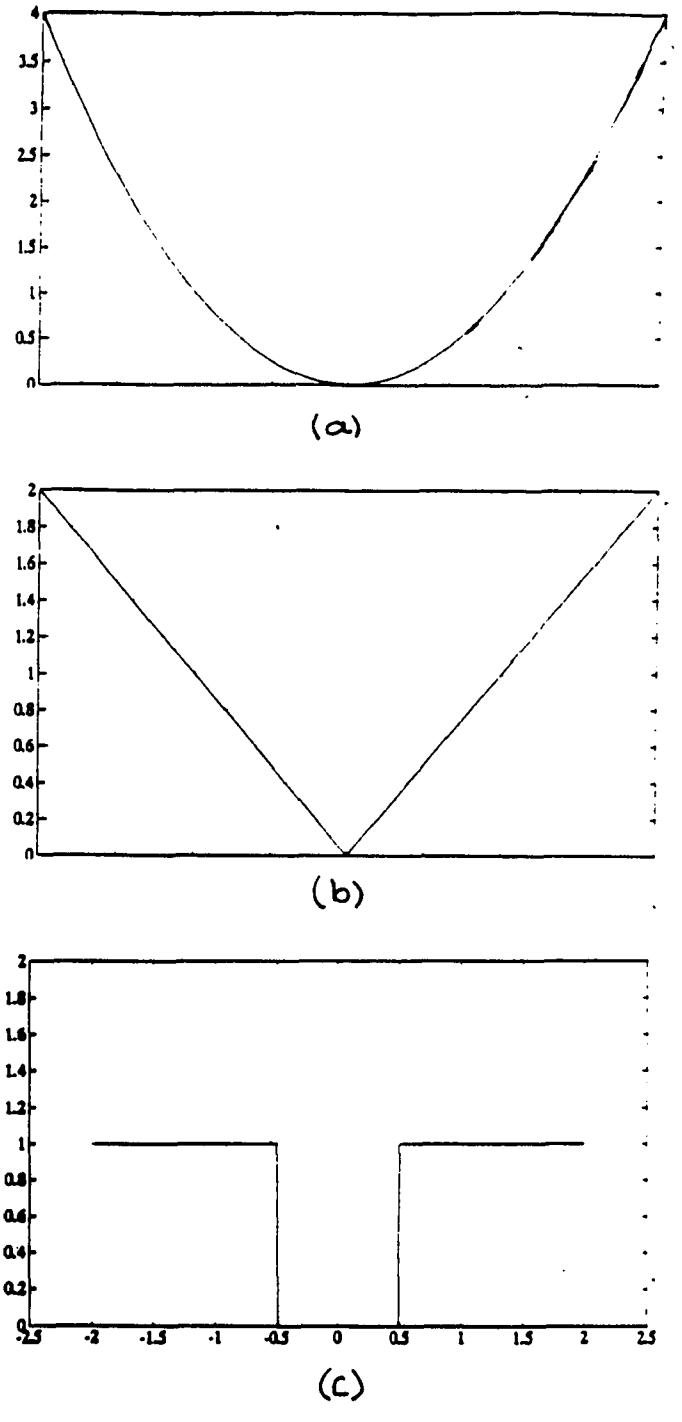

Figure 2.1: Cost functions. a) Square error. b) Absolute value of error. c) Uniform.

2.2.1 MINIMUM MEAN SQUARE ESTIMATE (MMSE)

An estimator which minimizes the risk function for the square error cost function $C(\tilde{\theta})$ is known as *Minimum Mean Square Estimate.* In this case the risk function is denoted by

$$R_{MMSE} = \int_{-\infty}^{\infty}\int_{-\infty}^{\infty} (\theta - \hat{\theta})^2 \, f_{\theta,Y}(\theta, y) \; dy \; d\theta \tag{2.17}$$

where

$$f_{\theta,Y}(\theta, y) = f_{\theta \,/\, Y}(\theta \mid y) \; f_Y(y) \tag{2.18}$$

Using EQ. (2.18) the risk function ,R_{MMSE}, can be rewritten as

$$R_{MMSE} = \int_{-\infty}^{\infty}\int_{-\infty}^{\infty} (\theta - \hat{\theta})^2 \, f_{\theta \,/\, Y}(\theta \mid y) \; f_Y(y) \; dy \; d\theta \tag{2.19}$$

$$R_{MMSE} = \int_{-\infty}^{\infty} f_Y(y) \; dy \int_{-\infty}^{\infty} (\theta - \hat{\theta})^2 \, f_{\theta \,/\, Y}(\theta \mid y) \; d\theta \tag{2.20}$$

Since the density function $f_Y(y)$ is always positive and the estimated value $\hat{\theta}$ dose not enter into the outer integral, minimizing R_{MMSE} is equivalent to minimizing the inner integral. Hence to obtain the minimum mean square estimate, we set the derivative of

the inner integral with respect to θ equal to zero, so that

$$\frac{d}{d\hat{\theta}} \int_{-\infty}^{\infty} (\theta - \hat{\theta})^2 \, f_{\theta / Y}(\theta \mid y) \, d\theta = 0 \tag{2.21}$$

By applying Leibnitz's, differentiation of an integral, theory[2] to EQ. (2.21) the minimum mean square estimate $\hat{\theta}_{MMSE}$ can be obtain, and is given by

$$\hat{\theta}_{MMSE} = \int_{-\infty}^{\infty} \theta \, f_{\theta / Y}(\theta \mid y) \, d\theta \tag{2.22}$$

or

$$\hat{\theta}_{MMSE} = E[\theta \mid Y] \tag{2.23}$$

The expression given by EQ. (2.23) is the conditional mean of $\hat{\theta}$ given the observation Y. Hence, the MMSE is the conditional mean estimate. Thus, the minimum risk R_{MMSE} and the conditional variance of $\hat{\theta}$ given observation Y can be defined as

$$R_{MMSE} = \int_{-\infty}^{\infty} f_Y(y) \, dy \int_{-\infty}^{\infty} (\theta - \hat{\theta}_{MMSE})^2 \, f_{\theta/Y}(\theta|y) \, d\theta \tag{2.24}$$

$$Var \, (\theta \mid Y) = \int_{-\infty}^{\infty} (\theta - \hat{\theta}_{MMSE})^2 \, f_{\theta / Y}(\theta \mid y) \, d\theta \tag{2.25}$$

respectively. Hence, R_{MMSE} is just the conditional variance of θ given Y, averaged over

---

[2]Leibnitz's differentiation of an integral theory:

$$\frac{d}{dx} \int_{a(x)}^{b(x)} F(u \, , \, x) \, du = \int_{a(x)}^{b(x)} \frac{\partial F}{\partial x} \, du + F[\, b(x) \, , x \,] \, \frac{db(x)}{dx} - F[\, a(x) \, , x \,] \, \frac{da(x)}{dx}$$

all values of Y.

2.2.2 ABSOLUTE ERROR (ABS)

In this case the cost function $C(\tilde{\theta})$ is denoted by

$$C(\tilde{\theta}) = | \tilde{\theta} | \tag{2.25}$$

Then the risk function, R_{ABS}, can be written as

$$R_{ABS} = \int_{-\infty}^{\infty}\int_{-\infty}^{\infty} | \theta - \hat{\theta} | f_{\theta / Y}(\theta | y) \, d\theta \, dy \tag{2.27}$$

This estimate can be interpreted from a Bayesian point of view by recognizing that it can equivalently be written as

$$R_{ABS} = \int_{-\infty}^{\infty} f_Y(y) \, dy \int_{-\infty}^{\infty} | \theta - \hat{\theta} | f_{\theta / Y}(\theta | y) \, d\theta \tag{2.28}$$

for any $C(\tilde{\theta})$ which is a monotonic function of $|\theta-\hat{\theta}|$. Since the cost function is monotonic and the density function $f_Y(y)$ is always positive, the risk function can be minimized by minimizing the inner integral of EQ. (2.28), which is given by

$$\Lambda = \int_{-\infty}^{\hat{\theta}} (\hat{\theta} - \theta) \, f_{\theta/Y}(\theta | y) \, d\theta + \int_{\hat{\theta}}^{\infty} (\theta - \hat{\theta}) \, f_{\theta/Y}(\theta | y) \, d\theta \tag{2.29}$$

the estimate of $\hat{\theta}_{ABS}$ can be obtained by differentiating EQ (2.29) with respect to θ, and

setting the result equal to zero. thus,

$$\frac{d\Lambda}{d\theta} = \int_{-\infty}^{\theta_{ABS}} f_{\theta \mid Y}(\theta \mid y)\ d\theta = \int_{\theta_{ABS}}^{\infty} f_{\theta \mid Y}(\theta \mid y)\ d\theta \qquad (2.30)$$

therefore $\hat{\theta}_{ABE}$ is just the median of the conditional density function $f_{\theta|Y}(\theta|y)$.

2.2.3 MAXIMUM A POSTERIORI ESTIMATE (MAP).

For the uniform cost function, the Bayes Risk becomes

$$R_{UCF} = \int_{-\infty}^{\infty} f_Y(y)\ \left[1 - \frac{1}{\varepsilon} \int_{\theta_{UCF} - \frac{\varepsilon}{2}}^{\theta_{UCF} + \frac{\varepsilon}{2}} f_{\theta \mid Y}(\theta \mid y)\ d\theta\right]\ dy \qquad (2.31)$$

let ε approach zero so that the cost function, $C(\tilde{\theta})$, becomes

$$C(\tilde{\theta}) = \delta(|\ \theta - \hat{\theta}\ |) \qquad (2.32)$$

the risk function R_{UCF} can be minimized by maximizing the $f_{\theta|Y}(\theta|y)$.

This is called the maximum a posteriori estimate, θ_{MAP}, which is defined by

$$\frac{\partial \ln f_{\theta \mid Y}(\theta \mid y)}{\partial \theta} = 0 \qquad (2.33)$$

This is known as the MAP equation. Using Bayes rule

$$f_{\theta \mid Y}(\theta \mid y) = \frac{f_{Y \mid \theta}(y \mid \theta)\ f_{\theta}(\theta)}{f_Y(y)} \qquad (2.34)$$

and taking the logarithm of the EQ. (2.34), we have

$$\ln f_{\theta/Y}(\theta \mid y) = \ln f_{Y/\theta}(y \mid \theta) + \ln f_{\theta}(\theta) - \ln f_{Y}(y) \qquad (2.35)$$

Therefore, EQ (2.33) can be written as

$$\left[\frac{\partial \ln f_{Y/\theta}(y \mid \theta)}{\partial \theta} + \frac{\partial \ln f_{\theta}(\theta)}{\partial \theta} \right] = 0 \qquad (2.36)$$

thus the MAP estimate can be obtained from EQ. (2.36).

2.3 PROPERTIES OF ESTIMATORS.

Some properties of estimators are as follows:

1. The estimator is unconditionally unbiased
2. The estimator is conditionally unbiased
3. The estimator is biased
4. The estimator is minimum - variance - unbiased
5. The estimator is consistent

Unconditional Unbiased Estimate:

An unconditional unbiased estimate is one whose expected value is the expected value of the quantity being estimated. Thus,

$$E[\hat{\theta}] = \theta \qquad \text{For all } \theta \qquad (2.37)$$

Conditional Unbiased Estimate:

A conditional unbiased estimate is one whose expected value is equal to the true value of the quantity being estimated. If $\hat{\theta}$ is a conditional unbiased estimate, then

$$E\ [\hat{\theta}\ |\ \theta]\ =\ \theta \tag{2.38}$$

or

$$E_Y(\theta)\ =\ \int \theta\ f\ (Y\ |\ \theta)\ dY\ =\ \theta \tag{2.39}$$

Biased Estimates:

Let us denote the expected value of $\hat{\theta}$ as follows:

$$E\ [\hat{\theta}]\ =\ \theta\ +\ B\ (\theta) \tag{2.40}$$

1. The estimator $\hat{\theta}$ has a known bias if B(θ) is independent of θ (B(θ)=B). That is, (θ-$\hat{\theta}$) is an unbiased estimate.

2. When B(θ) is not equal to B and is dependent on θ, an unbiased estimate cannot be obtained, hence θ is unknown. Therefore, the estimator has an unknown bias which cannot be subtracted out, since it depends upon θ, which is not known.

Unbiased Minimum Variance Estimate:

An estimator $\hat{\theta}$ is minimum variance unbiased, if it is unbiased and the variance of $\tilde{\theta}$ is less than the variance of any other unbiased estimator. That is, $\hat{\theta}$ has the smallest

variance among all unbiased estimates, θ' such that $E[\theta']=\theta$, of θ. Thus,

$$Var\ (\hat{\theta}) \leq Var\ (\theta') \qquad for\ all\ \theta' \tag{2.41}$$

Consistent Estimate:

It is desirable that an estimate become better as the number of observations increases. One measure of this desirable property is consistency. A consistent estimator is one which becomes better as the number of observation increases. Formally, this can be expressed as follows:

Let $\hat{\theta}$ represent the optimum parameter estimator of θ based upon K observations, the estimator is consistent if

$$\lim_{K\to\infty} E\ [\hat{\theta}] = \theta \tag{2.42}$$

and if

$$\lim_{K\to\infty} var\ [\hat{\theta}] = 0 \tag{2.43}$$

2.4 THE CRAMER-RAO INEQUALITY

It is not always possible to obtain an expression for the error variance and determine its consistency, but it is possible to establish lower bounds on the error variance of any estimator. This bound is called *Cramer - Rao Lower Bound (CRLB)* and its expression is called the *Cramer - Rao Inequality.* The CRLB is given by the following theorem:

Theorem: Let $\hat{\theta}$ be an estimator of the parameter whose true value is θ, and the vector $Y=(Y_1, \ldots, Y_K)$ represent K observations, then,

$$\sigma_{\hat{\theta}}^2 \geq \frac{\frac{\partial \overline{\theta}}{\partial \theta}^2}{E\left[\frac{\partial \ln f_{Y|\Theta}(y|\theta)}{\partial \theta}\right]^2} = -\frac{\frac{\partial \overline{\theta}}{\partial \beta}^2}{E\left[\frac{\partial^2 \ln f_{Y|\Theta}(y|\theta)}{\partial \theta^2}\right]} \qquad (2.44)$$

$$\overline{\theta} = E\,[\,\hat{\theta} \mid \theta\,] \qquad (2.45)$$

where $\overline{\theta}$ is mean value of $\hat{\theta}$ and $\sigma^2_{\hat{\theta}}$ represent the variance of the estimator $\hat{\theta}$. Either of the forms following the inequality sign in EQ. (2.44) is known as the Cramer - Rao Lower Bound.

If $\hat{\theta}$ is an unbiased estimator of θ, then the mean value of $\hat{\theta}$ is equal to θ. Therefore, CRLB becomes

$$\sigma_{\hat{\theta}}^2 = \frac{1}{E\left[\frac{\partial \ln f_{Y|\Theta}(y|)}{\partial \theta}\right]^2} = -\frac{1}{E\left[\frac{\partial^2 \ln f_{Y|\Theta}(y|\theta)}{\partial \theta^2}\right]} \qquad (2.46)$$

An unbiased estimator that achieves the CRLB dose not always exist. If such an

estimator existed, it would be unique and it would be a maximum likelihood estimator. Any estimate that satisfies the CRLB with an equality is called an *efficient estimate.*

CHAPTER THREE

POSSIBLE APPROACHES

3.0 INTRODUCTION

Since Fourier established the basis for defining a spectrum of a signal, the problem of spectral estimation, direction finding and location finding has progressed through many stages. The spectral estimation may be broken into two basic categories:

1. The spectral estimation methods based on Fourier analysis. This method can be categorized under two headings.

   i. The periodogram, proposed by Schuster in 1898

   ii. Blackman - Tukey spectral estimation, R. Blackman and J. Tukey in 1958

These methods are known as classical techniques which directly utilizes the theorems of Fourier on general data.

2. Estimation based on modelling (Parametric methods[1]) which consists of

   i. Selecting an appropriate model

   ii. Estimate the parameters of the model

   iii. Substituting the estimated values into the theoretical Power Spectrum Density, PSD, expressions.

The method of Burg, which maximizes the entropy defined for a particular model of signal and noise is in this category. Also, the Maximum Likelihood (ML) method (method of Capon) falls under this category.

The prime concern in this chapter will be to pose imprecise terms a small subset of different techniques which are being used in spectral estimation such as:

1. Classical Spectral Estimation
2. Autoregressive (AR)
3. Moving Average model (MA)
4. Autoregressive - Moving Average (ARMA)

---

[1]Originated with the work of Yule (1927) and subsequently developed and applied by Walker (1931), Bartlett (1948), Parzen (1957), Burg (1967), Capon (1969), and Pisarenko (1973).

In addition, before focusing on the Space Station robot tracking system, several alternate approaches which could be appropriate to some applications are discussed. Table 3.1 shows a partial list of different techniques that one can use for tracking and location finding.

3.1 CLASSICAL SPECTRAL ESTIMATION

In this section we discuss two basic methods, *PERIODOGRAM and BLACKMAN-TUKEY*, of classical estimation. Also, the major advantage and disadvantages of these two techniques are summarized.

Table 3.1 Partial list of different techniques.

TECHNIQUES	REFERENCE
Dead - reckoning method	[14], [24], [25]
Music	[31]
Conventional Beamforming	[16]
Cyclic Direction finding method	[29], [30]

3.1.1 PERIODOGRAM

The periodogram method of spectral estimation is based on the definition of power spectral density as the Fourier transform of the autocorrelation function. In other words the periodogram is defined as the squared magnitude of the discrete Fourier transform (DFT) of the sequence x[n] which is scaled by the number of samples in x[n]. Thus, we begin our discussion by estimation of autocorrelation function.

Let x(t) be a continuous time signal with a finite energy, that is,

$$E = \int_{-\infty}^{\infty} |x(t)|^2 dt < \infty \qquad (3.1)$$

The sequence x[n] denotes the result of sampling a signal x(t) at some uniform sampling rate f_s. To avoid spectral aliasing the signal bandwidth is limited to B hertz and the sampling frequency f_s must be greater than 2B. The Fourier transform of sequence x[n] (x[n], $-\infty < n < \infty$) is given by

$$X[f] = \sum_{n=-\infty}^{\infty} x[n] \exp^{-j2\pi fn} \qquad (3.2)$$

and the energy density spectrum[2] of the sampled signal, x[n], is

$$S_{xx}(f) = |X[f]|^2 \tag{3.3}$$

where the magnitude square of X[f] represents the distribution of signal energy as a function of frequency. The autocorrelation of the sampled signal is defined as

$$R_{xx}(m) = \sum_{n=-\infty}^{\infty} x^*[n]\, x[n + k] \tag{3.4}$$

From the Wiener-Khintchine theorem we have

$$S_{xx}(f) = \sum_{m=-\infty}^{\infty} R_{xx}(m)\, e^{-j2\pi fm} \tag{3.5}$$

That is, the power spectral density of an energy signal is the Fourier transform of its autocorrelation sequence. Therefore, the power spectral density function and the autocorrelation function are defined as a Fourier transform pair:

$$R_{xx}(m) = \sum_{n=-\infty}^{\infty} S_{xx}(f)\, e^{j2\pi fn} \leftrightarrow S_{xx}(f) = \sum_{m=-\infty}^{\infty} R_{xx}(m)\, e^{-j2\pi fm} \tag{3.6}$$

The power spectral density function can be directly determine from the Fourier transform of the autocorrelation function. However, the autocorrelation function is not known and it must be estimate based on a finite interval of sequence x[n]. In practice the sequence x[n] is assumed to be known only over a finite interval N. Since the sequence x[n] is not defined for n > N-1 and is limited to N points we multiply x[n] by a rectangular

---

[2]Parseval's theory

$$E = \sum_{n=-\infty}^{\infty} |x(t)|^2 = \sum_{n=-\infty}^{\infty} |X[f]|^2$$

window. As result

$$\hat{x}[n] = x[n]\,w[n] = \begin{cases} x[n] & 0 \le n \le N-1 \\ 0 & otherwise \end{cases} \qquad (3.7)$$

The frequency domain representation of x[n] can be found as follows

$$\begin{aligned} \hat{X}[f] &= \int_{-\frac{1}{2}}^{\frac{1}{2}} X[n]\,W[f-\alpha]\;d\alpha \\ &= X[n] * W[n] \end{aligned} \qquad (3.8)$$

That is, X[f] is the convolution of the desired frequency response with the Fourier transform of the window, since multiplication in time domain correspond to convolution in frequency domain. The effect of convolution with the window function is that it smooth X[f] if the spectrum of W[f] is relatively narrow compared to X[f].

If x[n] are samples of a single realization of the stationary random process X[f], its time average autocorrelation sequence is defined as

$$\begin{aligned} \hat{r}_N(m) &= \langle\, x[n]\; x^*[n+m] \,\rangle \\ &= \frac{1}{2N+1}\sum_{n=-N}^{N} x[n]\; x^*[n+m] \end{aligned} \qquad (3.9)$$

and has the Fourier transform

$$\hat{R}_N(f) = \sum_{m=-(N-1)}^{N-1} \hat{r}_N(m)\, e^{-j2\pi fm} \qquad (3.10)$$

Since the fourier transform of the real finite - length sequence x[n], 0<n<N-1, is

$$X[f] = \sum_{n=0}^{N-1} x[n]\, e^{-j2\pi fn} \tag{3.11}$$

Then the *periodogram spectral estimator* is defined as

$$\begin{aligned} \hat{R}_{PER}(f) &= \frac{1}{N} \left| \sum_{n=0}^{N-1} x[n]\, e^{-j2\pi fn} \right|^2 \\ &= \frac{1}{N} \left| X[f] \right|^2 \end{aligned} \tag{3.12}$$

Note that the periodogram spectral estimation is identical to the Fourier transform of an estimated autocorrelation sequence.

$$\hat{R}_{PER}(f) = \sum_{k=-(N-1)}^{N-1} \hat{r}_N(k)\, e^{-j2\pi fk} \tag{3.13}$$

where $\hat{r}_N(k)$ is the biased autocorrelation estimate, which is defined as

$$\hat{r}_N(k) = \frac{1}{N} \sum_{k=0}^{N-1-|k|} x[n]\; x[n + |k|] \tag{3.14}$$

The expected value of the periodogram autocorrelation is given by

$$\begin{aligned} E[\hat{R}_{PER}(f)] &= \sum_{k=(-N-1)}^{N-1} E[\hat{r}_N(k)]\, e^{-j2\pi fk} \\ &= \sum_{k=-(N-1)}^{N-1} \left[\frac{N - |k|}{N} \right] r_N(k)\, e^{-j2\pi fk} \\ &= F\{w_B[k]\, r_N[k]\} \\ &= \int_{-\frac{1}{2}}^{\frac{1}{2}} W_B(f - \xi)\, R_N(\xi)\, d\xi \end{aligned} \tag{3.15}$$

where $W_B(f)$ is the fourier transform of the Bartlett window, $w_B(k)$,

$$w_B[k] = \begin{cases} 1 - \frac{|k|}{N} & for \ |k| \leq N - 1 \\ 0 & for \ |k| > N - 1 \end{cases} \tag{3.16}$$

and is given by

$$W_B(f) = \frac{1}{N}\left(\frac{\sin \pi f N}{\sin \pi f}\right)^2 \tag{3.17}$$

3.1.2 BLACKMAN - TUKEY SPECTRAL ESTIMATION

In section 3.1.1 it was shown that the periodogram spectral estimation is identical to the Fourier transform of an estimated autocorrelation sequence which results a poor estimate of the power spectral density. The poor performance of the periodogram may be attributed to the poor performance of the autocorrelation function estimator. One way to avoid this problem is to use a lag window (w[k]). Thus,

$$\hat{P}_{BT}[f] = \sum_{k=-(N-1)}^{N-1} w[k]\, \hat{r}_{xx}[k]\, e^{-j2\pi fk} \tag{3.18}$$

where $P_{BT}[f]$ is called the *Blackman-Tukey spectral estimator* and w[k] is a lag window with the following properties:

1. $$0 \leq w[k] \leq w[0] = 1 \tag{3.19}$$

2. $$w[-k] = w[k] \tag{3.20}$$

$$3. \quad w[k] = 0 \qquad for\ all \quad |k| > M \tag{3.21}$$

where M ≤ N-1.

Using the above properties of a lag window then $P_{BT}[f]$ can be written as

$$\hat{P}_{BT} = \sum_{k=-M}^{M} w[k]\, \hat{r}_{xx}[k]\, e^{-j2\pi fk} \tag{3.22}$$

3.2 DEAD - RECKONING METHOD

The development of the "Dead - Reckoning" location finding system began in February 1971 and the system was delivered in August 1974. Dead reckoning methods can locate a vehicle if the initial position of a vehicle is known, its location at subsequent times can be computed, and when direction and distance changes are added vectorially as shown in Figure 3.1. This technique also requires that errors caused by thermal noise is negligible.

The system consist of a mobile unit which is installed on the vehicle and a base unit which is located inside the control room. The mobile unit block diagram is shown in Figure 3.2. This unit consist of one receiver, one transmitter, a data processing unit, a distance sensor, and a heading sensor. The distance sensor senses the distance traveled by the vehicle and the heading sensor senses the direction which vehicle is traveling. The information from the two sensors are transferred through vehicle data processor to the transmitter and then to the base unit.

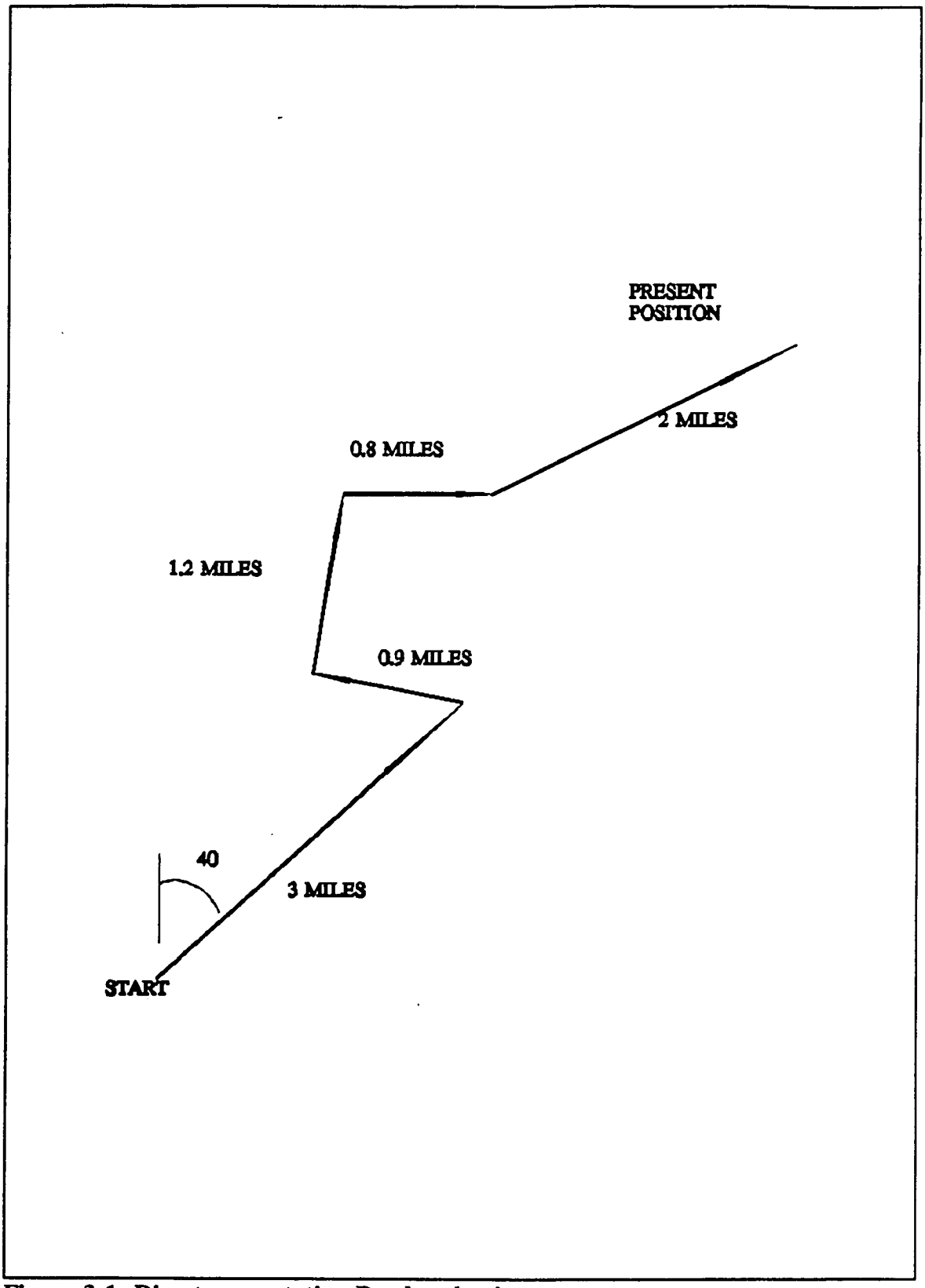

Figure 3.1: Direct computation Dead reckoning.

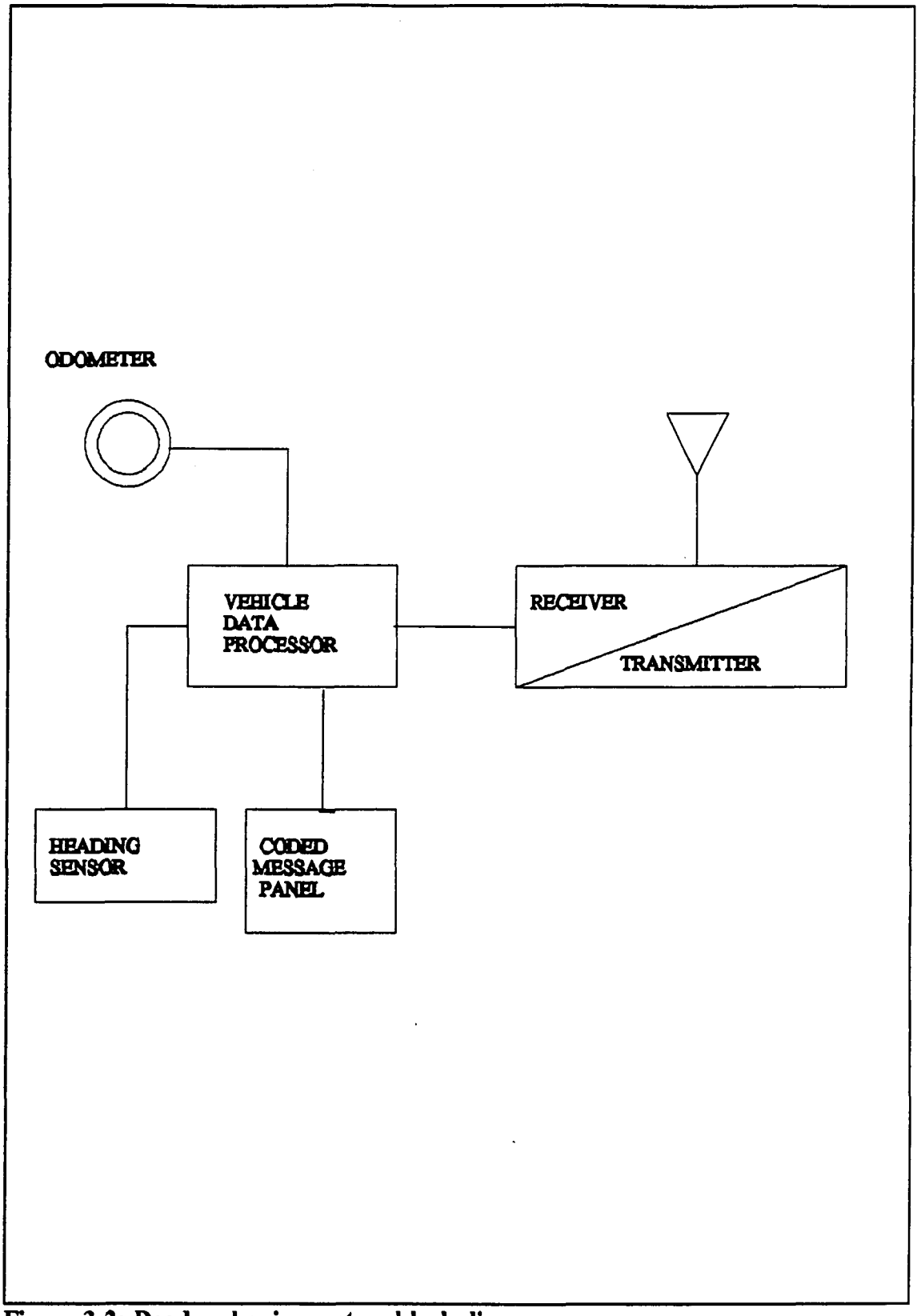

Figure 3.2: Dead reckoning system block diagram.

The base equipment includes all components of the system required to process the location and data received from the mobile equipment and display the location of the vehicle on a TV - type display. Block diagram of the base unit equipment is shown in Figure 3.3.

The vehicle's initial location are in the central processor unit. The vehicle position (via the mobil unit) is continuously transmitted to the central processor located at the base station as long as the vehicle is traveling. When the vehicle is at rest the central processor retains the vehicle last position for future initial position. Given the initial position X_i and Y_i the vehicle location can be computed as follow

$$X = X_i + \int_0^s \cos\theta(s)\, ds \qquad (3.23)$$

and

$$Y = Y_i + \int_0^s \sin\theta(s)\, ds \qquad (3.24)$$

where s is the distance traveled by the vehicle from the initial position (X_i, Y_i) and $\theta(s)$ is the vehicle heading as a function of the distance traveled. The distance measurements are made using a precision odometer (Distance sensor) and some compass type device to measure azimuth (Heading sensor).

Since the computed location depends upon all previous location estimates, errors in location due to noise tend to accumulate which can lead to sizeable position errors. One solution to this problem is manually up date the system with the initial location of the

vehicle on a regular basis. This process is not to difficult if the vehicle's routes are known, however, in case which the vehicle's routes are unknown sophisticated techniques would be needed to accomplish this.

This system operates in the UHF (450 - 470 MHZ) frequency band. The system is time synchronized by the base transmitter and accommodates 200 vehicles per mobile transmit frequency. Each vehicle transmits a 20 bits data massage every 1.215 second to the base receiver. A paper by Thomas W. Lezniak, Richard W. Lewis and R. A. McMillen [14] reports on tests of one such computer aided reckoning system.

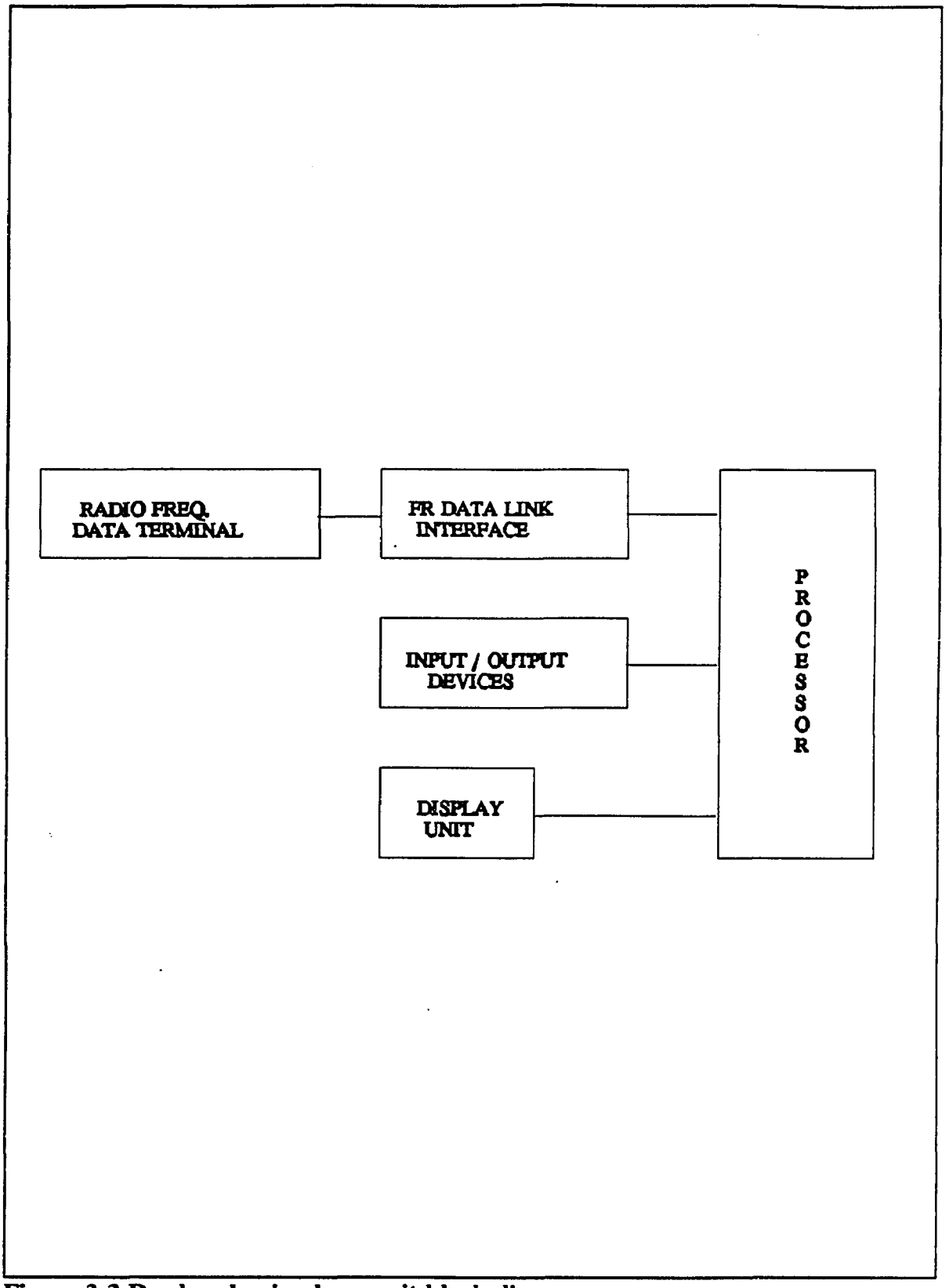

Figure 3.3 Dead reckoning base unit block diagram.

3.3 MUSIC

The MUltiple SIgnal Characterization[3] (MUSIC) algorithm is an implementation of the signal subspace approach to multiple source location and signal parameter estimation. The MUSIC algorithm can be use to provide asymptotically unbiased estimates of multiple wavefronts arriving at an antenna array from measurements made on the signal received at the array elements. These estimates may include

1. Number of signals
2. Direction of arrival
3. Polarization
4. Strength of noise and interference
5. Strengths and cross correlations among the emitted signals

3.3.1 MUSIC ALGORITHM

The MUSIC algorithm can be summarized in the following steps.

Step 1: Collect data (X) and form the covariance matrix (S) of the X vector.

Let M denote the number of the array elements, D denote the linear combination of

[3]R. U. Schmidt, "A signal Subspace Approach to Multiple Emitter Location" Ph.D. Thesis, Stanford, 1982

the incident wavefronts and noise received at the M array elements, and X denote the M vectors received. Thus,

$$Y_i = A(\theta) \times X_j + W_i \qquad where \begin{cases} i = 1,2,3....M \\ j = 1,2,3....D \end{cases} \qquad (3.25)$$

Where $X \in C^{Dx1}$ is the vector of complex signal amplitudes and phase, $W \in C^{Mx1}$ is an additive noise, and elements of Matrix $A(\theta) \in C^{MxD}$ are known function of the signal arrival angles and the array element locations. The Matrix $A(\theta)$ and the vector $a(\theta_j)$ are given by

$$A(\theta) = [a(\theta_1) \;\; a(\theta_2) \;\; \cdots \;\; a(\theta_D)] \qquad (3.26)$$

$$a(\theta_j) = [1 \;\; e^{i\theta} \;\; \cdots \;\; e^{i(M-1)\theta}]^T \qquad j = 1,2,3,.....D \qquad (3.27)$$

then using EQ. (3.4) and EQ. (3.5) the observed data vector can be rewritten as

$$\begin{bmatrix} Y_1 \\ Y_2 \\ \vdots \\ Y_M \end{bmatrix} = [a(\theta_1) \;\; a(\theta_2) \;\; \cdots \;\; a(\theta_D)] \times \begin{bmatrix} X_1 \\ X_2 \\ \vdots \\ X_D \end{bmatrix} + \begin{bmatrix} W_1 \\ W_2 \\ \vdots \\ W_M \end{bmatrix} \qquad (3.28)$$

or

$$Y = AX + W \qquad (3.29)$$

$a(\theta_j)$ is known as the jth direction of arrival (DOA) or mode vector. That is, the jth column of A is a "mode" vector $a(\theta_j)$ of responses to the direction of arrival θ_j of the jth signal.

The data covariance matrix S of the observation vector Y is given by

$$S \equiv \overline{YY^*} \equiv A\overline{XX^*}\,A^* + \overline{WW^*} \tag{3.30}$$

or

$$S = APA^* + \lambda S_w \tag{3.31}$$

under the following assumptions

$$1. \quad \lim_{M\to\infty} \frac{1}{M} \sum_{i=1}^{M} W_i = 0 \tag{3.32}$$

$$2. \quad \lim_{M\to\infty} \frac{1}{M} \sum_{i=1}^{M} W_i W_i^* = \lambda S_w \tag{3.33}$$

$$3. \quad P = \lim_{M\to\infty} \frac{1}{M} \sum_{i=1}^{M} X_i X_i^* \tag{3.34}$$

where the matrix P is nonsingular (positive definite) and D is less than M.

Note that S_w is the noise covariance matrix and λ denote the eigenvalues of the data covariance matrix S. Since the APA^* is singular and it has rank less than M then

$$|APA^*| = |S - \lambda S_w| = 0 \tag{3.35}$$

EQ. (3.33) is only satisfied if λ equal to one of eigenvalues of S in the metric of S_w. But, for A full rank and P positive define, APA^* must be nonnegative define. Therefore, the data covariance matrix can be written as

$$S = APA^* + \lambda_{\min} S_w \qquad \lambda_{\min} \geq 0 \tag{3.36}$$

For the case which the source vector X and the noise vector W are independent then the

expected data covariance matrix $\hat{S}$ is

$$\hat{S} = APA^* + \sigma^2 S_w \tag{3.37}$$

where σ^2 is the average sensor noise power. Thus,

$$\sigma^2 = \frac{1}{M} tr\ (\sigma^2 S_w) \tag{3.38}$$

$$tr\ (S_w) = M \tag{3.39}$$

Where tr(◦) denotes the matrix trace operation. If the antenna noises are uncorrelated and of equal power then the S_w matrix is the identity matrix. Thus,

$$S_w = I \tag{3.40}$$

and

$$\hat{S} = APA^* + \sigma^2 I \tag{3.41}$$

Therefore, the data covariance matrix can be consistently estimated from the observed data Y.

$$\hat{S} = \frac{1}{M} \sum_{i=1}^{M} Y(i)\, Y(i)^* \tag{3.42}$$

where $\hat{S}$ is an estimate of S.

Step 2: Determine the number of signals D.

In general, the number of signals with no noise is equal to the rank of APA^* and the number of signals with noise is the "pseudo-rank" of the number of eigenvalue having

the threshold set by noise. Therefore, the number of incident signals estimator is

$$\hat{D} = M - \hat{N} \tag{3.43}$$

$$D = rank\ [APA^*] \tag{3.44}$$

where $\hat{N}$ is the multiplicity of λ_{min} of S in metric of S_w. The rank of APA^* can be determined from the eigenvalues of the data covariance matrix in the metric of S_w.

Step 3: Evaluate $P_{MU}(\theta)$ and the MUSIC spectrum.

Let D denote the number of signals, the eigenvectors corresponding to the largest D eigenvalues are called the signal eigenvectors and the remainder are called the noise eigenvectors. The noise eigenvectors are orthogonal to the DOA vectors of the signals present. Thus the MUSIC spectrum is

$$SP_{MU}(\theta) = \left[\frac{a^*(\theta)\, E_n E_n^*\, a(\theta)}{a^*(\theta)\, a(\theta)}\right]^{-1} \tag{3.45}$$

where E_n is a MxN matrix whose columns are N noise eigenvectors. Then using the noise eigenvector, the "angle spectrum" is

$$P(\theta) = \frac{a^*(\theta)\ a(\theta)}{a(\theta)\ E_n^*\ a^*(\theta)} \tag{3.46}$$

and the effects of polarization diversity among the array elements is given by

Hence, the vector of polarization parameters q are determine from the eigenvectors

$$P_{MU}(\theta) = \frac{1}{a^*(\theta) E_n E_n^* a(\theta)} \qquad (3.47)$$

corresponding to λ_{min} and the peaks in EQ. (3.24) represents the direction of arrival.

Step 4: Evaluate the Angle of Arrival (AOA).

The angle of arrival of the incident signals can be determined directly from the spectrum, that is, the location of the peaks in the spectrum are the estimate of the angles of arrival of the incident signals.

Once the direction of arrival is known then the A matrix becomes available and the P matrix can be expressed as

$$P = (A^* S_w^{-1} A)^{-1} A^* S_w^{-1} (S - \lambda_{min} S_w) S_w^{-1} A (A^* S_w^{-1} A)^{-1} \qquad (3.48)$$

where P is a DxD matrix of cross and auto powers. Since

$$APA^* = S - \lambda_{min} S_w \qquad (3.49)$$

then the P matrix can be rewritten in terms of $(S - \lambda_{min} S_w)$ and A. As result

$$P = (A^* A)^{-1} A^* (S - \lambda_{min} S_w) A (A^* A)^{-1} \qquad (3.50)$$

Note that for MUSIC algorithm the number of antennae (M) needed in order to unambiguously determine arrival angles must be greater than the number (D) of incident signals received. That is,

$$M \geq D + 1 \qquad (3.51)$$

For a single strong source the MUSIC algorithm is very accurate, fast, and gives

unambiguous estimates of the angel of arrival.

CHAPTER FOUR

LINEAR FREQUENCY MODULATION

4.0 INTRODUCTION

The primary function of a high resolution direction and location finding system is to obtain information which determine the relative object position. This information may include the distance from the object to the receiver, angular position such as azimuth and elevation, etc. One technique which can be use to accomplished this information is Frequency Modulation (FM). This modulation may by *sinusoidal or linear.* Linear

Frequency Modulation (LFM) or *CHIRP*[1] signals are common in different areas of engineering such as communication, radar, ...etc. For example, chirp signals can be used to estimate the location of an object with respect to fixed receivers. Chirp signal is a sinusoidal waveform whose instantaneous frequency varies linearly with time. Mathematically, it can be represented as

$$s(t) = A\cos(\omega_c t + \frac{1}{2}\mu t^2) \qquad (4.1)$$

where A is the amplitude, ω_c is the carrier frequency, and μ is the rate of change of frequency.

This chapter contains a discussion of the most widely used forms of modulation, frequency modulation and linear frequency modulation. The details of chirp signal generation is considered and the resulting signal waveforms and power spectra are calculated. In addition, parameter estimation of chirp signal is discussed.

4.1 FREQUENCY MODULATION

Frequency modulation (FM) is a form of angle modulation in which the instantaneous frequency changes with respect to the modulating signal. The spectrum of a FM signal depends on amplitude of the baseband signal as well as the frequency of the spectral

---

[1]A common term for LFM signals used by B. M. Oliver in an internal Bell Laboratories Memorandum entitled "Not with a Bang, But a Chirp" in 1951.

components. A frequency modulated signal is given by

$$v(t) = A \cos (\omega_c t + 2 \pi k_f \int_{-\infty}^{t} m(\lambda) d\lambda) \tag{4.2}$$

where ω_c is the angular velocity of the carrier, k_f a constant representing frequency sensitivity of the modulator in hertz per volt, and m(t) is the modulating signal. For a sinusoidal function the instantaneous angular velocity is equal to the time rate of change of the argument. That is

$$\begin{aligned} \omega_i(t) &= \frac{d}{dt} [\omega_c t + 2 \pi k_f \int_{-\infty}^{t} m(\lambda) d\lambda] \\ &= \omega_c + 2 \pi k_f m(t) \end{aligned} \tag{4.3}$$

or

$$f_i(t) = f_c + k_f m(t) \tag{4.4}$$

From EQ. (4.4), it can be observed that the instantaneous frequency is directly proportional to the modulating waveform. As result the frequency the frequency modulated signal changes frequency whenever the modulation changes level.

4.2 LINEAR FREQUENCY MODULATION

There are two basic approaches to generation of the linear FM signal active and passive signal generation. Active signal generation is based on controlling the frequency of an oscillator with a voltage derived from a function generator. The passive generation of the frequency modulated signal is based on exciting a conjugate matched-filter

network with an impulse. Figure 4.1 shows the basic techniques for active generation of a linear FM signal, in a frequency modulation device in which the frequency is linearly proportional to the voltage present on the control element of the oscillator. If the oscillator is a phase modulation device, such that the frequency is proportional to the derivative of the voltage at the control element, then a square-law voltage vs. time function is required. Figure 4.2 shows the basic block diagram of a square-law oscillator control voltage. For both cases the use of gating circuit and frequency multiplication serve the purpose of larger frequency deviation before transmission. The block diagram for the passive generation of a linear FM is shown in Figure 4.3.

4.2.1 ACTIVE GENERATION OF A LINEAR FM SIGNAL

Let y(t) be a modulating signal of duration T_p

$$y(t) = \begin{cases} t & , \quad |t| < T_p / 2 \\ 0 & , \quad elsewhere \end{cases} \tag{4.5}$$

and x(t) is the emitted signal of the form

$$x(t) = A\ rect(\frac{t}{T_p})\ \cos(\omega_c t) \tag{4.6}$$

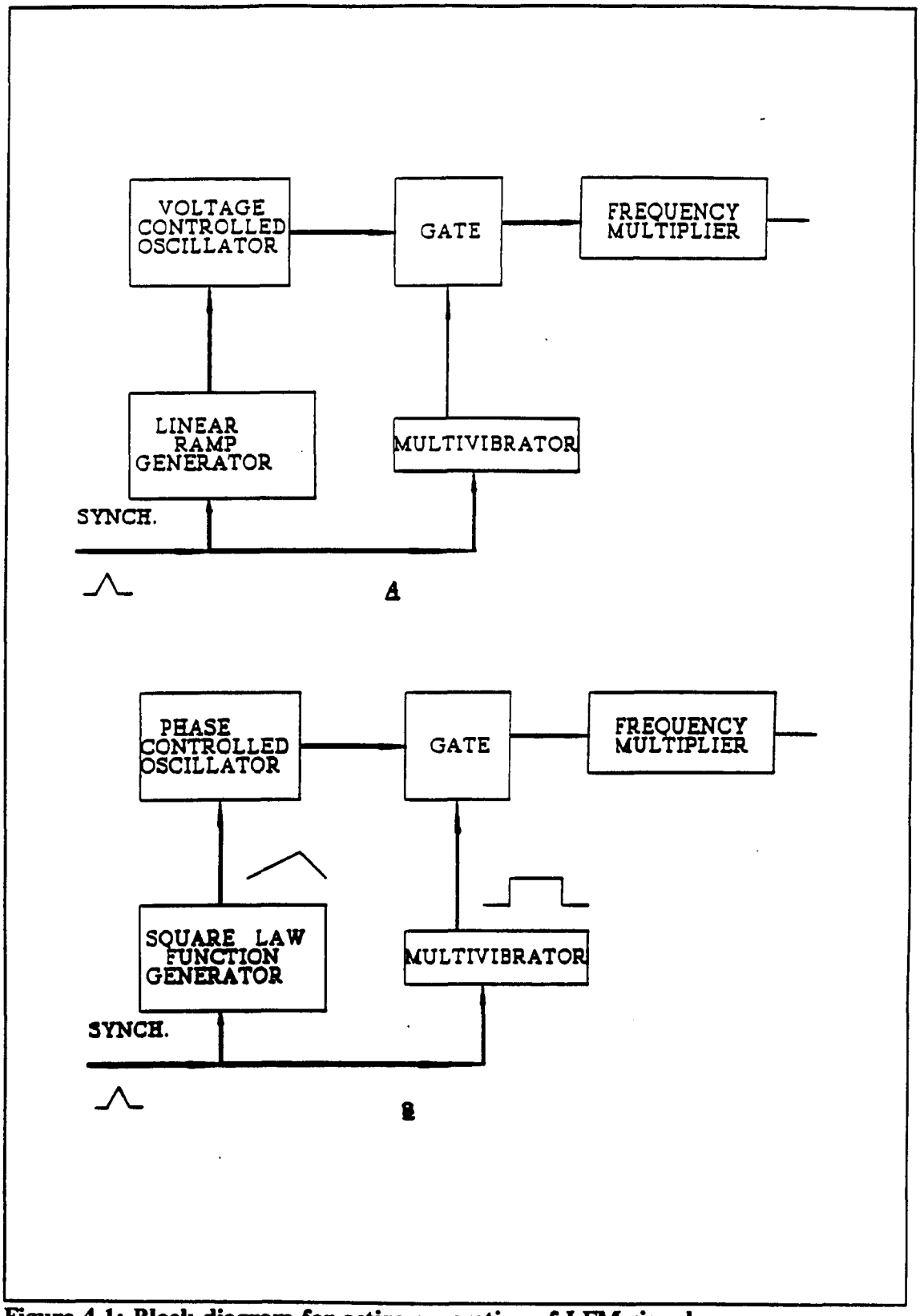

Figure 4.1: Block diagram for active generation of LFM signal.

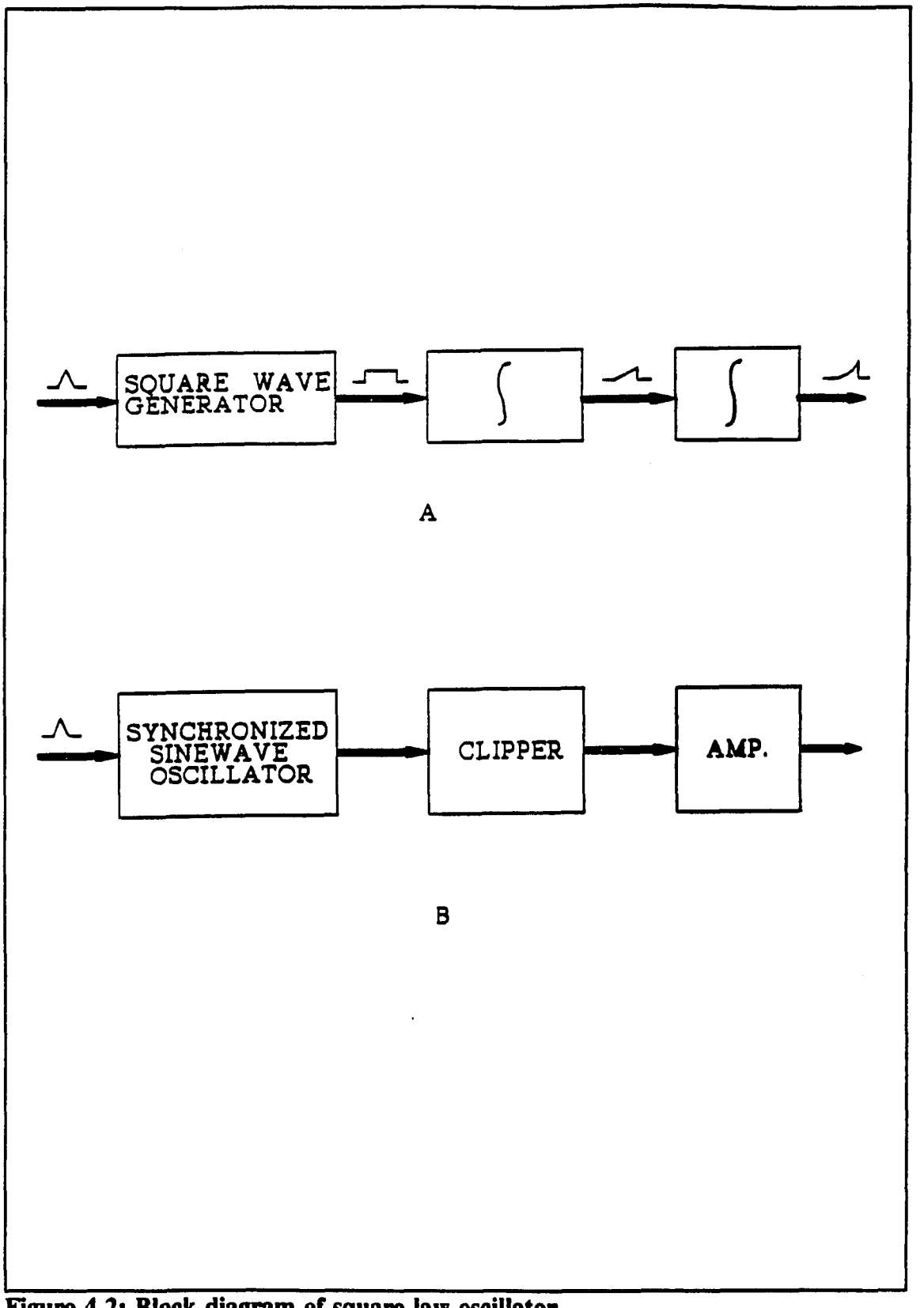

Figure 4.2: Block diagram of square law oscillator.

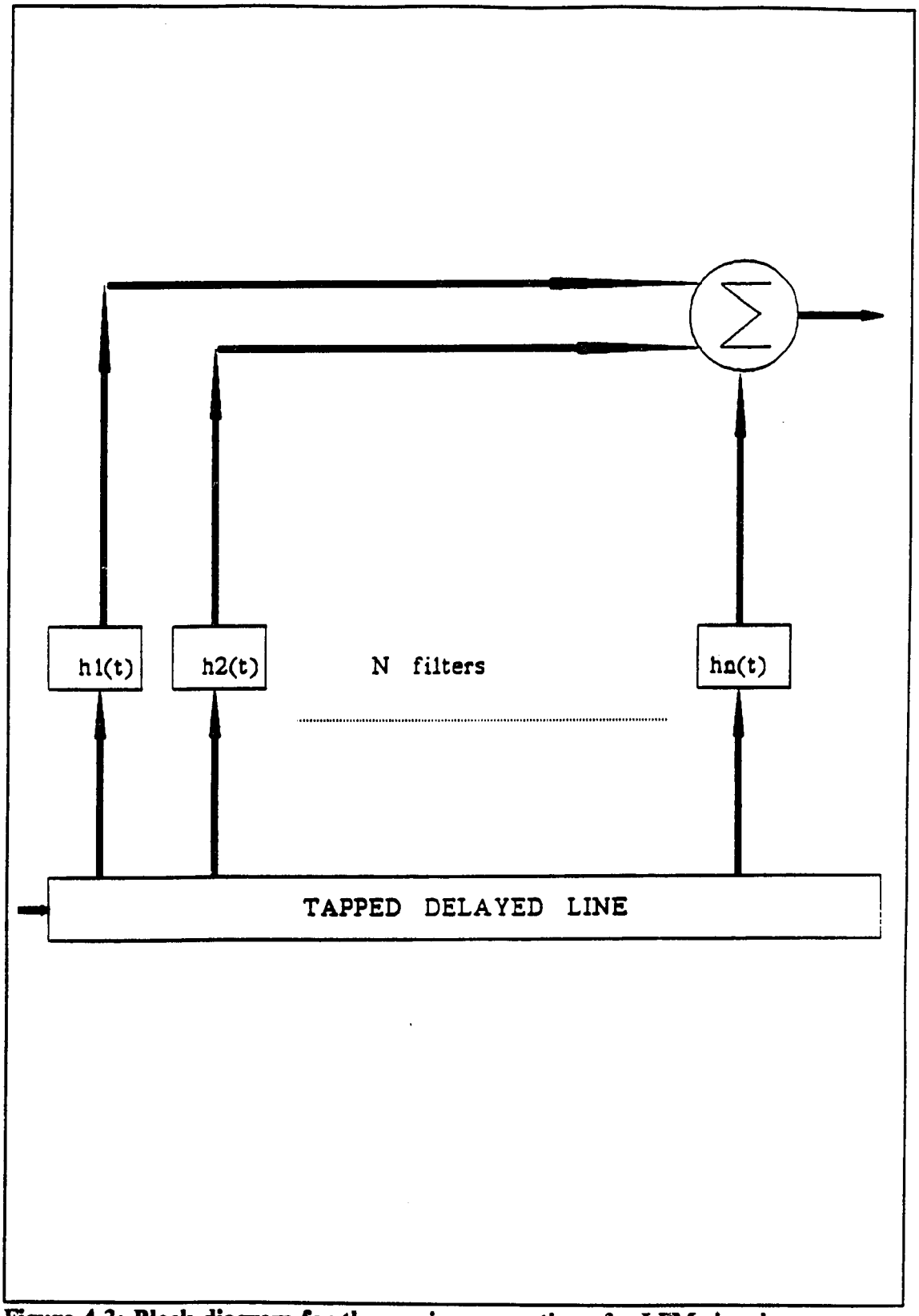

Figure 4.3: Block diagram for the passive generation of a LFM signal.

where A is the amplitude of the rectangular pulse, and ω_c is the carrier frequency in rad/sec. With the signal of EQ. (4.5) FM modulating the carrier of EQ. (4.6), the instantaneous frequency of the carrier will be

$$\omega_i(t) = \begin{cases} \omega_c + \mu t & , \quad |t| < T_p / 2 \\ 0 & , \quad elsewhere \end{cases} \tag{4.7}$$

where μ is the rate of change of frequency and may be either positive or negative. This means that the carrier frequency is linearly swept during the pulse duration T_p covering a band of frequencies (Δ) at a rate of μ rad/sec^2, centered at a frequency f_c as shown in Figure 4.4.

The angle of the modulated wave, $\theta_i(t)$, can be obtain by taking the integral of the instantaneous frequency. Thus,

$$\begin{aligned} \theta_i(t) &= \int \omega_i(t)\, dt \\ &= \omega_c t + \frac{1}{2}\mu t^2 + \varphi \end{aligned} \tag{4.8}$$

that is, the phase angle change is quadratic. Therefore the LFM signal s(t) can be written as

$$s(t) = A\ rect(\frac{t}{T_p})\ \cos(\omega_c t + \frac{1}{2}\mu t^2 + \varphi) \qquad -\frac{T_p}{2} \le t \le \frac{T_p}{2} \tag{4.9}$$

where φ is a constant phase assumed uniformly distributed in [0 - 2π]. EQ. (4.9) is

known as a *CHIRP* signal. Since rect(t/T_p) is defined as

$$rect(\frac{t}{T_p}) = \begin{cases} 1 & for \quad -T_p/2 \le t \le T_p/2 \\ 0 & elsewhere \end{cases} \tag{4.10}$$

then EQ. (4.9) can be written as

$$s(t) = A\cos(\omega_c t + \frac{1}{2}\mu t^2 + \varphi) \qquad -\frac{T_p}{2} \le t \le \frac{T_p}{2} \tag{4.11}$$

This is a cosine of duration T_p seconds, whose frequency is swept (chirped) linearly over the pulse length, T_p, around ω_c, as shown in Figure 4.5. The net frequency sweep, Δ, is

$$\begin{aligned} \Delta &= (\omega_c + \mu\frac{T_p}{2}) - (\omega_c - \mu\frac{T_p}{2}) \\ &= \mu T_p \end{aligned} \tag{4.12}$$

Figure 4.6 schematically illustrates a signal processing a linear FM. This signal finds extensive use in radar application.

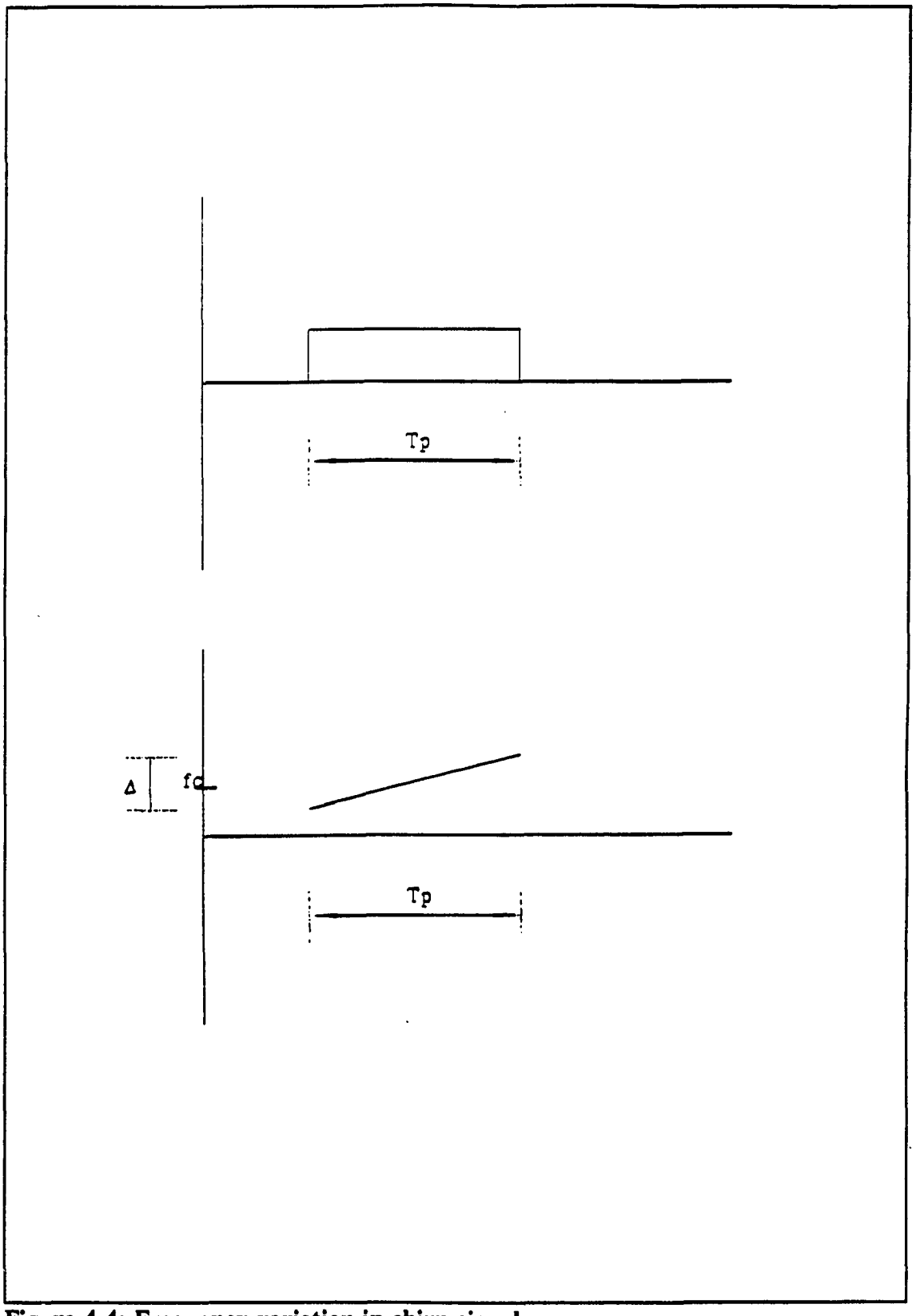

Figure 4.4: Frequency variation in chirp signal.

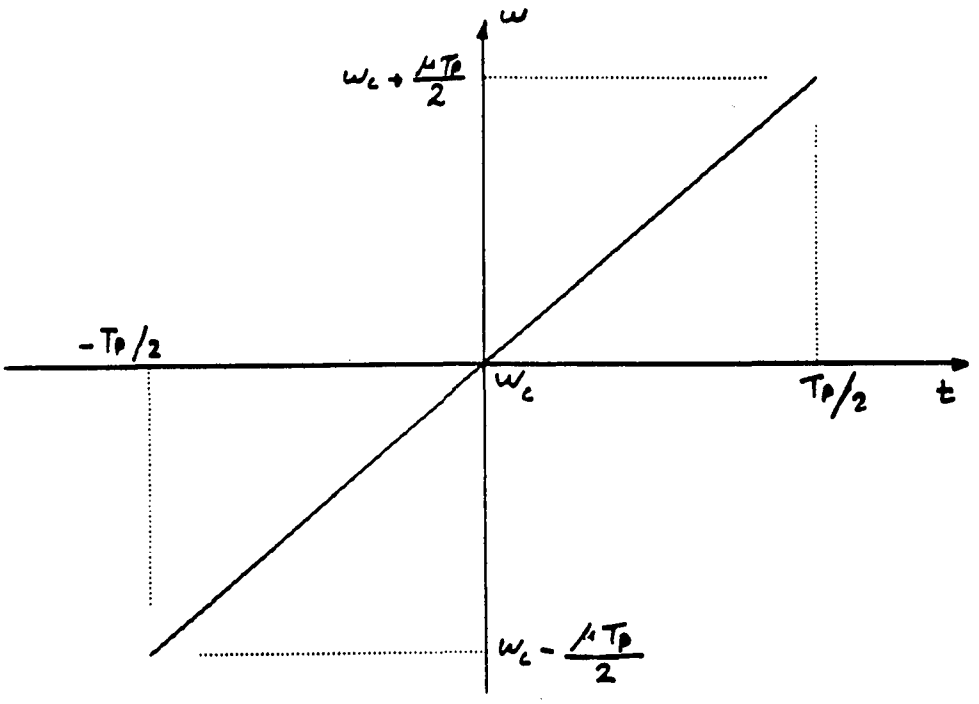

Figure 4.5: Net frequency sweep of a chirp signal.

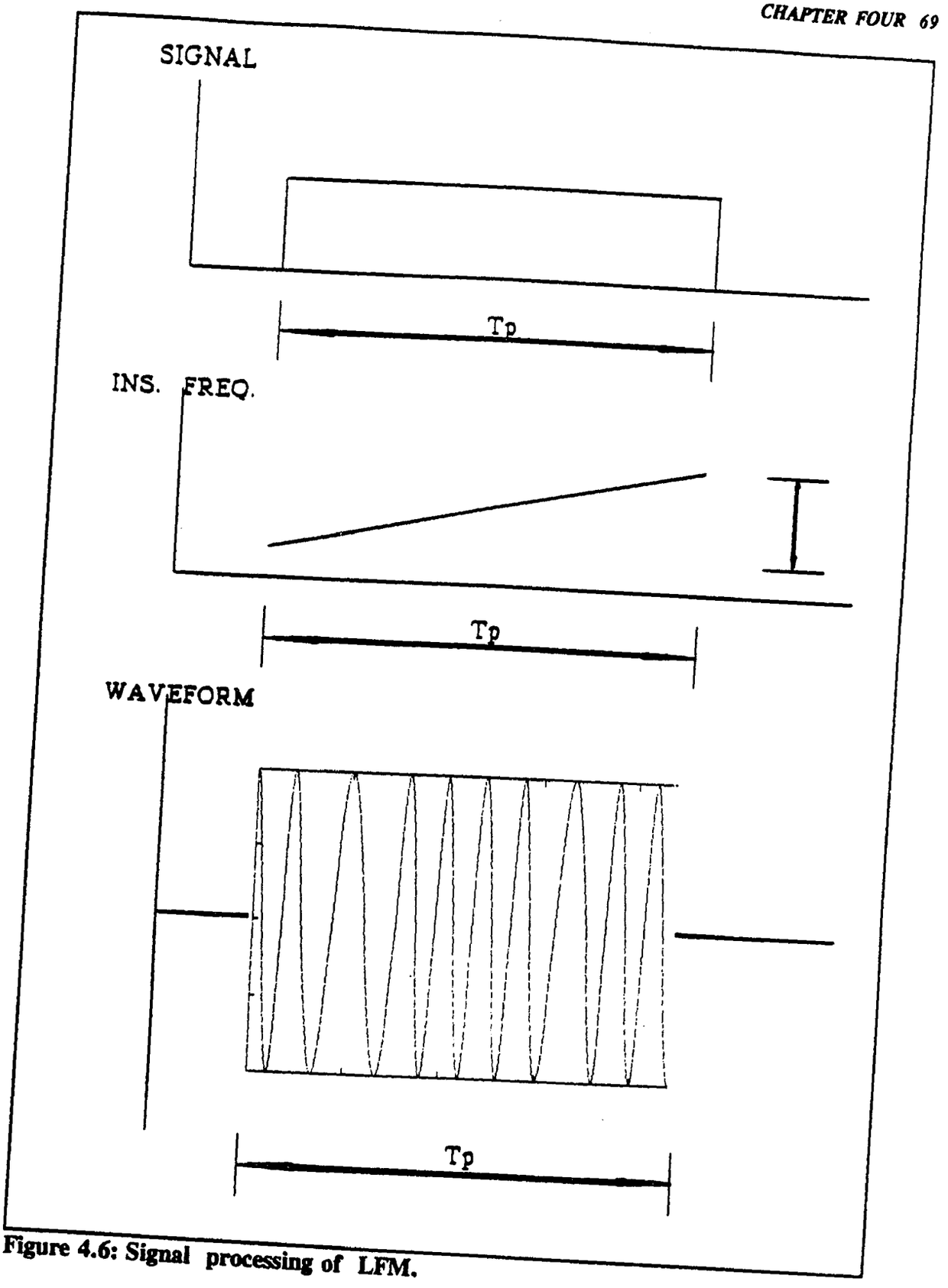

Figure 4.6: Signal processing of LFM.

4.3 SPECTRUM OF A CHIRP SIGNAL

Let A(ω) denote the Fourier transform of an arbitrary function of time, a(t). Thus,

$$A(\omega) = F\{a(t)\} \tag{4.13}$$

The transform of the signal s(t) becomes

$$\begin{aligned} F\{s(t)\} = S(\omega) &= \int_{-\frac{T_p}{2}}^{\frac{T_p}{2}} s(t)e^{-j\omega t}dt \\ &= \int_{-\frac{T_p}{2}}^{\frac{T_p}{2}} \cos(\omega_c t + \frac{1}{2}\mu t^2)e^{-j\omega t}dt \\ &= \frac{1}{2}\int_{-\frac{T_p}{2}}^{T-\frac{p}{2}} e^{j[(\omega_c - \omega) + \frac{1}{2}\mu t^2]}dt \\ &\quad + \frac{1}{2}\int_{-\frac{T_p}{2}}^{\frac{T_p}{2}} e^{-j[(\omega_c + \omega) + \frac{1}{2}\mu t^2]}dt \end{aligned} \tag{4.14}$$

By completing the square of the bracket term in S(ω) the following expression for the

spectrum is obtained:

$$S(\omega) = \frac{1}{2} e^{-j\left(\frac{(\omega - \omega_c)^2}{2\mu}\right)} \int_{-\frac{T_p}{2}}^{\frac{T_p}{2}} e^{\frac{j\mu}{2}\left(t - \frac{\omega - \omega_c}{\mu}\right)^2} dt \tag{4.15}$$

After a series of algebraic manipulation the spectrum becomes

$$S(\omega) = \frac{1}{2}\sqrt{\frac{\pi}{\mu}} e^{-j\left(\frac{(\omega - \omega_c)^2}{2\mu}\right)} \int_{-x_1}^{x_2} e^{j\frac{\pi x^2}{2}} dx \tag{4.16}$$

where

$$x_1 = \frac{\frac{\mu T_p}{2} + (\omega - \omega_c)}{\sqrt{\pi\mu}} \tag{4.17}$$

$$x_2 = \frac{\frac{\mu T_p}{2} - (\omega - \omega_c)}{\sqrt{\pi\mu}} \tag{4.18}$$

This yields

$$S(\omega) = \frac{1}{2}\sqrt{\frac{\pi}{\mu}} e^{-j\left(\frac{(\omega - \omega_c)^2}{2\mu}\right)} \left[S(x_1) + jS(x_1) + C(x_2) + jC(X_2) \right] \tag{4.19}$$

where

$$C(x) = \int_0^x \cos\left(\frac{\pi \alpha^2}{2}\right) d\alpha \tag{4.20}$$

and

$$S(x) = \int_0^x \sin\left(\frac{\pi \alpha^2}{2}\right) d\alpha \tag{4.21}$$

are called the Fresnel integral, which have the property

$$C(-x) = -C(x) \qquad \textit{and} \qquad S(-x) = -S(x) \tag{4.22}$$

The Fresnel integral can not be calculated in closed form. However, it can be found in tabulated form in Tables of Fresnel integral. These two integral are shown in Figure 4.7.

Expressing the spectrum function in the form

$$S(\omega) = e^{-\alpha_s - j\beta_s} \tag{4.23}$$

then the three major components of Linear FM spectrum are given as follows:

1. **Amplitude Term**

$$\begin{aligned} e^{-\alpha_s} &= |S(\omega)| \\ &= \frac{1}{2}\sqrt{\frac{\pi}{\mu}}\sqrt{[C(x_1) + C(x_2)]^2 + [S(x_1) + S(x_2)]^2} \end{aligned} \tag{4.24}$$

2. Square-Law Phase Term

$$\phi_1(\omega) = \frac{(\omega - \omega_c)^2}{2\mu} \tag{4.25}$$

3. Residual Phase Term

$$\phi_2(\omega) = -\tan^{-1}\left[\frac{S(x_1) + S(x_2)}{C(x_1) + C(x_2)}\right] \tag{4.26}$$

Thus, the spectrum phase function is

$$\beta_s = \phi_1 + \phi_2 \tag{2.27}$$

and the time-bandwidth product (TBW) is

$$\begin{aligned} TBW = T \times BW &= \frac{T\Delta}{2\pi} \\ &= \frac{\mu T^2}{2\pi} = \frac{\mu T_p^2}{2\pi} \end{aligned} \tag{4.28}$$

For large values of TBW the ratio

$$\frac{S(x_1) + S(x_2)}{C(x_1) + C(x_2)} \triangleq 1 \tag{4.29}$$

over the significant interval of the variables, and ϕ_2 approximates a constant phase angle, $\pi/4$, in this ratio. The linear FM spectra are, functionally, dependent only on the TBW factor and not on the absolute bandwidth parameters. Figure 4.8 through. 4.11 illustrates various spectrum of the linear FM signal for different TBW products. It can be seen that

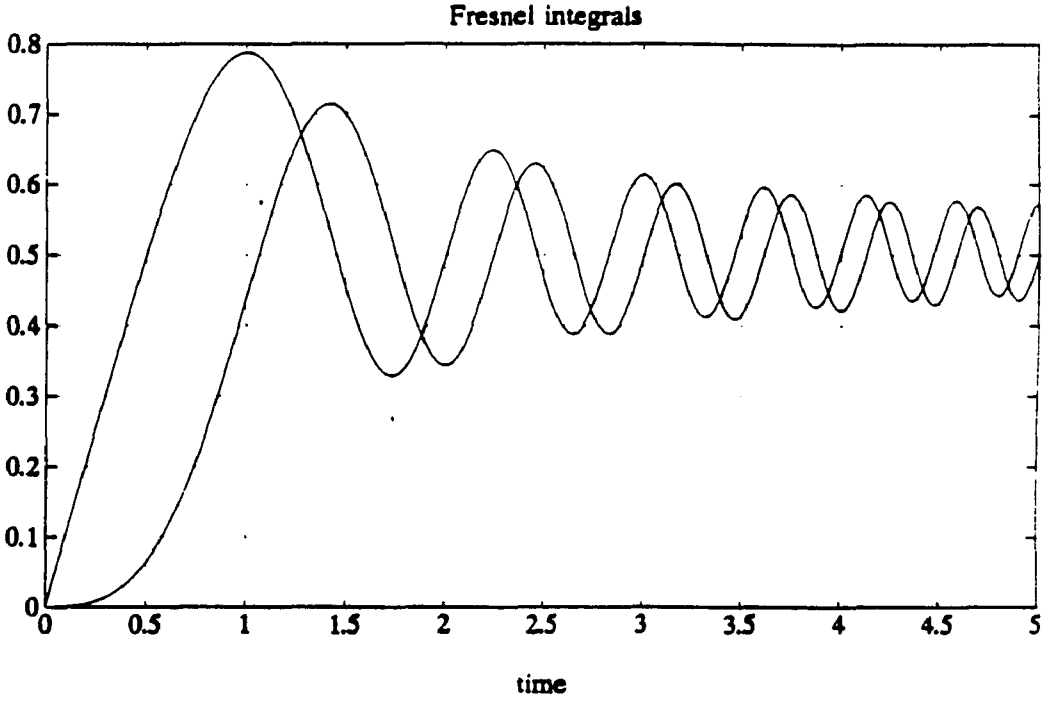

Figure 4.7: Two fresnel integral.

as the TBW is increased, the spectrum shape becomes more nearly rectangular, with a total Bandwidth approaching Δ. Therefore for large value of TBW the envelope function approximated a rectangular time envelope, and the residual modulation term approximates a constant phase angle, $\pi/4$. About 95% of the spectra energy is contained in the band Δ for TBW's as low as 10; and 98% to 99% of the energy is confined between $f_c - \Delta/2$ and $f_c + \Delta/2$ for TBW=100.

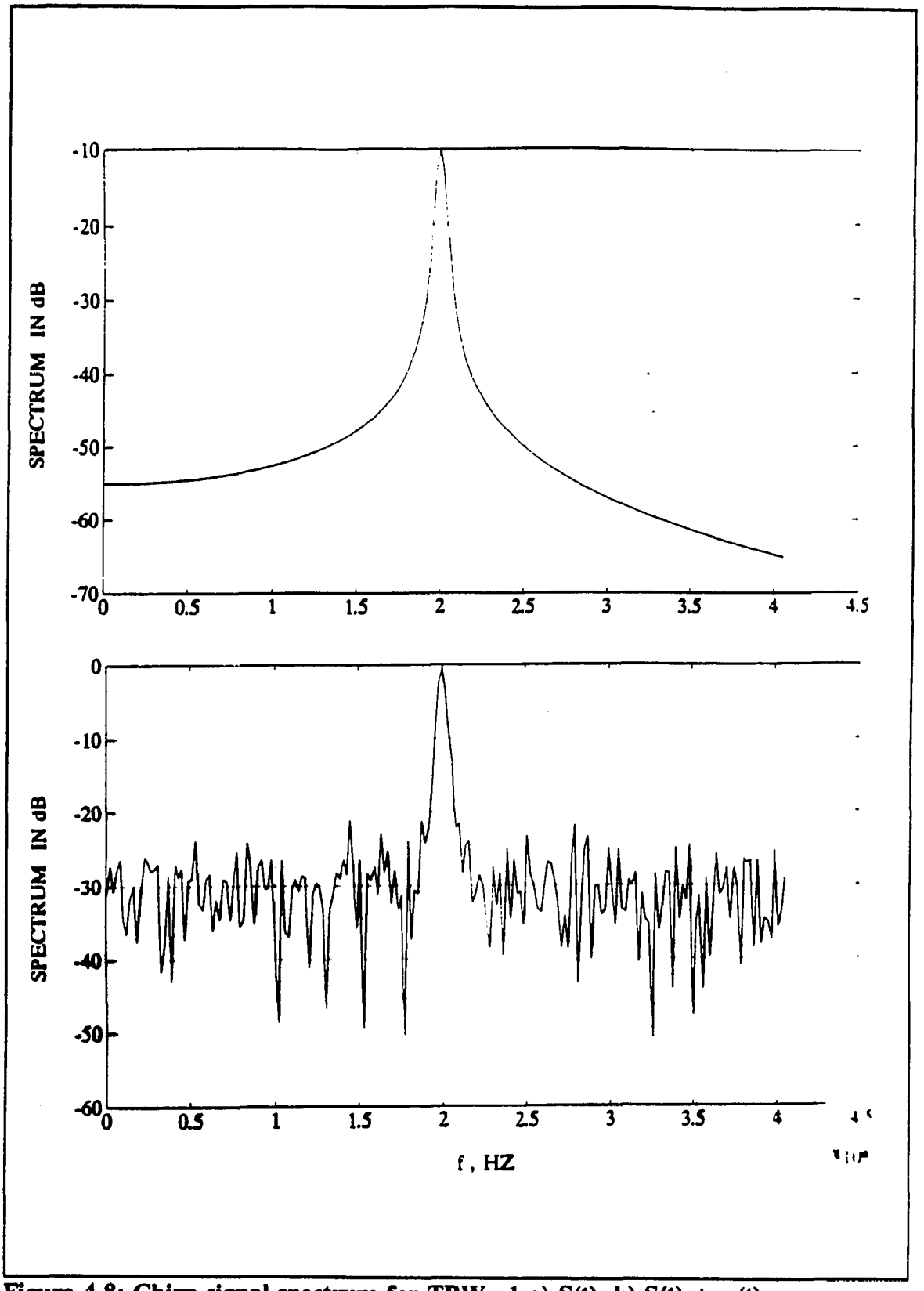

Figure 4.8: Chirp signal spectrum for TBW=1 a) S(t) b) S(t) + n(t).

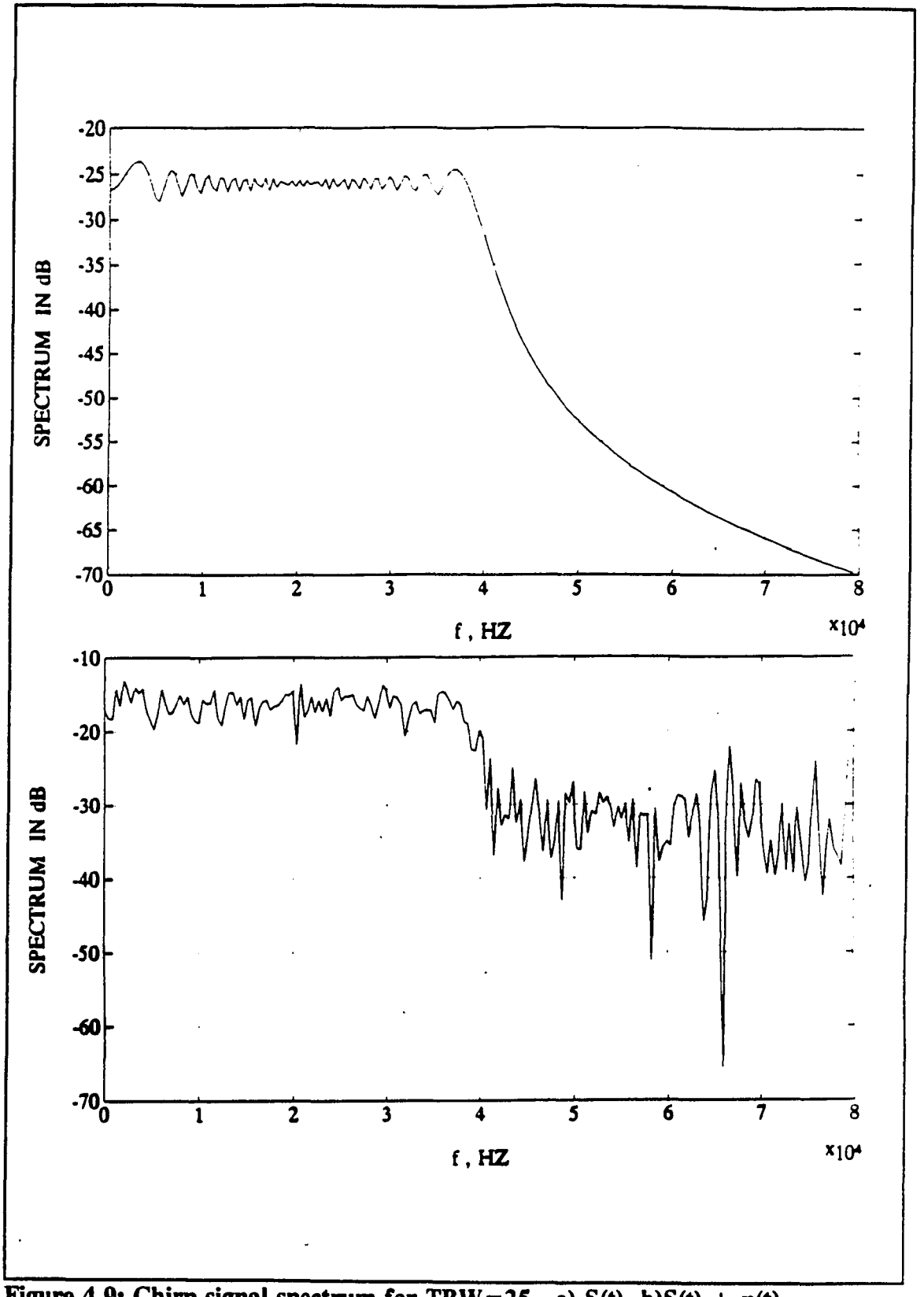

Figure 4.9: Chirp signal spectrum for TBW=25. a) S(t) b)S(t) + n(t).

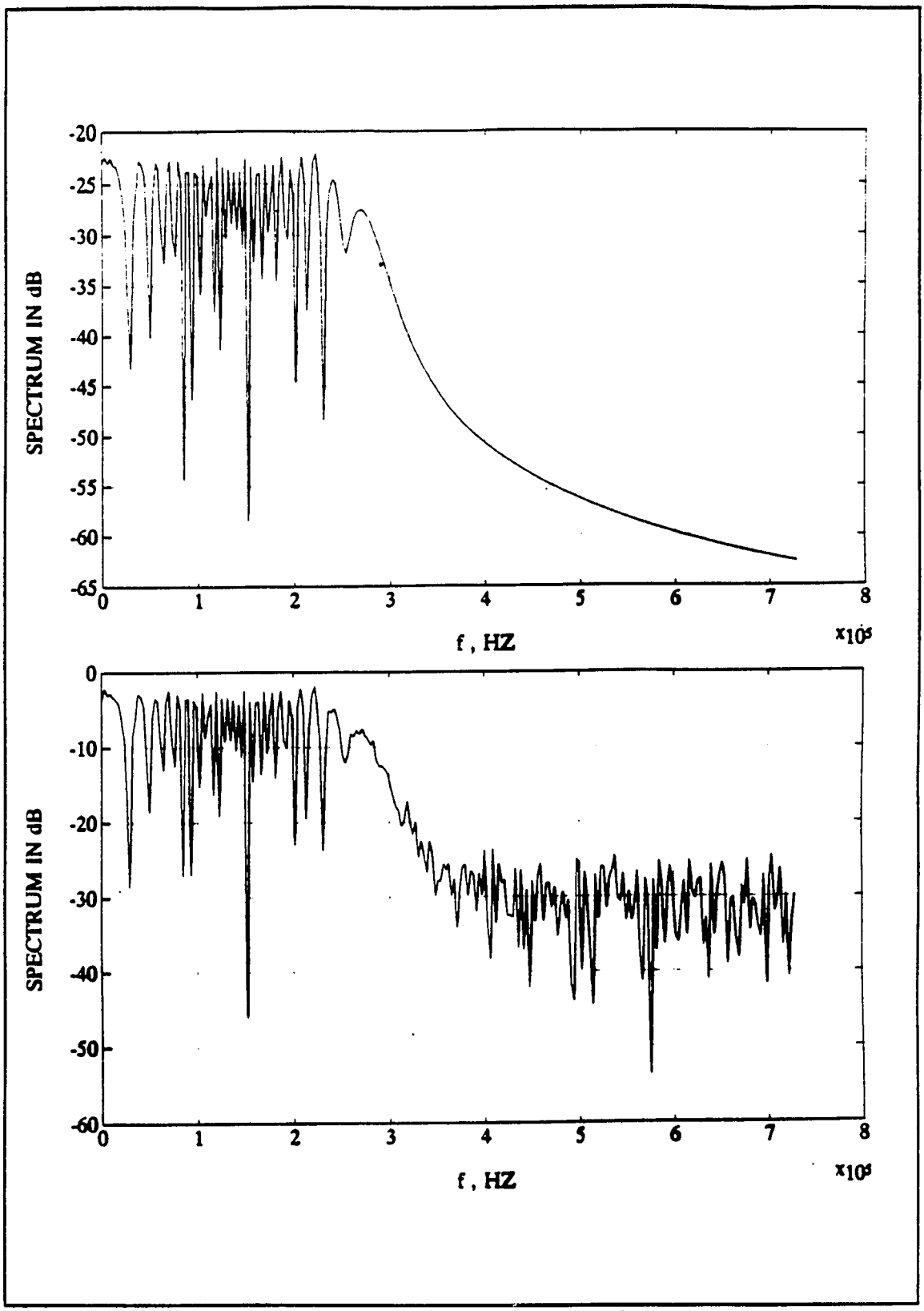

Figure 4.10: Chirp signal spectrum for TBW=46. a) S(t) b) S(t) + n(t).

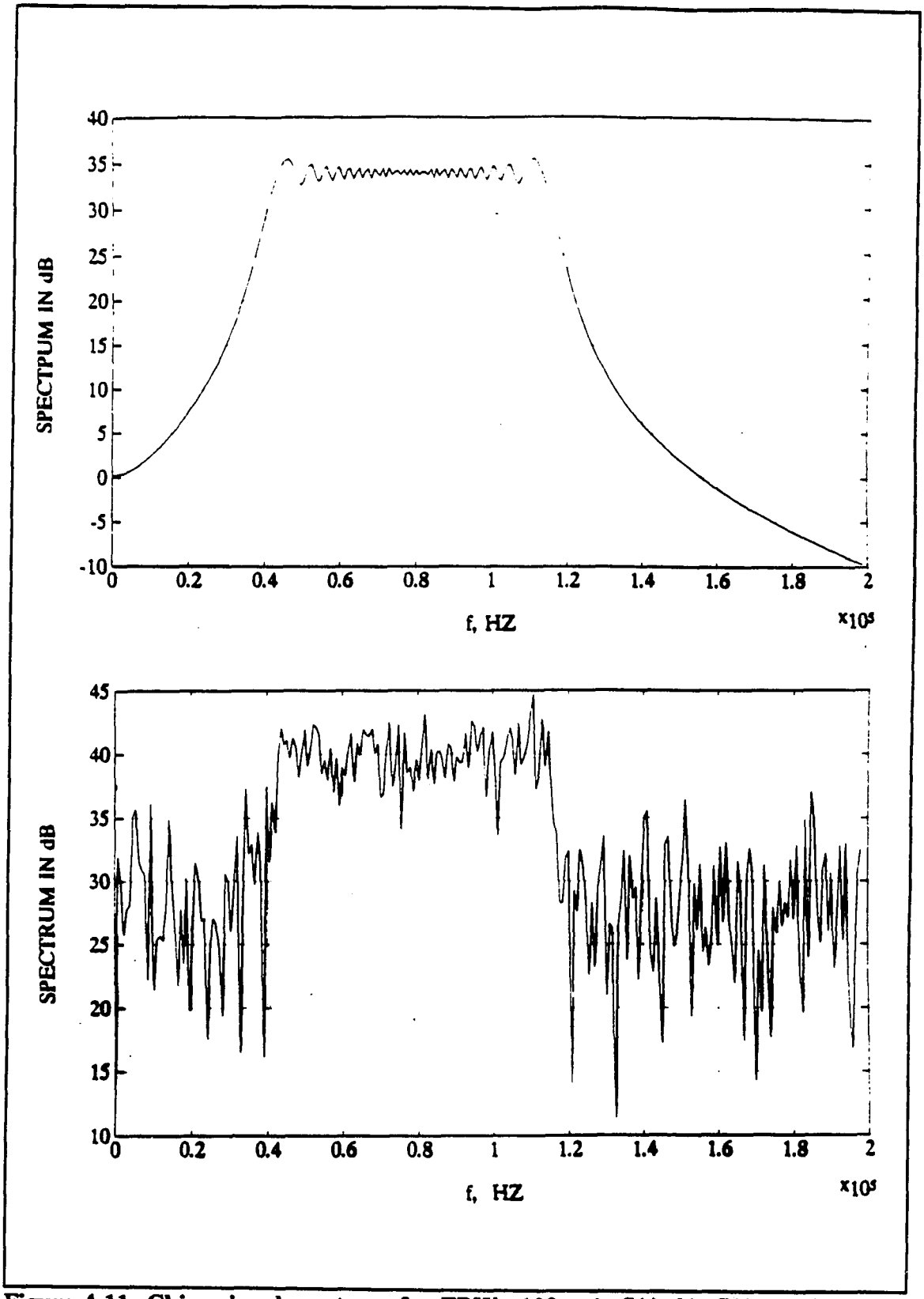

Figure 4.11: Chirp signal spectrum for TBW=100. a) S(t) b) S(t) + n(t).

4.4 Matched Filter for Chirp

The characteristic of matched filters can be described by either frequency or time response function, where the frequency response function and time response function are related to each other by a Fourier transform operation. The transfer function, $H(\omega)$, of a matched filter in frequency domain is

$$H(\omega) = A\ F^*(\omega)e^{-j\omega t_d} \tag{4.30}$$

where $F^*(\omega)$ is the complex conjugate function of the spectrum f(t), t_d is an arbitrary delay constant of the filter, and A is the normalizing factor. The corresponding time domain characteristics of matched filter is obtained from the inverse Fourier transform of $H(\omega)$. Thus,

$$h(t) = a\ f(t_d - t) \tag{4.31}$$

Generally the delay constant, t_d, and the normalizing factor, a, are ignored. Therefore, the characteristics function of matched filter in frequency domain and time domain can be written respectively as follows:

$$H(\omega) = F^*(\omega) \tag{4.32}$$

$$h(t) = h(-t) \tag{4.33}$$

Hence, matched filtering is equivalent to correlation processing. The matched filter

impulse response for the signal, s(t),

$$s(t) = \begin{cases} \cos(\omega_c t + \frac{1}{2}\mu t^2) & -\frac{T_p}{2} \le t \le \frac{T_p}{2} \\ 0 & -\frac{T_p}{2} \le t \le \frac{T_p}{2} \end{cases} \tag{4.34}$$

is a time inversion of s(t) given by

$$h(t) = \sqrt{\frac{2\mu}{\pi}}\cos(\omega_c t - \frac{1}{2}\mu t^2) \quad for \quad -\frac{T_p}{2} \le t \le \frac{T_p}{2} \tag{4.35}$$

where $\sqrt{2\mu/\pi}$ is the factor that gives the filter unity gain. The output of the matched filter, $g(\tau)$, is

$$g(t) = \int_{-\infty}^{\infty} f(t)\, h(\tau - t)\, dt \tag{4.36}$$

When f(t) and h(t) are matched, $g(\tau)$ represents the autocorrelation function of the input signal and when these are not matched $g(\tau)$ represents the cross-correlation of the two function. For the linear FM (received signal is mismatched to the filter) function, the Doppler-shifted signal is

$$s(t) = \cos\left((\omega_c - \omega_d)t + \frac{\mu t^2}{2}\right) \quad for \quad -\frac{T_p}{2} \le t \le \frac{T_p}{2} \tag{4.37}$$

From EQ. (4.37) it has been shown that the general output of a Linear FM matched filter

is

$$g(\tau,\omega_d) = \int_a^b s(t)\, s(\tau - t)\, dt \tag{4.38}$$

where

$$a = \begin{cases} \tau - \dfrac{T_p}{2} & \text{for} \quad \tau > 0 \\ -\dfrac{T_p}{2} & \text{for} \quad \tau < 0 \end{cases} \tag{4.39}$$

and

$$b = \begin{cases} \dfrac{T_p}{2} & \text{for} \quad \tau > 0 \\ \tau + \dfrac{T_p}{2} & \text{for} \quad \tau < 0 \end{cases} \tag{4.40}$$

Therefore, the output of the Linear FM matched filter is obtained by

$$g(\tau,\omega_d) = \sqrt{\frac{2\mu}{\pi}} \int_a^b \cos\left[(\omega_c + \omega_d)t + \frac{1}{2}\mu t^2\right] \times \cos\left[(\omega_c(\tau - t) - \frac{\mu}{2}(\tau - t)^2\right] dt \tag{4.41}$$

After a series of trigonometric manipulation, and dropping the higher frequency terms,

the matched filter output is

$$g(\tau\ ,\ \omega_d) = \frac{1}{2}\sqrt{\frac{2\mu}{\pi}}\int_a^b \cos\left[(\omega_c - \frac{1}{2}\mu\tau)\tau + (\omega_d + \mu\tau)t\right] dt$$
$$= \frac{1}{2}\sqrt{\frac{2\mu}{\pi}}\left[\frac{\sin\left((\omega_c - \frac{1}{2}\mu\tau)\tau + (\omega_d + \mu\tau)t\right)}{\omega_d + \mu\tau}\right]_{t=a}^{t=b} \qquad (4.42)$$

For $\tau>0$ and $\tau<0$ the output of the matched filter, $g(\tau,\omega)$, respectively are as follows

$$g(\tau\ ,\ \omega_d) = \frac{1}{2}\sqrt{\frac{2\mu}{\pi}}\frac{\sin(\omega_c\tau + \frac{\omega_d T_p}{2} + \frac{\mu\tau}{2}(T_p - \tau))}{\omega_d + \mu\tau}$$
$$- \frac{\sin(\omega_c\tau + \omega_d\tau - \frac{\omega_d T}{2} - \frac{\mu\tau}{2}(T - \tau)}{\omega_d + \mu\tau}$$
$$= \frac{1}{2}\sqrt{\frac{2\mu}{\pi}}\frac{\sin\left((\omega_c + \omega_d)\tau + \frac{\omega_d T_p}{2} + \frac{\mu\tau}{2}(T_p + \tau)\right)}{\omega_d + \mu\tau} \qquad (4.43)$$
$$- \frac{\sin(\omega_c\tau - \frac{\omega_d T_p}{2} - \frac{\mu\tau}{2}(T_p + \tau))}{\omega_d + \mu\tau}$$

Thus, the final expression for the matched-filter output is[2]

$$g(\tau,\omega_d) = \sqrt{\frac{2\mu}{\pi}} \frac{\sin\left(\frac{\omega_d + \mu\tau}{2}(T_p - |\tau|)\right)}{\frac{\omega_d + \mu\tau}{2}} \cos\left(\omega_c + \frac{\omega_d}{2}\right)\tau \tag{4.44}$$

For the case $\omega_d=0$ (autocorrelation), the output of matched filter is

$$g(\tau) = \sqrt{\frac{2\mu T_p^2}{4\pi}} \frac{\sin\left(\frac{\mu\tau}{2}(T_p - |\tau|)\right)}{\frac{\mu\tau T_p}{2}} \cos(\omega_c\tau) \tag{4.45}$$

Thus, for $\tau << T_p$ the autocorrelation function, $g(\tau)$, can be approximated by

$$g(\tau) \approx \sqrt{\frac{\mu T_p^2}{2\pi}} \frac{\sin\left(\frac{\mu\tau T_p}{2}\right)}{\frac{\mu\tau T_p}{2}} \tag{4.46}$$

$$= sinc\left(\frac{\mu\tau T_p}{2}\right) \qquad |\tau| \le T_p$$

Figure 4.12 shows the linear FM auto-correlation waveforms for different time bandwidth product.

The typical envelope of the output power pulse, $\psi^2(t)$, is shown in Figure 4.13, along with corresponding input pulse s(t). ($\psi(t)$ is the resulting output from passing s(t)

---

[2]Cook, C. E., "General Matched-Filter Analysis of Linear FM Pulse Compression" IRE Tran. Mil. Elec., Vol. Mil. - 5, No. 2 April 1961 pp 109-116.

through h(t)). Thus,

$$\psi(t) = \sqrt{\frac{\mu T_p}{2\pi}} \frac{\sin\left(\frac{\mu T_p t}{2}\right)}{\frac{\mu T_p t}{2}} Re\left[e^{j(\omega_c t + \frac{1}{2}\mu t^2 + \frac{\pi}{4})}\right] \tag{4.47}$$

An important feature of linear FM is its relative insensitivity to degradation in response to Doppler-shifted signals.

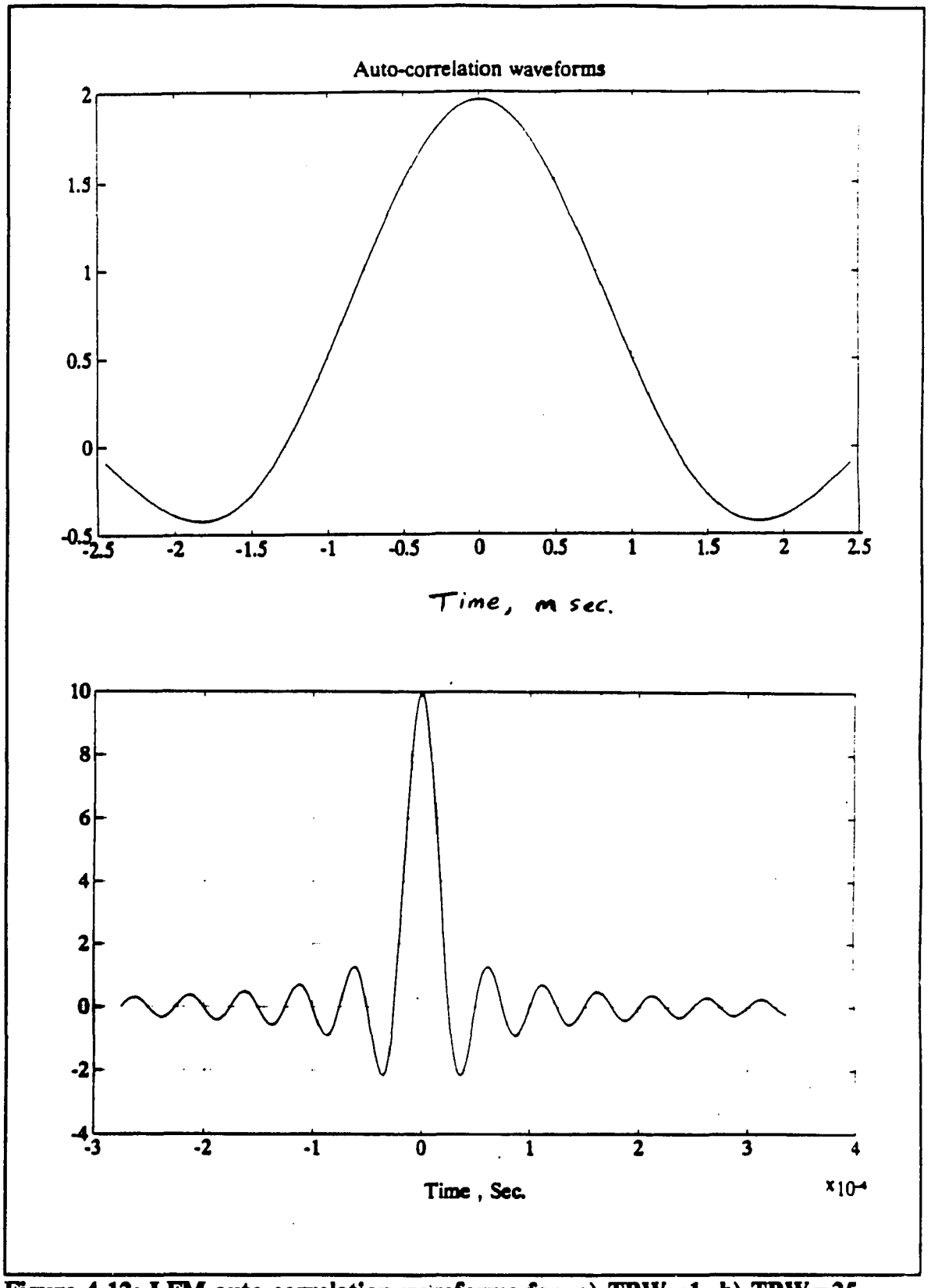

Figure 4.12: LFM auto-correlation waveforms for a) TBW=1 b) TBW=25.

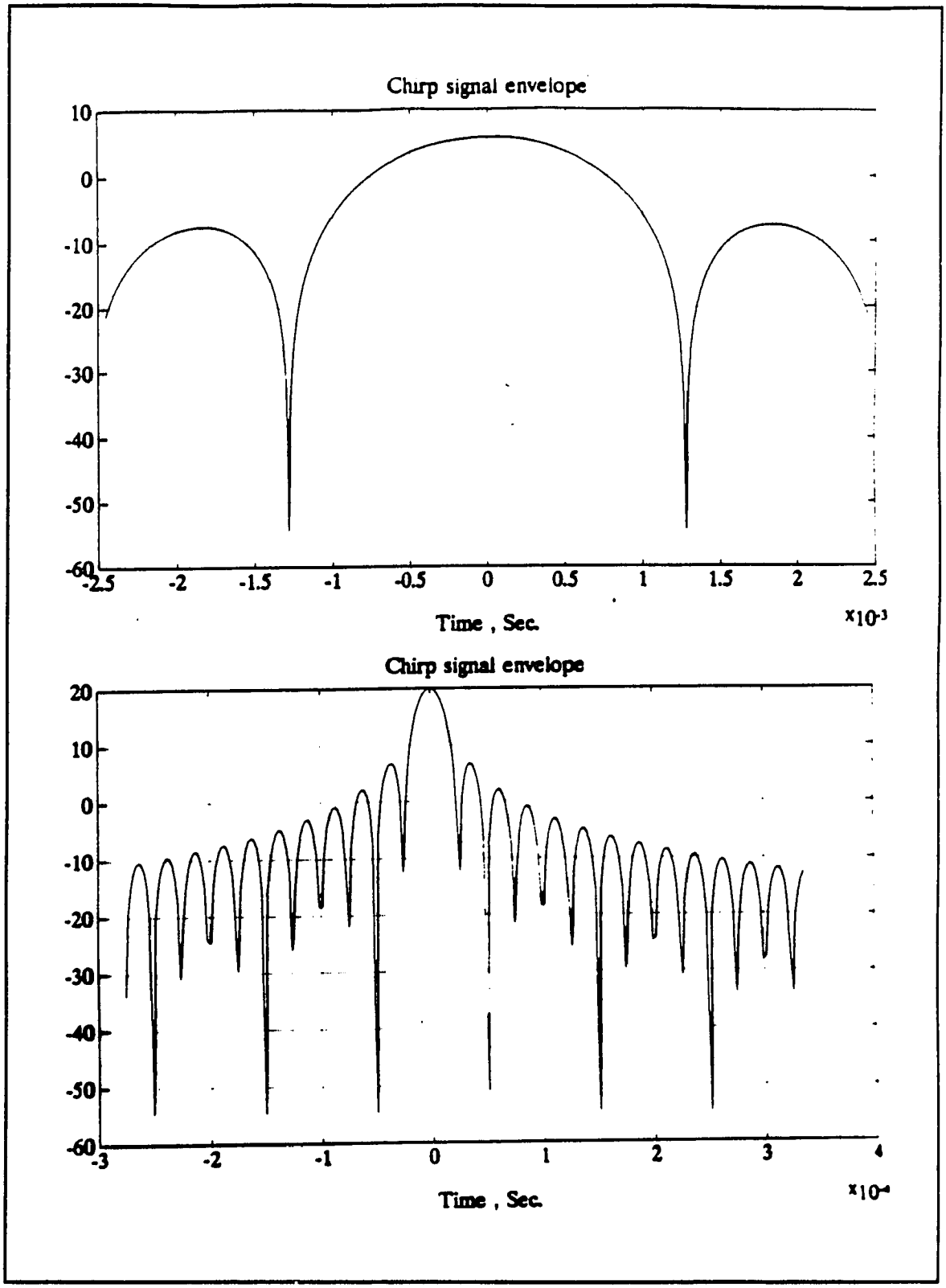

Figure 4.13: Typical envelop of the output power pulse for a) TBW=1 b) TBW= 25

CHAPTER FIVE

A NEW APPROACH

5.0 INTRODUCTION

Our specific objective is to achieve an overall system design and a detailed block diagram design of the robot tracking and three dimensional direction finding system. In this chapter we describe a new signal processing technique for a Space Station robotic tracking system. The particular application of interest is that of estimating the locations of extra-vehicular robots as they operate external to the Space Station. The proposed system contains block level design and study of a communication system for a space station involving spread spectrum and digital processing of signal techniques. The system utilizes a chirp signal matched filter technique to discriminate against multipath and other undesired signals. In addition, utilizes FFT hardware chips to implement cross correlation and detection procedures in order to provide additional discrimination against

multipath as well as redundant signals.

The system under consideration must be able to identify each robot and estimate the location of individual robots in a few fraction of a second. In order to determine the position of the robot, one technique is to transmit a very narrow, ideally an impulse, and measure the propagation delay (provided that there is direct line of sight) of its reflection from the robot. However, impulses are not practical signals. One signal that can be used to discriminate against small delays is a spread spectrum signal such as Chirp signal. Utilization of a chirp signal, S(t),

$$S(t) = A\cos(\omega_c t + \frac{1}{2}\mu t^2 + \phi) \qquad (5.1)$$

allows for individual robot identification and discriminates against multipath signals as a limiting factor to location accuracy. This signal is sinusoidal waveform whose frequency varies linearly with time and easily provides a large time bandwidth products.

5.1 APPROACH

The approach taken is to estimate the distance between the individual robot moving outside the Space Station and at least three receiving antennae placed at different locations on the space station as shown in Figure 5.1.

To obtain the three distances (D_1, D_2, D_3), we measure the propagation delay between the transmitting antennae to the robot and back to the receiving antennae located on the Space Station. Therefore, the distances from antennae A_1, A_2, and A_3 to the robot can

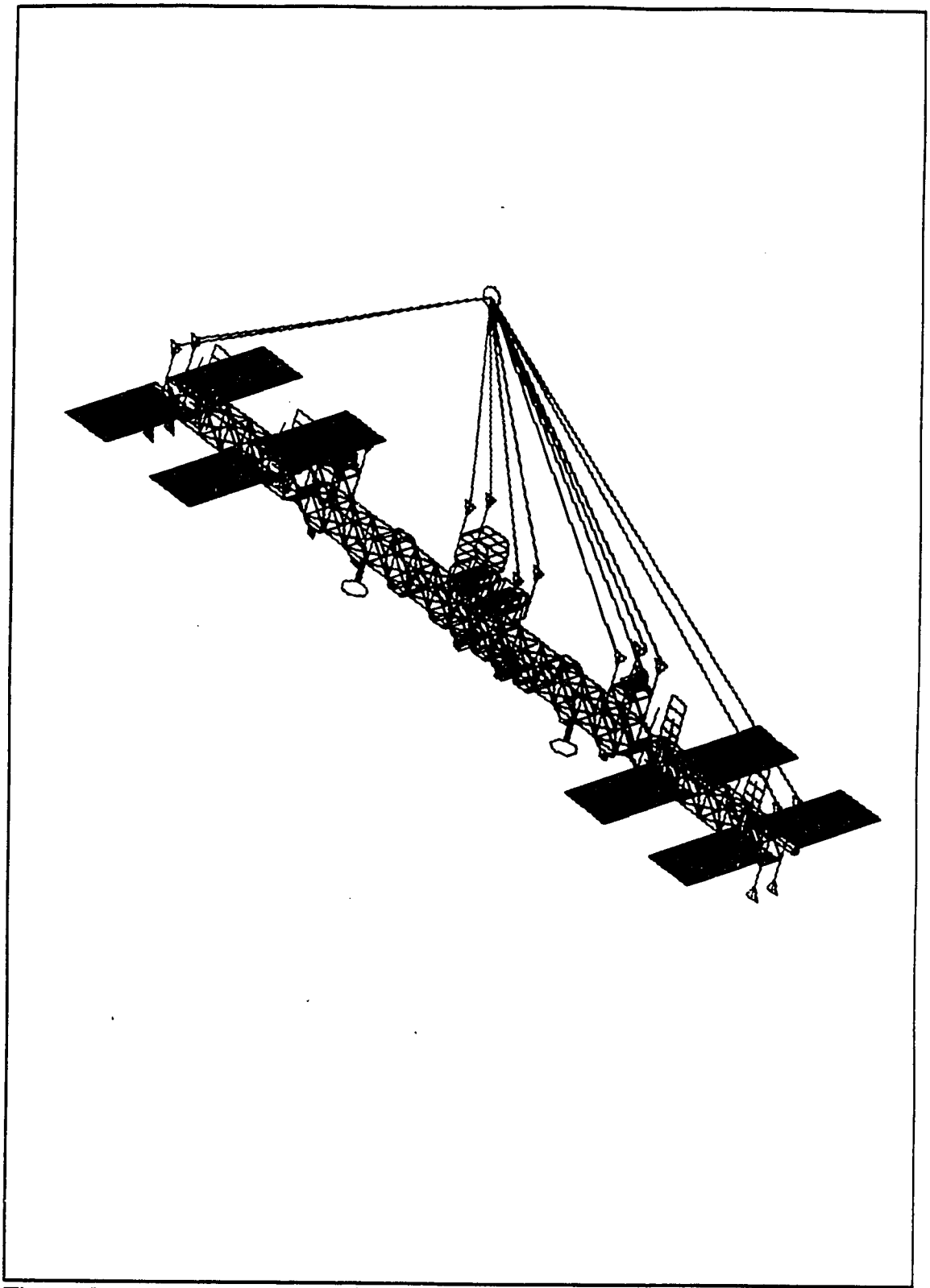

Figure 5.1: Received plane wave arriving from robot to receiving antennae placed at Space Station .

be determined. Thus,

$$D_i = \frac{1}{2}\tau_i C \qquad i = 1 , 2 , 3 \qquad (5.2)$$

where τ_i is the signal travel time and C is the speed of light (C=2.997 x 10^{10} cm/s). The factor 1/2 is the result of the round trip travel time. Given the distances D_i the robot is then located on the surface of a sphere centered at A_i and having a radius r_i. Thus,

$$r_i = D_i \qquad i = 1,2,3,\cdots,M \qquad (5.3)$$

where M is the number of receiving antennae. Therefore, the location of robots can be denoted by a point in space along a predefined coordinate system (x,y,z) as shown in Figure 5.2.

The location of the robot with respect to coordinate system (x,y,z) can be found by determining the common intersection of the three spheres of radius r_1, r_2, and r_3 centered on antennae A_1, A_2, A_3 respectively. In Figure 5.3, the surfaces for three spheres for a three receiving antennae system is shown.

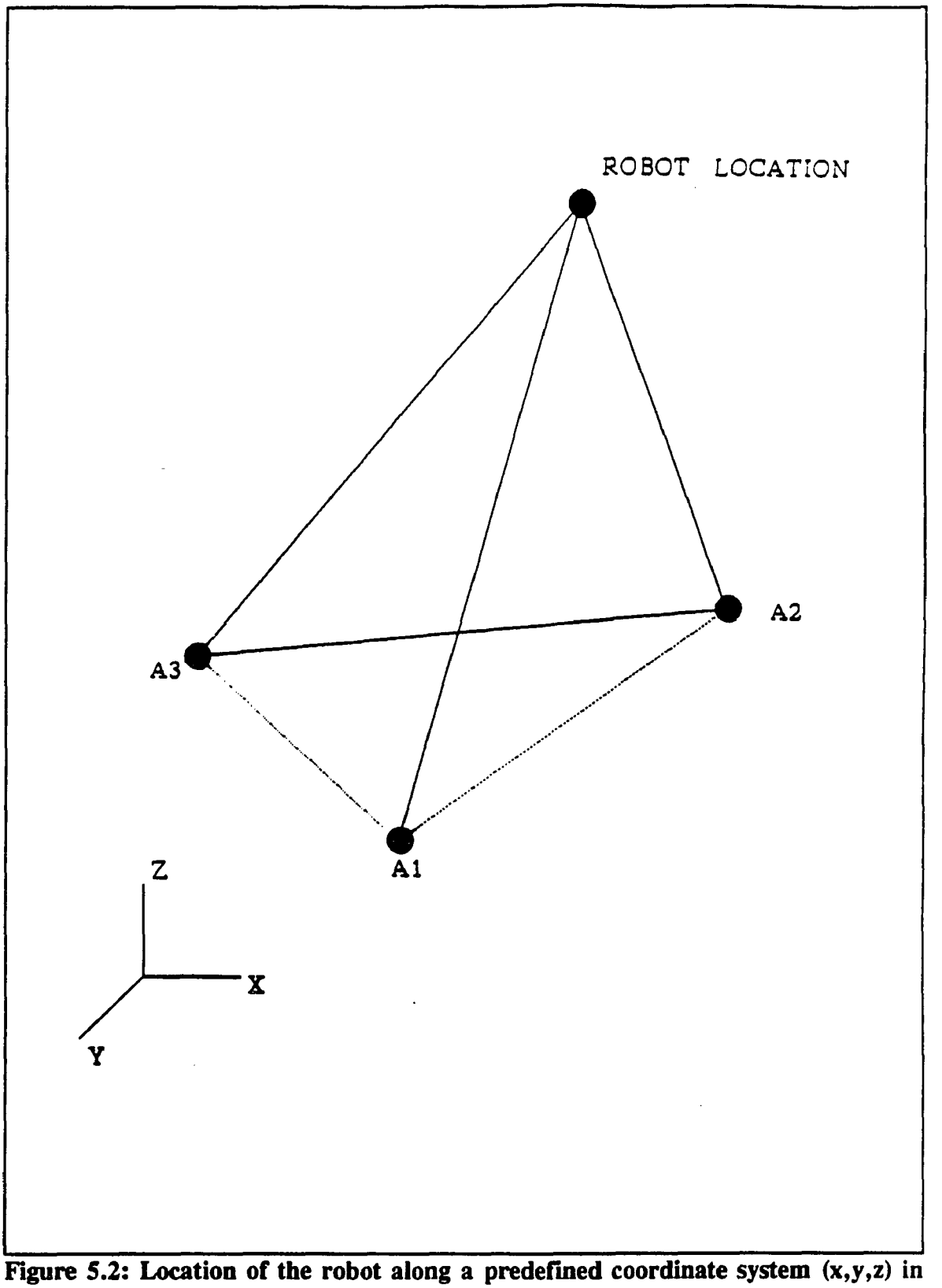

Figure 5.2: Location of the robot along a predefined coordinate system (x,y,z) in space.

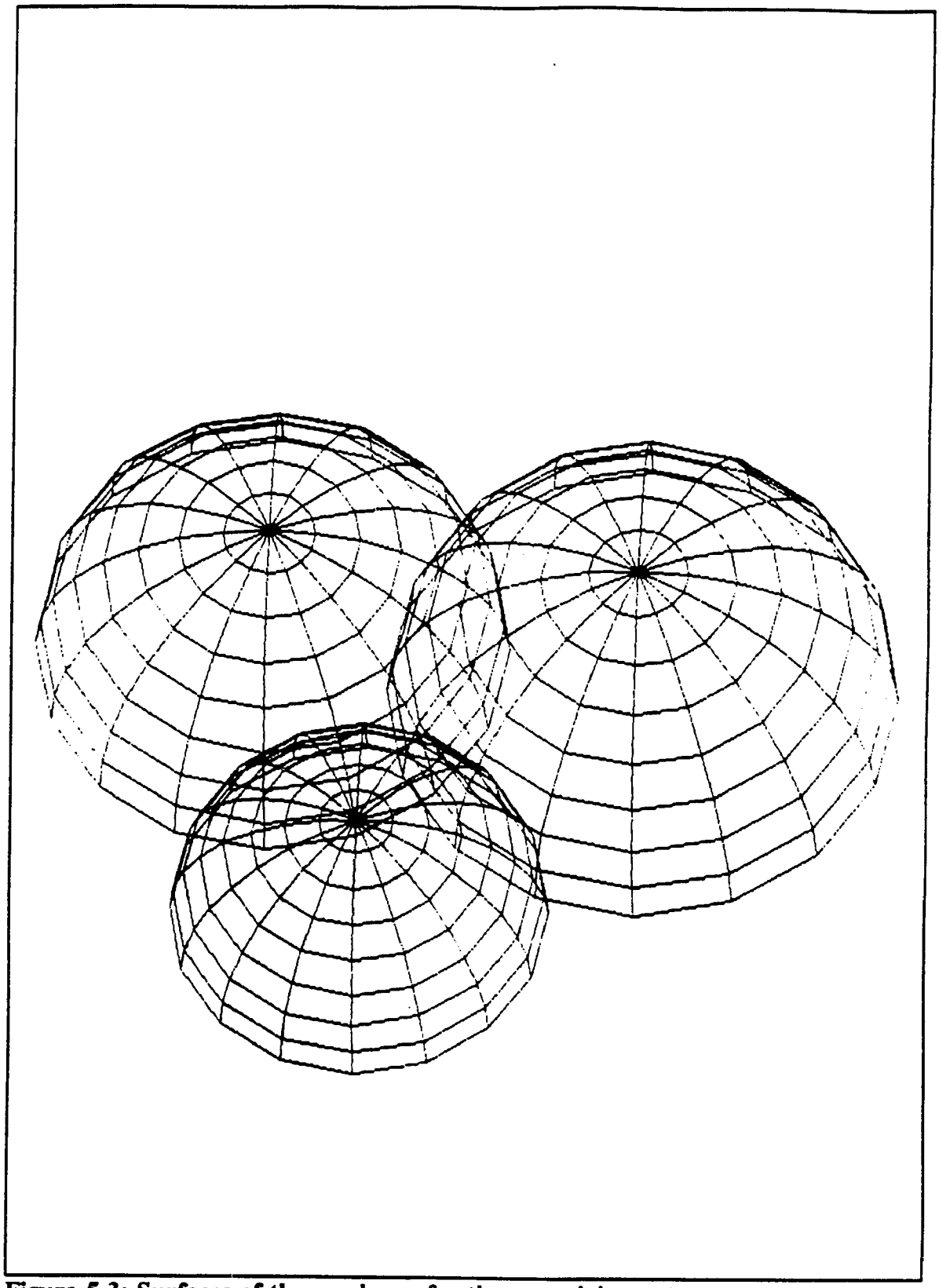

Figure 5.3: Surfaces of three spheres for three receiving antennae.

5.2 SYSTEM STRUCTURE

The process of finding the location of an extra vehicular robot in space station environment involves a transmitter with a transmitting antenna and a receiver with at least three receiving antennae. The receiving and transmitting antennae are located at various locations on the space station and the processing unit which include a transmitter and number of receiver is located inside the Space Station's central room. In addition, each robot is carrying a small repeater which is connected to one receiving and one transmitting antennae. The function of the repeater is response to any signal transmitted from a transmitting antenna on the Space Station.

The function of the overall system can be describe as follows:

1. The controller will choose a search region outside the space station.

2. Each robot is assumed to have an address. In another word each robot is assigned a certain tone frequency. This tone frequency is selected by assigning different value to μ of the transmitting chirp signal. All the robots are normally in a listening mode waiting to receive it's particular tone. Each, upon receiving its tone, robot will respond to it's tone for a limited time interval and then goes back to listening mode.

3. If the robot response is positive to the addressing tone then a chirp signal will

be transmitted via a transmitting antenna located inside the search region.

4. After the robot receive the initial transmitting signal it will retransmit the same signal to the receiving antennae located inside the search region.

5. The received chirps will be correlated with the chirp signal initially transmitted.

6. The result of the correlations process will then be used to determine the location of specific robot.

5.2.1 TRANSMITTING AND RECEIVING UNIT

The transmitter under consideration for our system consists of a linear frequency modulation signal generator, a tone generator, and a transmitting filter. The block diagram of such transmitter is show in Figure 5.4.

The tone generator will generate the address of any robot and is connected to the transmitting filter during the addressing period. The LFM generator will generate the chirp signal for the location finding process and is connected to the transmitting filter during the location finding period. The output of the transmitting filter is connected to one of the transmitting antennae via a multiplexer as shown in Figure 5.5.

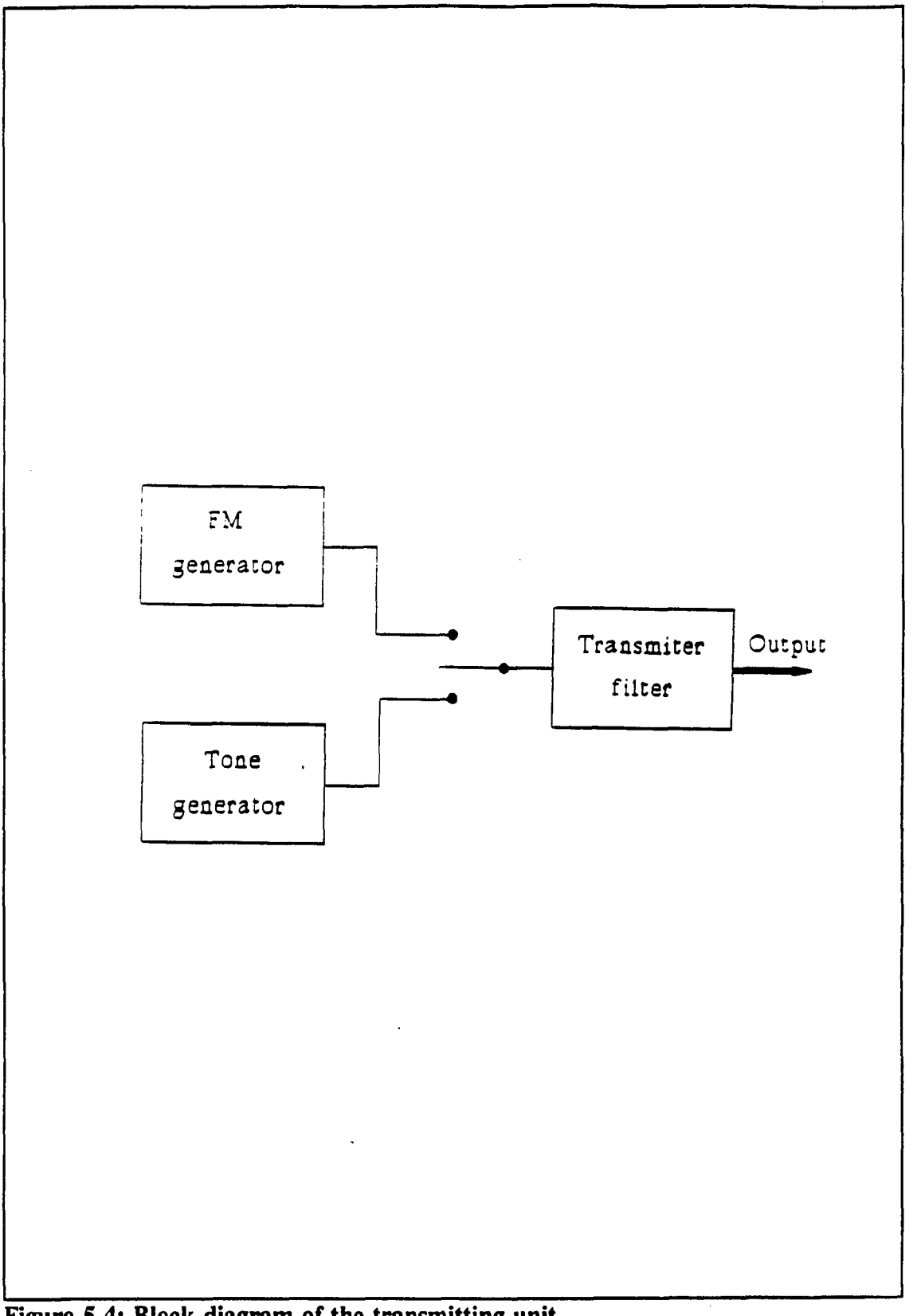

Figure 5.4: Block diagram of the transmitting unit.

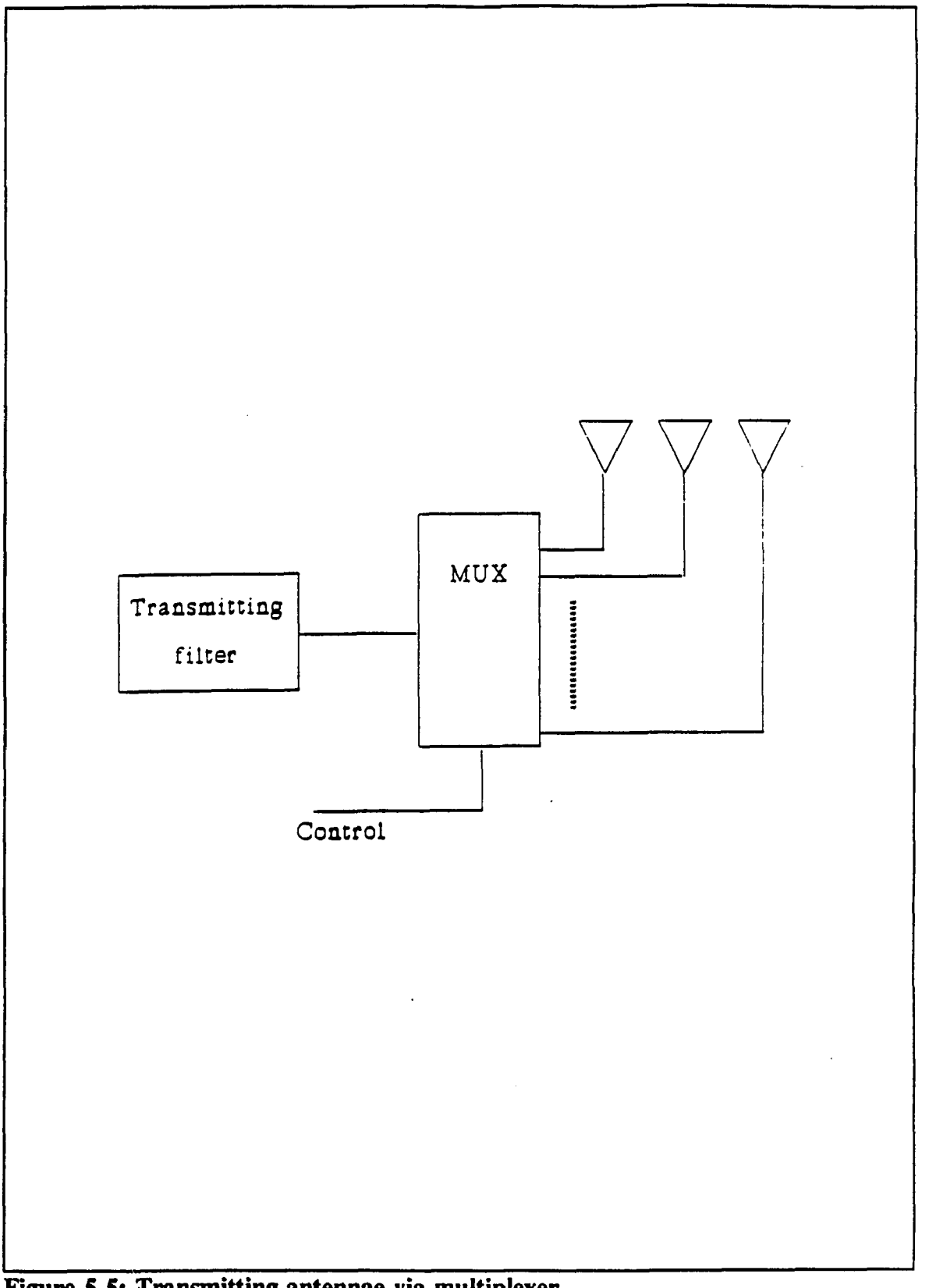

Figure 5.5: Transmitting antennae via multiplexer.

The receiving unit block diagram is shown in Figure 5.6. It consists of a group of receiving antennae which are connected to a demultiplexer. At least three of the receiving antennae are connected to the receiving filters via the demultiplexer. Each of the receiving filters' output is now connected to an identical set of subsystems as shown in Figure 5.7. These subsystems consist of a tone detector, power measurement circuit and a controller. The tone detector determines if the robot is present or not.

The total power measurement circuit will provide the controller with information about the background noise. If the addressed robot responds to a tone transmitted (tone is determined as present by the controller), then the signal is routed to the dechirping circuit which perform the correlation process. If the tone is determined as not present, then the controller will disregard the received signal.

The power measurement circuit is an energy detector which consists of a receiving filter, followed by a squarer and an integrator. The block diagram of such a circuit is shown in Figure 5.8.

The tone detector circuit is also an energy detector identical to the total power measurement circuit with one exception. The tone detector operates on a bandwidth matched to the tone of particular robot under consideration, whereas the total power measurement circuit operates on the whole bandwidth occupied by the chirp signal. The local oscillator in Figure 5.7 is used to shift the tone of a particular robot under consideration inside the tone detector. The tone detector determines if the robot is present or not.

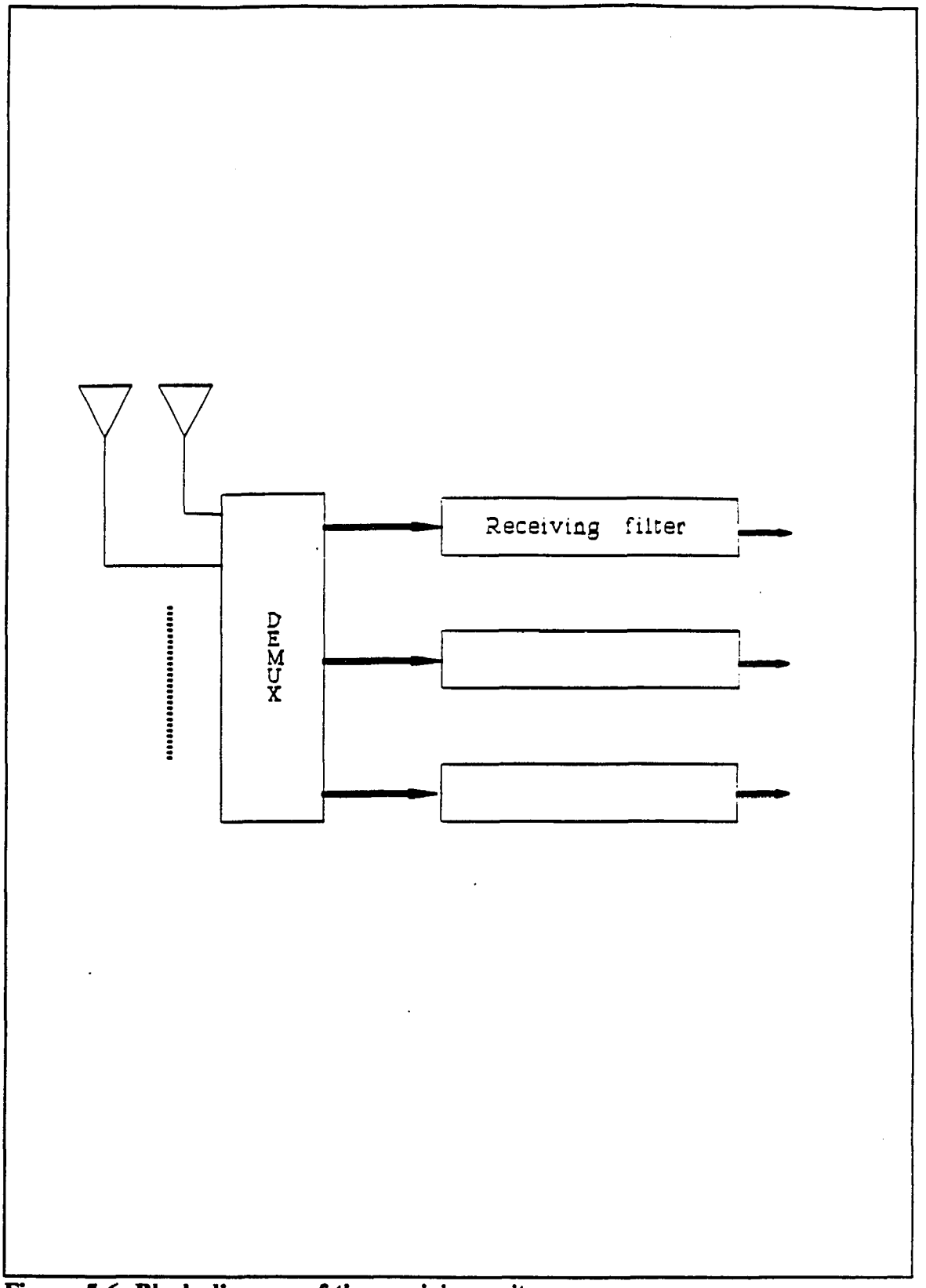

Figure 5.6: Block diagram of the receiving unit.

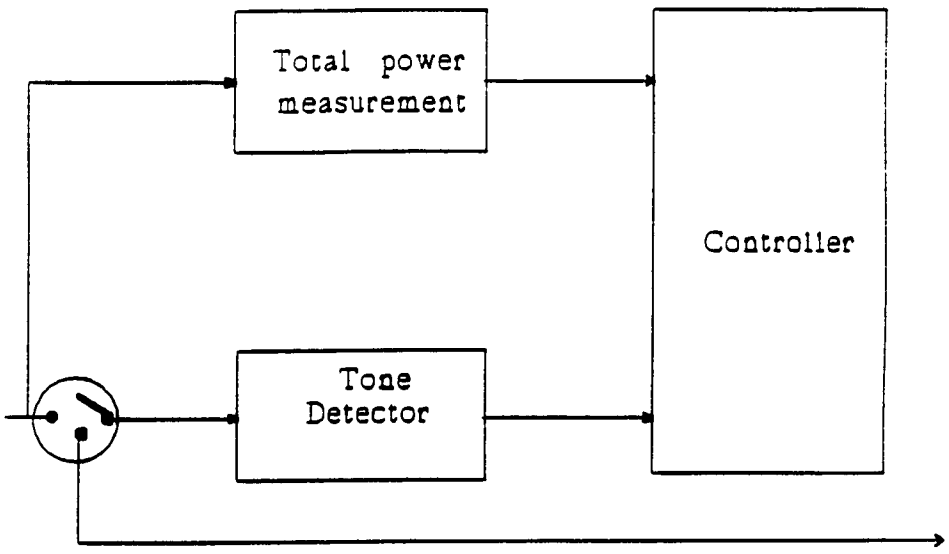

Figure 5.7: Subsystem for each receiving filter.

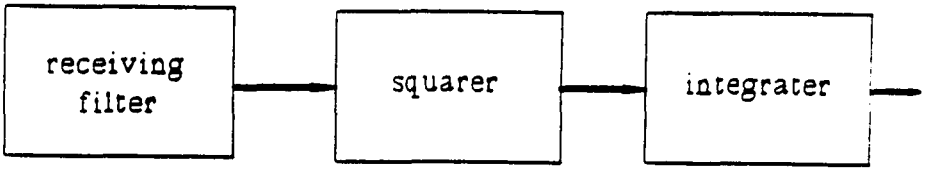

Figure 5.8: Block diagram for the power measurement circuit.

5.2.2 TRANSMITTED CHIRP SIGNAL

The system under consideration utilizes a chirp signal which enables the system to discriminate multipath signal components and provide accurate location of the robots outside the Space Station. The chirp signal mathematically , it can be represented as

$$X(t) = A\cos(\omega_c t + \frac{1}{2}\mu t^2) \qquad -\frac{T}{2} \le t \le \frac{T}{2} \qquad (5.4)$$

Where A is the amplitude, ω_c is the carrier frequency, μ is the rate of change of frequency, θ is a constant phase which uniformly distributed in (0 - 2π) and T is the period of the signal. The phase of X(t) is given by

$$\phi(t) = \omega_c t + \mu t \qquad (5.5)$$

The instantaneous frequency of the signal X(t) is

$$\frac{d\phi(t)}{dt} = \omega_c + \mu t \qquad (5.6)$$

From EQ. (5.6) we see that the instantaneous frequency of the signal X(t) change from ω_c - μT/2 to ω_c + μT/2. This mean that the carrier frequency is linearly swept during the pulse duration T covering a band of frequencies at a rate of μ rad/sec^2. Figure 5.9 shows the signal X(t) and it's frequency variation.

In section 4.3 it was shown that the spectrum of this signal is relatively flat within it's frequency variation. Thus, the approximate bandwidth occupied by the signal is

$$BW = \frac{\mu T}{2\pi} \qquad (5.7)$$

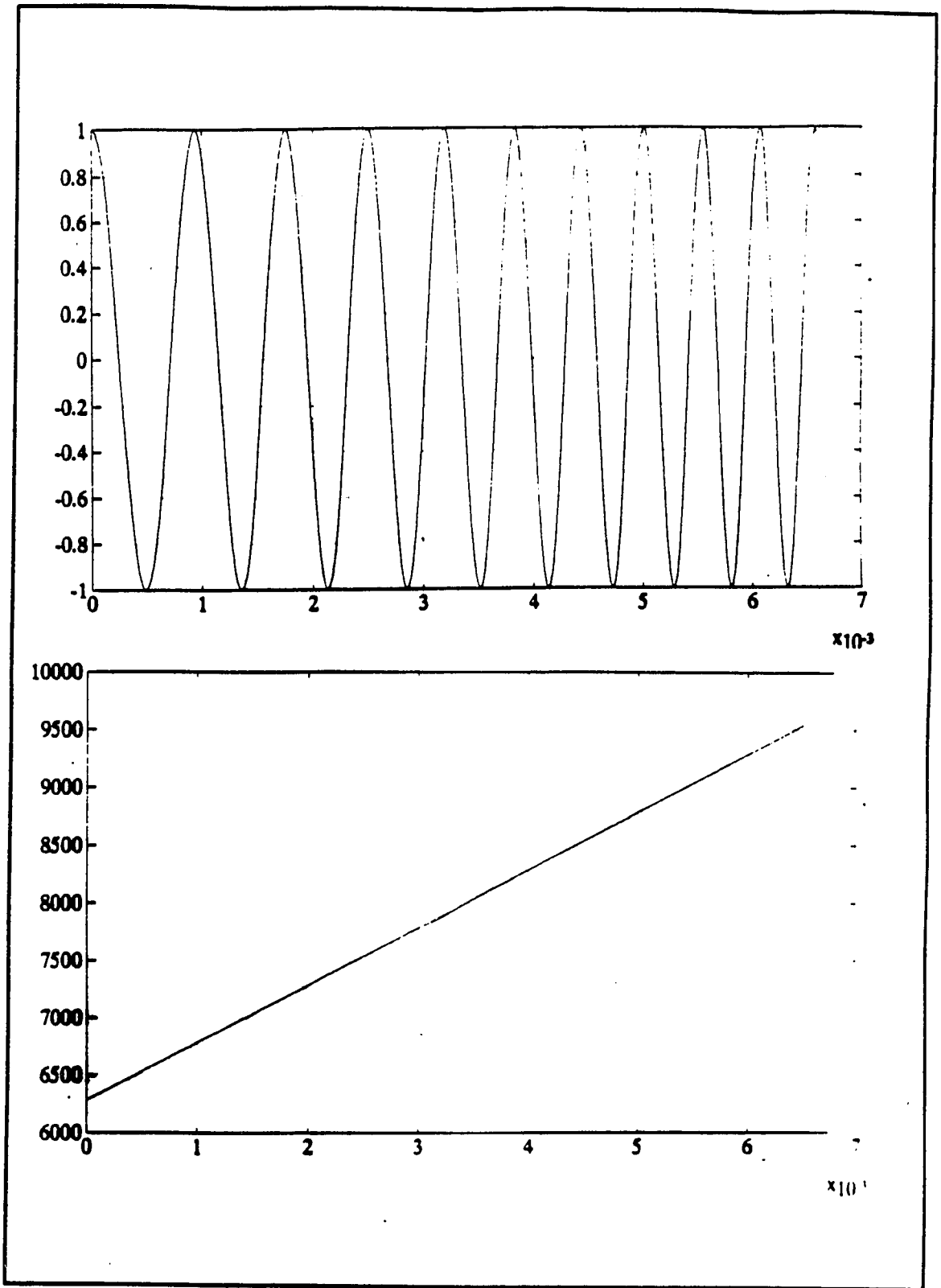

Figure 5.9: a) Chirp signal X(t) b) Instantaneous frequency variation of chirp signal X(t).

It can be seen that the spectrum of these signals depends only on their time bandwidth product (TBW). As TBW product is increased these pulses obtain nearly square-pulse. However, to obtain a accurate location in fraction of a second (Due to the structure of the Space Station) we need to have very large bandwidth. Therefore, a single pulse chirp signal with a constant μ is not practical. However, a similar signal can be obtain by changing the sign of μ every T second. Also the carrier phase of this signal must remain constant throughout it's duration. Thus,

$$S(t) = A\cos(\omega_c t + \psi(t) + \theta) \qquad 0 \le t \le 2T \qquad (5.8)$$

The instantaneous frequency of this signal can be found by taking the derivative of the phase of S(t) with respect to time. Hence,

$$\psi(t) = \begin{cases} \omega_c t + \frac{1}{2}\mu t^2 & , \quad 0 \le t \le T \\ \omega_c t - \frac{1}{2}\mu t^2 & , \quad T \le t \le 2T \end{cases} \qquad (5.9)$$

$$\frac{d\psi(t)}{dt} = \begin{cases} \omega_c + \mu t & , \quad 0 \le t \le T \\ \omega_c - \mu t & , \quad T \le t \le 2T \end{cases} \qquad (5.10)$$

Figure 5.10 shows the signal S(t) and it,s frequency variation.

The spectrum of this signal will approximately represent the shape of the single pulse chirp spectrum. Thus,

$$F[S(t)] = \int_{-T}^{T} S(t)\, e^{-j\omega}\, dt \qquad (5.11)$$

Figure 5.11 shows a line spectrum of such signal.

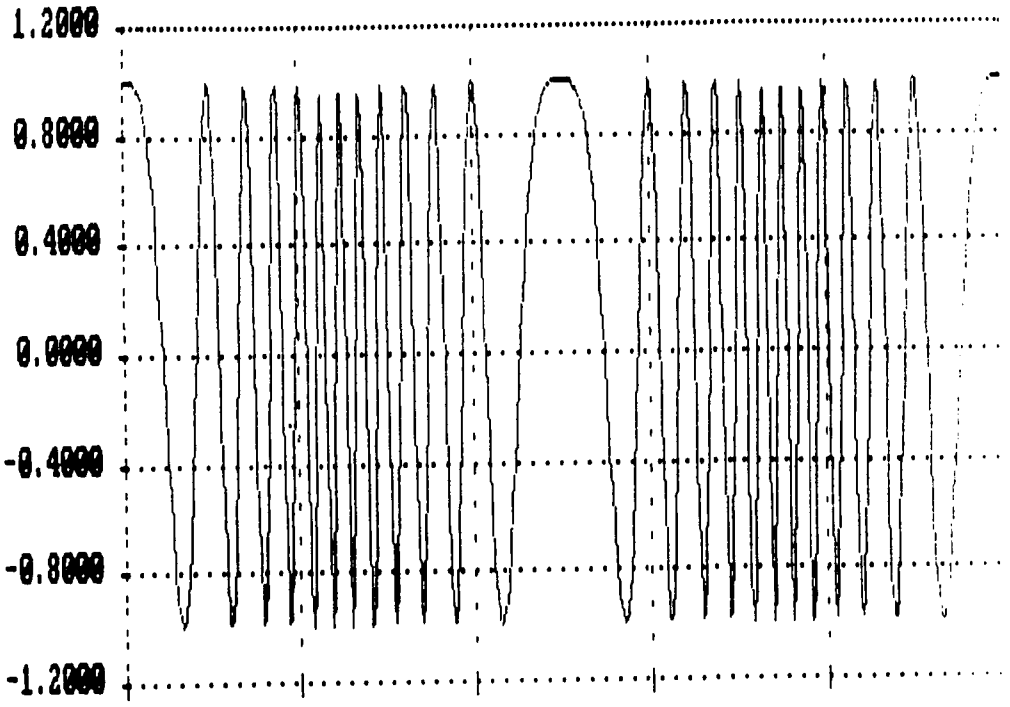

Figure 5.10: Chirp signal S(t).

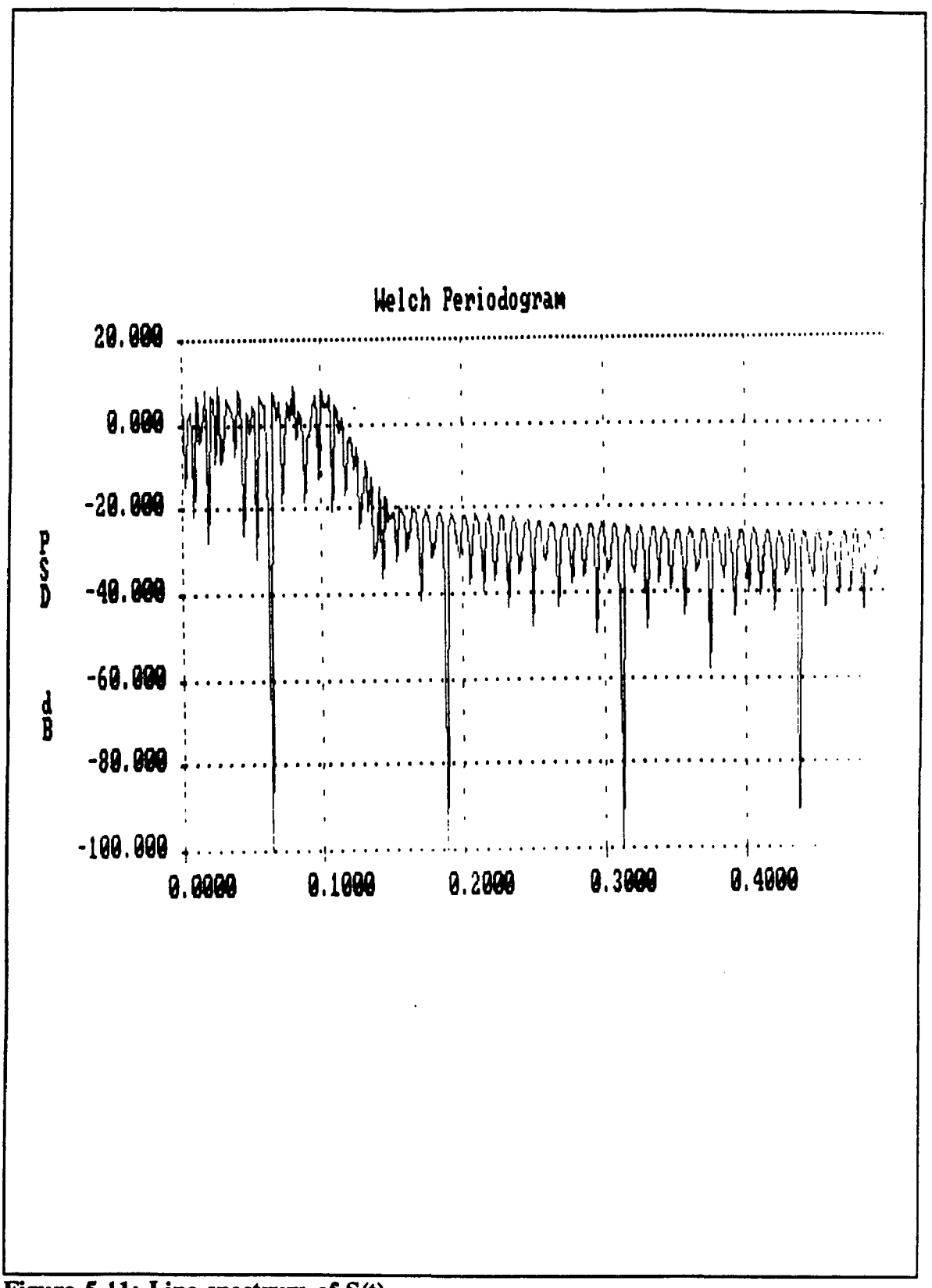

Figure 5.11: Line spectrum of S(t).

5.2.3 DECHIRPING CIRCUIT

The function of the dechirping circuit is to perform the correlation process between the received chirp signal and the transmitted chirp signal. The block diagram of such a circuit is shown in Figure 5.12. The correlation process is performed as follows:

1) The received signals, $r_i(t)$, are multiplied by the locally generated LFM (x(t)). The transmitted signal is given by

$$x(t) = \begin{cases} A\cos\left(\omega t + \frac{1}{2}\mu t^2\right) & , \quad 0<t<T_p \\ 0 & , \quad elsewhere \end{cases} \tag{5.12}$$

and the received signal is

$$r_i(t) = \begin{cases} B\cos\left(\omega(t+T_{d_i}) + \frac{1}{2}\mu(t+T_{d_i})^2 + \phi_i\right) & , \quad 0<t<T_p \quad i=1 \\ 0 & , \quad elsewhere \end{cases} \tag{5.13}$$

where i is the number of receiving antennae in the selected search region.

The product of the transmitted and the received signal is

$$y(t) = x(t) \times r(t) \tag{5.14}$$

After disregarding the double frequency components of y(t) then EQ. (5.14) can be

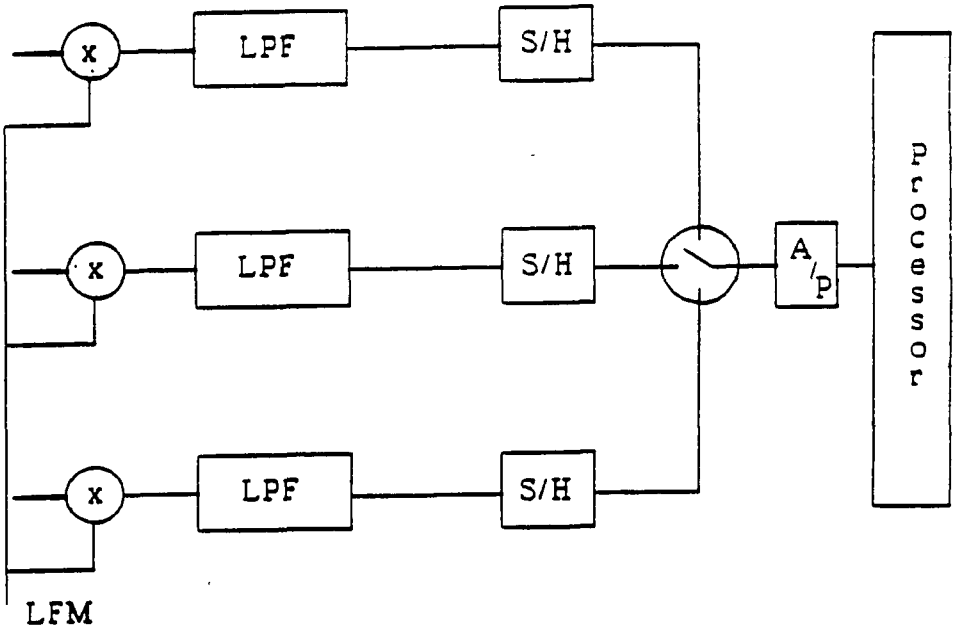

Figure 5.12: Block diagram of the dechirping circuit.

written as

$$y_i(t) = \sqrt{\frac{P}{2}} \cos(\omega_d t + \varphi_i) \qquad (5.15)$$

Where p is the carrier power of the received signal and φ_i is a random and uniformly distributed phase in the range of [0 , 2π]. This multiplication process will remove the quadratic dependence from the received chirp. Therefore, $y_i(t)$ is a pure sinusoidal wave whose frequency depends on relative time delays of the received signal $r_i(t)$ as compared to the signal x(t). After the multiplication process each output is low-pass filtered and sampled. Then the output of the S/H are first multiplexed and digitalized so that the FFT processor can be used as means of determining ω_{di}. The frequency ω_{di} is directly proportional to the propagation delay T_{di}. Thus,

$$\omega_{d_i} = \mu T_{d_i} \qquad (5.16)$$

Hence, the distance between the receiving antennae and the particular robot can be determined by:

$$D_i = T_{d_i} C \qquad (5.17)$$

The problem under consideration is not as simple as what we discussed so far because the received signals are combinations of multipath components from different directions with a direct ray from the robot to the receiving antennae. The delays between the direct ray and multipath components can be in order of few nanosecond. If the bandwidth and the duration of the transmitted chirp signal are BW and T respectively , then we can

discriminate between two tones located more than 1/ T HZ apart. Hence,

$$\mu \left| T_{d_0} - T_{d_1} \right| \geq \frac{1}{T} \tag{5.18}$$

Therefore,

$$\left| T_{d_0} - T_{d_1} \right| \geq \frac{1}{\mu T} = \frac{1}{BW} \tag{5.19}$$

where T_{d0} and T_{d1} are the time delay of the direct signal and the time delay of the first multipath. Therefore, if single chirp signal with bandwidth BW is used then we discriminate between signal which arrive 1/BW seconds apart. However, if we use multiple pulse chirp with bandwidth W, as described by EQ. (5.8), is used we can discriminate between signals much less than 1/W apart.

Now let us begin assuming that the transmitted chirp signal consists of a single up-going and a single down going pulse as shown in Figure 5.10. The received signal will be of the form

$$r(t) = \begin{cases} \sqrt{2}\bar{p}\cos\left(\omega(t - T_d) + \frac{1}{2}\mu(t - T_d)^2\right) & 0 \leq t \leq T \\ \sqrt{2}\bar{p}\cos\left(\omega(t - T_d) - \frac{1}{2}\mu(t - T_d)^2\right) & T \leq t \leq 2T \end{cases} \tag{5.20}$$

The product of the transmitted signal S(t) and the received signal r(t) after filtering is

$$y(t) = \begin{cases} \sqrt{\frac{\bar{p}}{2}}\cos\left(\mu T_d t + \theta\right) & 0 \leq t \leq T \\ \sqrt{\frac{\bar{p}}{2}}\cos\left(-\mu T_d t + \theta\right) & T \leq t \leq 2T \end{cases} \tag{5.21}$$

where θ is assumed random and uniformly distributed in [0 , 2π]. Figure 5.13 shows the instantaneous frequency versus time function of the received and transmitted signals.

Once the signal has been dechirp it's output, y(t), is a sinusoidal wave whose frequency is the difference between $\Psi'(t)$ and $\Psi'(t - T_d)$. Where,

$$\Psi'(t) = \begin{cases} \omega + \mu t \\ \omega - \mu t \end{cases} \tag{5.22}$$

$$\Psi'(t - T_d) = \begin{cases} \omega + \mu (t - T_d) \\ \omega - \mu (t - T_d) \end{cases} \tag{5.23}$$

$$Y(t) = \Psi'(t) - \Psi'(t - T_d) = \begin{cases} \mu T_d \\ -\mu T_d \end{cases} \tag{5.24}$$

$$| Y(t) | = \mu T_d \tag{5.25}$$

The frequency of y(t) will be equal to μT_d . Where, the phase of y(t) though constant during the up-swing and down-swing times, it will change it's polarity as shown in Figure 5.14.

Since y(t) is been detected coherently we can collect samples of y(t) only during up-swing/down-swing times. This results in a sinusoidal signal which has a continuous phase and a constant frequency. However, this signal is set to zero during down-swing/up-swing times, since data are only collected during up-swing/down-swing times as shown in Figure 5.15. Thus, if n pieces of T duration each are collected and Fourier transformed, the resolution of the FFT corresponding to time of arrival will be 1/nW seconds.

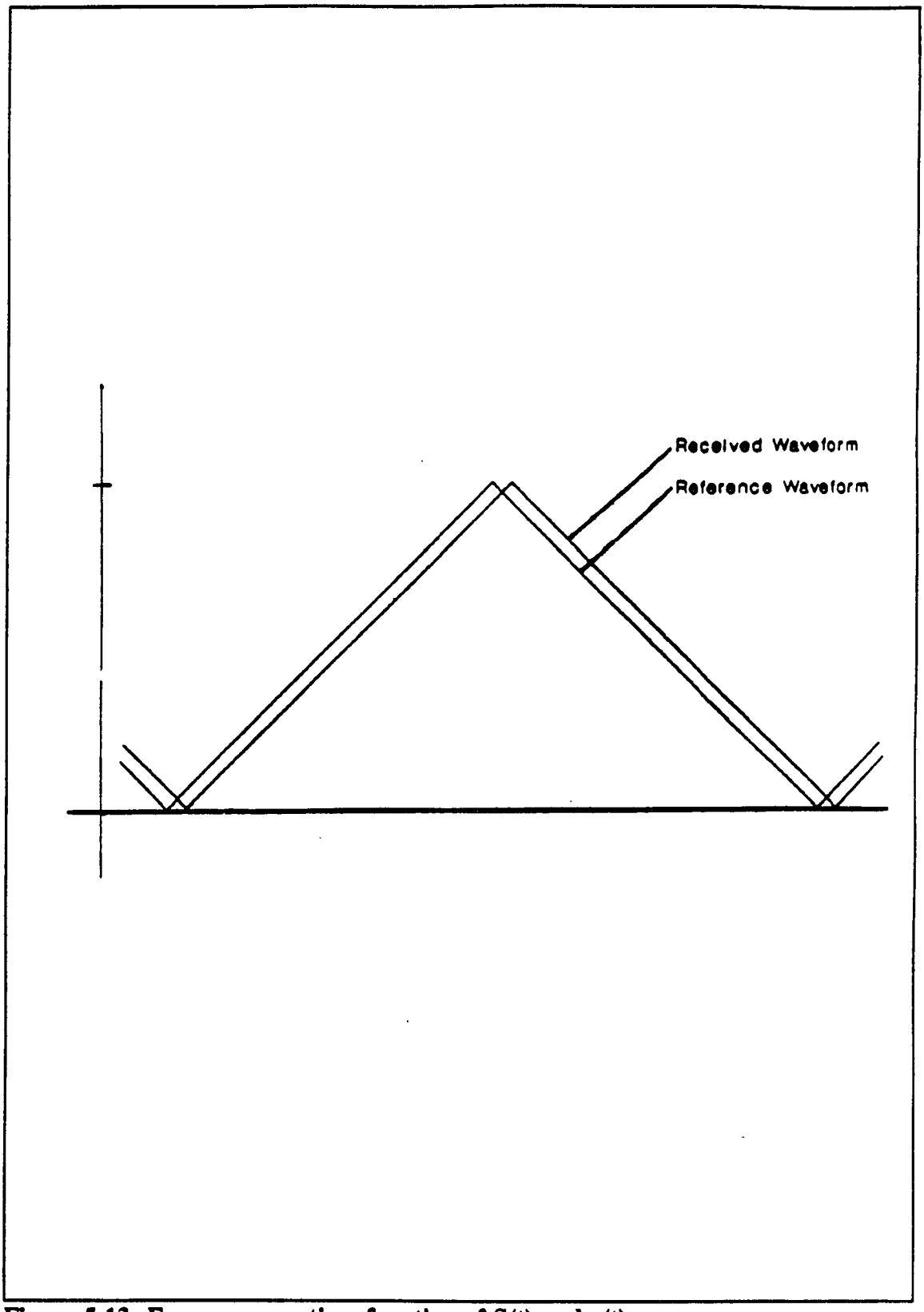

Figure 5.13: Frequency vs. time function of S(t) and r(t).

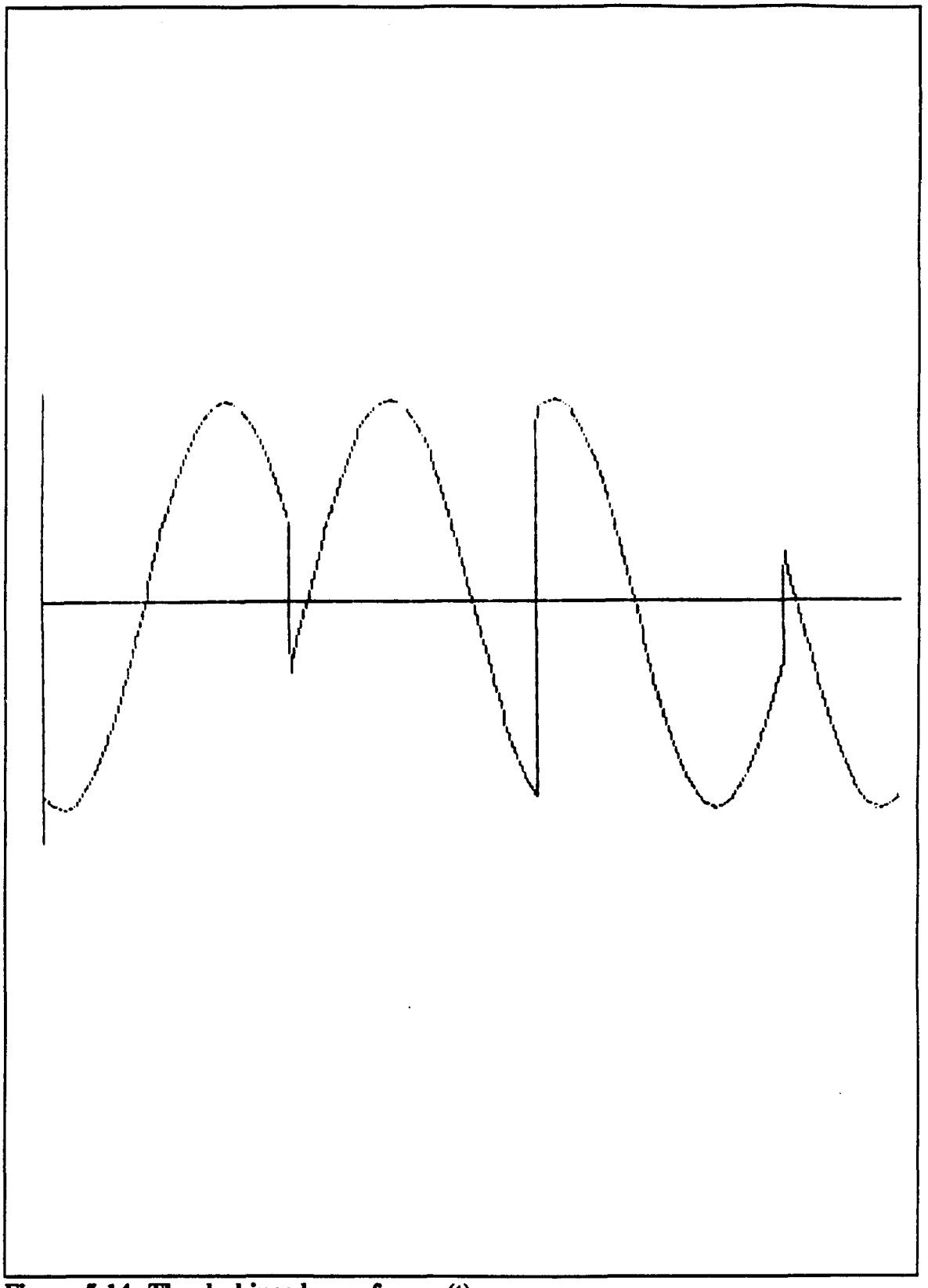

Figure 5.14: The dechirped waveform y(t).

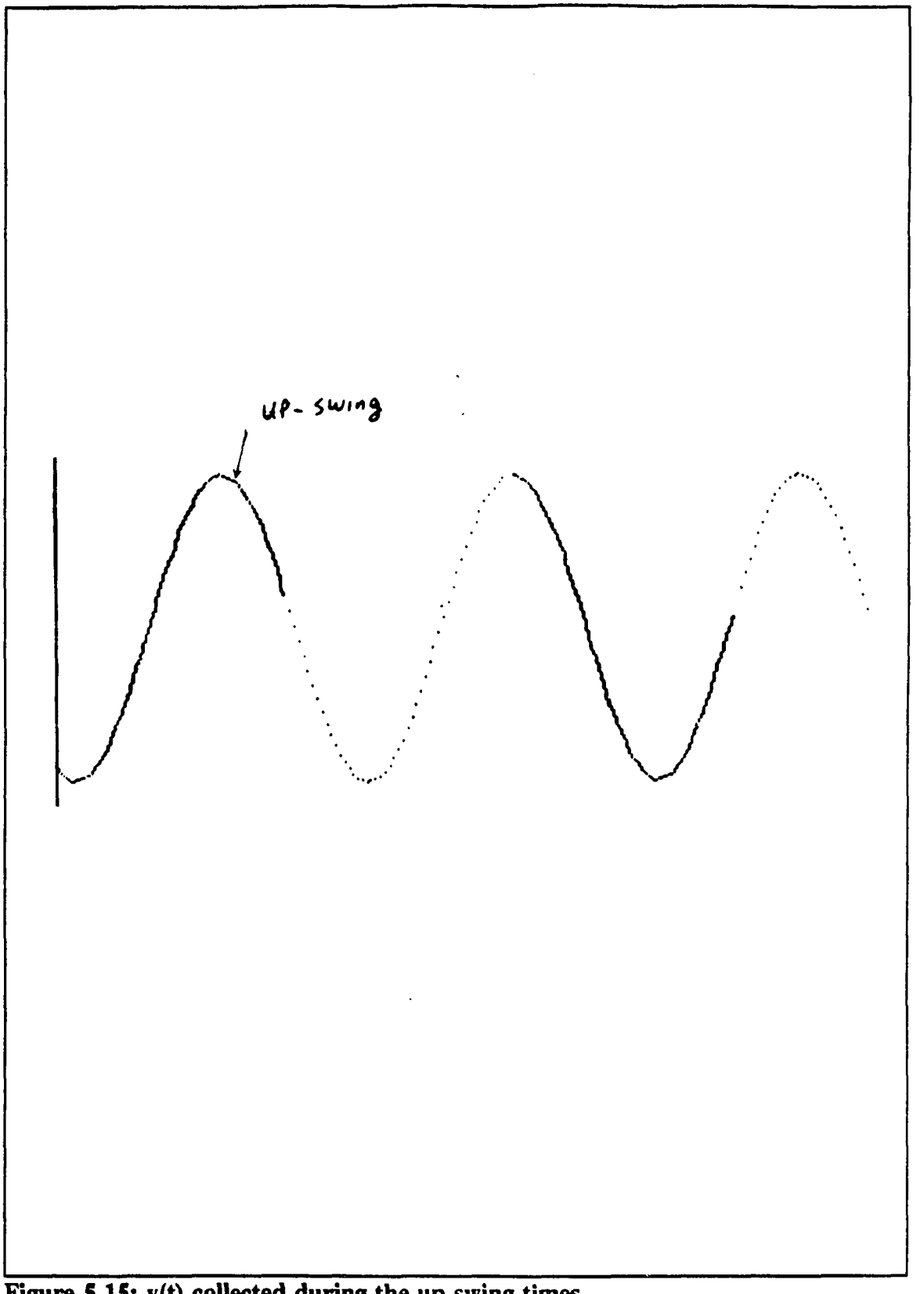

Figure 5.15: y(t) collected during the up-swing times.

5.3 POWER MEASUREMENT CIRCUIT ANALYSIS

The total power measurement circuit is a energy detector which supplies the controller with information about the background noise. This circuit is similar to the tone detector circuit except that the total power measurement circuit operates on the whole bandwidth occupied by the LFM signal, whereas the tone detector operates on a bandwidth matched to the tone of a particular robot under consideration. The output of the total power measurement circuit will be used as means of determining the threshold at the output of the FFT.

The threshold setting device it consist of a squaring device, integrator, and a bandpass filter that contain a narrow notch at the pilot frequency (in order to remove the pilot tone), otherwise flat unity gain throughout the remaining bandwidth. The block diagram of the threshold setting device is shown in Figure 5.8.

A bandpass gaussian noise can be represented in term of it's quadrature components $n_c(t)$ and $n_s(t)$. That is

$$y(t) = n_c(t)\cos(2\pi f_c t) - n_s(t)\sin(2\pi f_c t) \qquad (5.26)$$

in which f_c is the center frequency of the bandpass filter. However , if y(t) is bandlimited white gaussian noise of spectral density $N_o/2$ then the quadrature components of y(t) have flat power spectral densities of N_o over $|f| \leq BW/2$. The normalized

output of the integrator can be represented by

$$\begin{aligned} Z(t) &= \frac{2}{N_o}\int_{t-T}^{T} y^2(\tau)\, d\tau \\ &= \frac{2}{N_o}\int_{0}^{T} y^2(t)\, dt \end{aligned} \tag{5.27}$$

Where T is equal to the observation interval. Assuming time bandwidth product is very large and $f_c \gg$ BW then Z(t) can be approximated as

$$Z(t) = \frac{1}{N_o}\int_{0}^{T} n_c^2(t)\, dt + \frac{1}{N_o}\int_{0}^{T} n_s^2(t)\, dt \tag{5.28}$$

Using sampling theorem the in phase and quadrature components of the noise can be express as

$$n_c(t) = \sum n_c(nT)\, sinc(\omega(t - nT)) \tag{5.29}$$

and

$$n_s(t) = \sum n_s(nT)\, sinc(\omega(t - nT)) \tag{5.30}$$

$$\int_{0}^{T} sinc(\omega t - j)\, sinc(\omega t - i)\, dt \approx 0 \qquad i \neq j \tag{5.31}$$

From the following properties of the sinc function

$$\int_{0}^{T} sinc(\omega t - j)\, dt \approx \int_{-\infty}^{\infty} sinc(\omega t - i)\, dt = \frac{1}{BW} \qquad 0 < i \leq TBW \tag{5.32}$$

$$\int_0^T sinc(\omega t - i)\, dt \approx 0 \qquad i \leq 0 \quad or \quad i > TBW \qquad (5.33)$$

We can represent Z(t) as

$$Z(t) = \frac{1}{N_o \omega} \sum_{i=1}^{2TBW} [n_c^2(nT) + n_s^2(nT)] \qquad (5.34)$$

It can be shown $n_c(nT)$ and $n_s(nT)$ are independent gaussian random variable having the following autocorrelation function.

$$R(\tau) = N_o \omega\, sinc(\omega \tau) \qquad (5.35)$$

Since $n_c(n_iT)$ and $n_s(n_iT)$ are statistically independent of $n_c(n_jT)$ and $n_s(n_jT)$ for $i \neq j$ respectively then Z(t) can be expressed as

$$Z(t) = \frac{1}{N_o BW} \sum_{i=1}^{2TBW} A_i^2 \qquad (5.36)$$

Where the A_i, i = 1, 2, ...2TBW, are statistically independent and identically distributed gaussian random variable with

$$E[A_i] = 0 \qquad (5.37)$$

and

$$E[A_i^2] = N_o BW \qquad (5.38)$$

Thus,

$$E[Z] = 2TBW \qquad (5.39)$$

and

$$\sigma_z = 4TBW \tag{5.40}$$

Therefore, the characteristic and power density function of Z can be written respectively as follows:

$$\psi_z(j\nu) = \frac{1}{(1 - j2\nu\sigma^2)^{N/2}} \tag{5.41}$$

$$p_Z(z) = \frac{1}{2^\gamma \Gamma(\gamma)} z^{\gamma-1} e^{-\frac{z}{2}} \qquad \gamma = 2TBW \tag{5.42}$$

Where $\Gamma(\gamma)$ is the gamma function, defined as

$$\Gamma(\gamma) = \int_0^\infty t^{\gamma-1} e^{-t}\, dt \qquad \gamma > 0 \tag{5.43}$$

$$\Gamma(\gamma) = (\gamma - 1)! \qquad \gamma \text{ an integer}, \quad \gamma > 0 \tag{5.44}$$

$$\Gamma(\tfrac{1}{2}) = \sqrt{\pi} \qquad \Gamma(\tfrac{3}{2}) = \frac{\sqrt{\pi}}{2} \tag{5.45}$$

Hence, the pdf of a variable q can be defined as

$$p_Q(q) = \frac{q^{\frac{\gamma}{2}-1}}{(\sigma^2)^{\frac{\gamma}{2}} 2^{\frac{\gamma}{2}} \Gamma(\frac{\gamma}{2})} e^{-\frac{q}{2\sigma^2}} \tag{5.46}$$

$$q = \frac{1}{TBW} \sum_{i=1}^{2\gamma} A_i^2$$

and

$$E[q] = 2N_oBW \tag{5.48}$$

This pdf is called a chi-square (gamma distribution) pdf with γ degree of freedom. Figure 5.16 shows the pdf of Z for various value of γ. The impulsive nature of $p_Z(z)$ cab be seen for large γ's. This is an indication, that for large TBW, a good estimate of the noise floor can be obtained.

At this point we can prove that if the pilot tone or the LFM signal are present at the input of the threshold setting device, we will still obtain a good estimate of the noise statistic. To prove this, let

$$S(t) = S_c(t)\cos(\omega_c t) - S_s(t)\sin(\omega_s t) \tag{5.49}$$

where $S_c(t)$ and $S_s(t)$ are the low-pass component of S(t). Using the sampling theorem for stochastic processes and the properties of the sinc function then the output of the integrator can be express as follows

$$\begin{aligned} Z &= \frac{1}{N_oBW}\left[\sum_{i=1}^{TBW}\left[S_c\left(\frac{i}{BW}\right) + n_c\left(\frac{i}{BW}\right)\right]^2 + \sum_{i=1}^{TBW}\left(S_s\left(\frac{i}{BW}\right) + n_s\left(\frac{i}{BW}\right)\right]^2\right] \\ &= \sum_{i=1}^{TBW} A_i^2 + \sum_{i=1}^{TBW} B_i^2 \end{aligned} \tag{5.50}$$

using the statistical independence property for the noise terms we obtain the following means.

$$E[A_i] = \frac{1}{\sqrt{N_oBW}} S_c\left(\frac{i}{BW}\right) \tag{5.51}$$

$$E[B_i] = \frac{1}{\sqrt{N_o BW}} S_s\left(\frac{i}{BW}\right) \tag{5.52}$$

The sum terms in EQ. (5.50) has noncentral χ^2 distribution with TBW degree of freedom and noncentral parameter

$$\lambda_1 = \sum E[A_i]^2 \tag{5.53}$$

and

$$\lambda_2 = \sum E[B_i]^2 \tag{5.54}$$

Since the two χ^2 variables are independent, Z has a χ^2 distribution with 2TBW degrees of freedom and parameter λ. Thus,

$$\begin{aligned}
\lambda &= \lambda_1 + \lambda_2 \\
&= \frac{1}{N_o BW}\left[\sum_{i=1}^{TBW} S_c^2\left(\frac{i}{BW}\right) + \sum_{i=1}^{TBW} S_s^2\left(\frac{i}{BW}\right)\right] \\
&\approx \frac{1}{N_o}\int_0^T [S_c^2(t) + S_s^2(t)]\, dt \\
&\approx \frac{2}{N_o}\int_0^T S^2(t)\, dt \\
&= \frac{2\varepsilon}{N_o}
\end{aligned} \tag{5.55}$$

where ε is the signal energy. The mean and the variance of Z can be defined by

$$E[Z] = \lambda + 2TBW \tag{5.56}$$

$$Var[Z] = 4\lambda + 4TBW \tag{5.57}$$

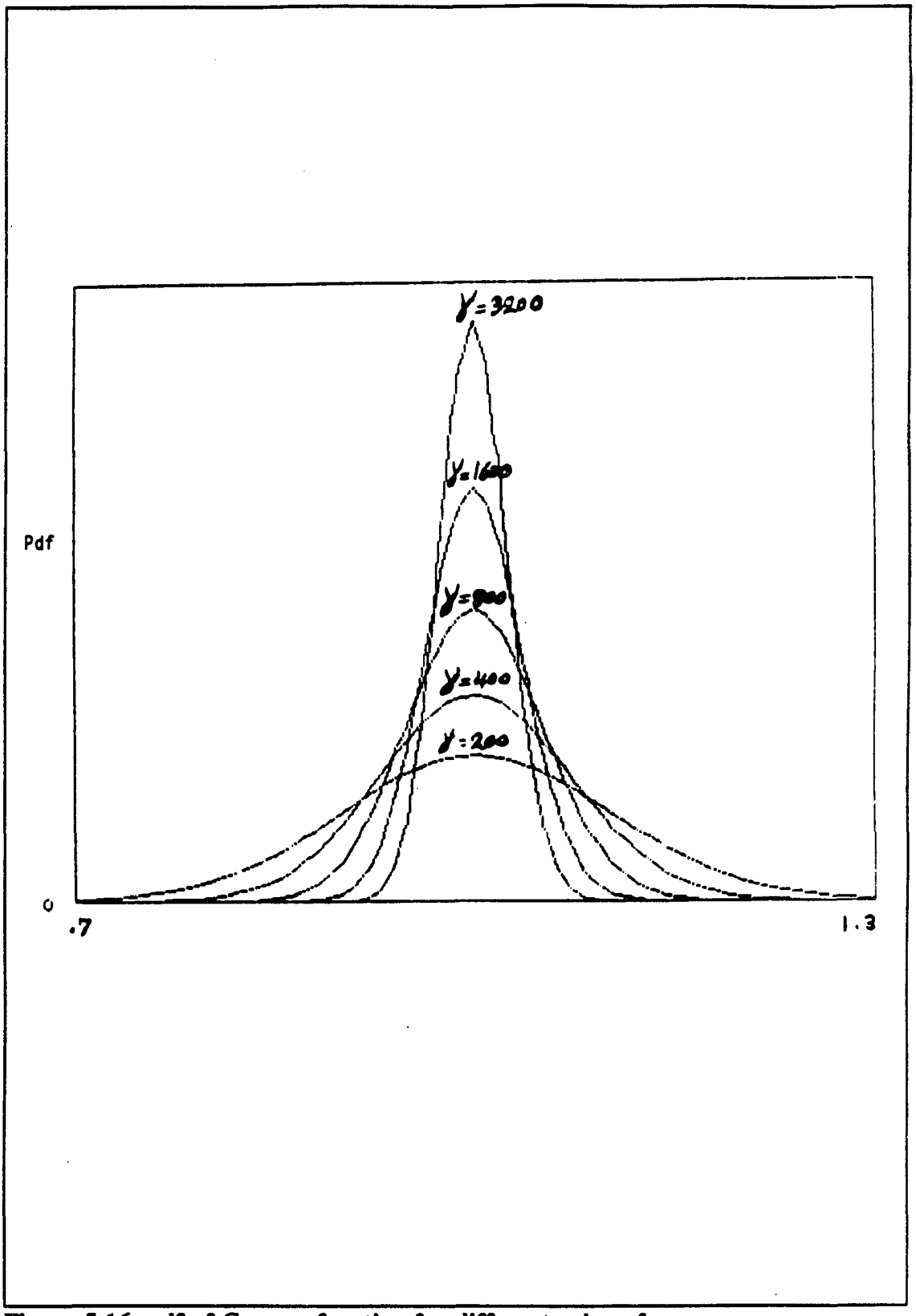

Figure 5.16: pdf of Gamma function for different value of γ.

Hence, the χ^2 distribution of Z is

$$p_Z(z) = \frac{1}{2}\left(\frac{z}{\lambda}\right)^{\frac{(\lambda-1)}{2}} e^{-\frac{z+\lambda}{2}} I_{\lambda-1}(\sqrt{z\lambda}) \qquad z \geq 0 \tag{5.58}$$

where $\gamma = 2TBW$. After a series of algebraic manipulation the mean and the variance of q can be obtain as follows

$$\begin{aligned} E[q] &= 2p_s + 2N_oBW \\ &= 2p_s + 2p_n \end{aligned} \tag{5.59}$$

$$Var[q] = 8p_s\frac{p_n^2}{(TBW)^2} + 4\frac{P_n^2}{TBW} \tag{5.60}$$

where

$$q = \left[\frac{N_o}{T}\right]Z \tag{5.61}$$

and

$$p_s = \frac{\mathcal{E}}{T} \tag{5.62}$$

We see that if the signal is present, but disregarded from the threshold setting device, the inclination introduced will be in the order of one percent from the one acquired when only noise is present. Consequently, the threshold setting device, does not need to notch out the pilot tone nor stop when the LFM signal is being received. This also allows the estimate of the noise floor to have a smaller variance due to the increased integration time. Furthermore, the threshold device does not need estimates of when the pilot tone stops and the LFM signal starts. It can simply use the total receiving period before

supplying the threshold setting to the robot location-finder processor.

5.4 DETECTOR ANALYSIS

The detection circuit is supposed to detect the existence of a robot without being confused by noise. A simple detection circuit consists of a narrow bandpass filter followed by an envelope detector which typically has a linear or square-law characteristic and the last stage is a threshold circuit in which the output of the envelope detector is compared to a preset threshold. The block diagram of such detector is shown in Figure 5.17.

In this problem the threshold comparator circuit is used to observe the returned signal from the robot and to determine whether the robot is present or absent. This situation can be described as follows:

The source emitting two possible outputs at different instants of time. These outputs referred to the hypotheses H_0 and H_1. Hence,

$$H_0 : \quad r(t) = n(t) \tag{5.63}$$

$$H_1 : \quad r(t) = n(t) + s(t) \tag{5.64}$$

where the hypothesis H_0 represents that the received signal, r(t), is only noise and the hypothesis, H_1, present that the output will be noise plus the emitted signal s(t). If each observation is represented by a random variable and each hypothesis corresponds to one

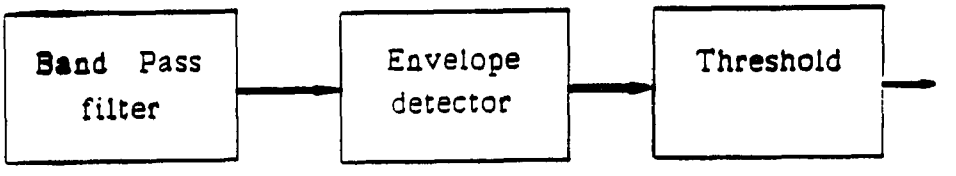

Figure 5.17: Detector block diagram.

or more observations, then one can establish the fact that outputs under the hypothesis H_0 and H_1 are random variables. These random variables contain the probability density functions of $f_{Y|H0}(y|H_0)$ and $f_{Y|H1}(y|H_0)$ where y is a particular value of the random variable Y corresponding to each hypothesis. Thus,

$$p_0(y) = f_{Y|H_0}(y|H_0) \tag{3.65}$$

$$p_1(y) = f_{Y|H_1}(y|H_1) \tag{3.66}$$

where $p_0(y)$ and $p_1(y)$ presents the distribution of Y under hypothesis H_0 and H_1 respectively. Therefore, if the decisions are made based on some preset threshold, l, under this hypothesis testing, there are four possible cases that can occur:

1. Decision made: H_0 Correct decision: H_0
2. Decision made: H_1 Correct decision: H_1 (Detection)
3. Decision made: H_0 Correct decision: H_1 (Miss)
4. Decision made: H_1 Correct decision: H_0 (False alarm)

Where cases 1 and 2 represent that the receiver makes a correct decision, while cases 3 and 4 represents that the receiver makes an error. For our problem, case 2 is called a detection, case 3 a miss, and case 4 a false alarm.

Suppose that each robot will transmit a signal ($S_i(t)$) with preset frequency f_i and the received signal is

$$r_i(t) = s_i(t) + n_i(t) \tag{5.67}$$

after passing the signal $s_i(t)$ through a bandpass filter and an envelope detector we will compare the output of the envelope detector with threshold level l. When the output of

the envelope detector passes the threshold, the existence of a robot is assumed at the corresponding delay (t_{di}). If the output of envelope detector is below *l*, we assume that the received signal is noise. When the threshold is above all but the highest noise peak, only one noise peak is mistaken for a target. This is called a false alarm. By lowering the threshold, the probability of detection will increase, and at the same time, the probability of the false alarm will increase.

Assume an input consists of a sinusoidal signal with additive white Gaussian noise. We will seek two power spectrum densities of the envelope:

1. when only the noise is present (H_0)
2. when both noise and signal are present (H_1)

with a preset threshold and the two PDF we can determine the probability of detection P_D, and the probability of false alarm P_{fa}.

When white Gaussian noise is passed through a narrow bandpass filter, the output noise can be described by

$$n(t) = X(t)\cos(\omega_c t) + Y(t)\sin(\omega_c t) \qquad (5.68)$$

where X(t) and Y(t) are independent random variables having a Gaussian PDF with a zero mean and the same variance as n(t).

For a filter with a rectangular response with bandwidth f_B and the two-sided noise spectral power density $N_o/2$ the variance of X(t) and Y(t) are

$$X^2(t) = Y^2(t) = n^2(t) = f_B N_o \qquad (5.69)$$

The signal with frequency W_c and duration τ ($f_B >> 1/\tau$) will pass the filter almost

unchanged. The signal at the output could be described by

$$S_o(t) = A\cos(\omega_c t - \phi_s) \tag{5.70}$$

$$S_o(t) = a\cos(\omega_c t) + b\cos(\omega_c t) \tag{5.71}$$

where

$$A = \sqrt{a^2 + b^2} \tag{5.72}$$

and

$$\phi_s = \arctan\frac{b}{a} \tag{5.73}$$

The output signal of the filter will be the sum of the noise and signal. Thus,

$$\begin{aligned} V(t) &= s_o(t) + n(t) \\ &= a\cos(\omega_c t) + b\sin(\omega_c t) + X(t)\cos(\omega_c t) + Y(t)\sin(\omega_c t) \\ &= (a + X(t))\cos(\omega_c t) + (b + Y(t))\sin(\omega_c t) \\ &= r(t)\cos(\omega_c t + \phi) \end{aligned} \tag{5.74}$$

where

$$r(t) = \sqrt{(a + X(t))^2 + (b + Y(t))^2} \tag{5.75}$$

and

$$\phi = \arctan\frac{b + Y(t)}{a + X(t)} \tag{5.76}$$

X(t) and Y(t) are independent Gaussian random variables with zero average. Hence,

$$r(t) = \sqrt{X_1(t)^2 + Y_1(t)^2} \tag{5.77}$$

where $X_1(t)$ and $Y_1(t)$ are Gaussian random variables with an average a and b and their PDF can be described as follows:

$$p_1(X_1) = \frac{1}{\beta\sqrt{2\pi}} e^{-\frac{(X_1 - a)^2}{2\beta^2}} \tag{5.78}$$

$$p_1(Y_1) = \frac{1}{\beta\sqrt{2\pi}} e^{-\frac{(Y_1 - b)^2}{2\beta^2}} \tag{5.79}$$

where β is the standard deviation for X_1 and Y_1 that is equal to Root Mean Square (RMS) value of the noise n(t).

$$\beta = \sqrt{n(t)^2} = \sqrt{N_o f_\beta} \tag{5.80}$$

Since X_1 and Y_1 are independence from each other, their two-dimensional joint PDF is equal to $p(X_1, Y_1)$. Thus,

$$\begin{aligned} p(X_1, Y_1) &= p_1(X_1)\ p_1(Y_1) \\ &= \frac{1}{2\pi\beta^2} e^{\frac{(X_1 - a)^2 + (Y_1 - b)^2}{2\beta^2}} \end{aligned} \tag{5.81}$$

Let $X_1 = r \cos\phi$ and $Y_1 = r \sin\phi$ where

$$r = \sqrt{X_1^2 + Y_1^2} \quad , \quad \phi = \arctan\frac{Y_1}{X_1} \tag{5.82}$$

then

$$p(r, \phi) = \frac{p(X_1, Y_1)}{|J(X_1, Y_1)|} \tag{5.83}$$

$J(X_1, Y_1)$ is the Jacobian of the transformation

$$J(X_1, Y_1) = \begin{vmatrix} \frac{\partial r}{\partial X_1} & \frac{\partial r}{\partial Y_1} \\ \frac{\partial \phi}{\partial X_1} & \frac{\partial \phi}{\partial Y_1} \end{vmatrix} = \frac{1}{r} \tag{5.84}$$

using EQ.(5.82), EQ.(5.83), and EQ.(5.84) it yields

$$p(r,\phi) = \frac{r}{2\pi\beta^2} e^{\frac{r^2 + a^2 + b^2 - 2ra\cos\phi - 2rb\sin\phi}{2\beta^2}} \tag{5.85}$$

under the hypothesis H_1, the PDF of the envelope is the integral of $p(r,\phi)$ over all the phases.

$$\begin{aligned} p_{H_1}(r) &= \int_0^{2\pi} p(r,\phi)\, d\phi \\ &= \int_0^{2\pi} \frac{r}{2\pi\beta^2} e^{-\frac{r^2 + a^2 + b^2 - 2ra\cos\phi - 2rb\sin\phi}{2\beta^2}} \\ &= \frac{r}{\beta^2} e^{-\frac{r^2 + A^2}{2\beta^2}} \int_0^{2\pi} e^{\frac{rA}{\beta^2}\cos(\phi - \phi_s)}\, d\phi \\ &= \frac{r}{\beta^2} e^{-\frac{r^2 + A^2}{2\beta^2}} I_o\left(\frac{rA}{\beta^2}\right) \end{aligned} \tag{5.86}$$

where ϕ_s and A are the phase and the amplitude of the signal and $I_o(rA/\beta^2)$ is the modified Bessel function of order zero. EQ.(5.86) can be rewritten as

$$p_1(r) = \frac{r}{2\varepsilon N_o} e^{-\frac{r^2 + 4\varepsilon^2}{4\varepsilon N_o}} I_o\left(\frac{r}{N_o}\right) \tag{5.87}$$

where ε is the received signal energy in T seconds and $N_o/2$ denotes the two sided noise

power spectral density. On the other hand, the power density function of decision variable y under hypothesis H_o is

$$p_0(y) = \frac{y}{\sigma_n^2} e^{-\left(\frac{y^2}{2\sigma_n^2}\right)} \qquad y \geq 0 \tag{5.88}$$

Therefore, the decision variable Y will have a Rayleigh distribution and Rician distribution under the two hypothesis H_o and H_1 respectively. From Bayes rule, we have

$$P(D_i, H_j) = P(D_i | H_j)\ P(H_j) \qquad i,j = 0,1 \tag{5.89}$$

where D_0 denotes "decide H_0", D_1 denotes "decide H_1", and $P(H_j)$ is the probability of occurrence of hypothesis H_j. Hence, the conditional density function $P(D_i \mid H_j)$ in terms of the regions shown in Figure 5.18 are

$$P(D_0 | H_0) = \int_{Z_0} f_{Y|H_0}(y | H_0)\ dy = 1 - P_{fa} \tag{5.90}$$

$$P(D_1 | H_1) = \int_{Z_0} f_{Y|H_1}(y | H_1)\ dy = P_D \tag{5.91}$$

$$P(D_0 | H_1) = \int_{Z_0} f_{Y|H_1}(y | H_1)\ dy = P_m \tag{5.92}$$

$$P(D_1 | H_0) = \int_{Z_1} f_{Y|H_0}(y | H_0)\ dy = P_{fa} \tag{5.93}$$

The probabilities P_{fa}, P_d and P_m represent the probability of false alarm, probability of detection, and probability of miss respectively. Therefore, under the two hypothesis H_0 and H_1 for a preset threshold, l, the probability of detection and the probability of the

false alarm are :

$$P_D = \int_{1\sqrt{2\varepsilon N_o}}^{\infty} v\, e^{-\frac{v^2 + 4\alpha^2}{2}}\, I_0(\alpha y)\, dy \qquad (5.94)$$

$$P_{fa} = \int_{1}^{\infty} \frac{y}{\sigma_n^2}\, e^{-\frac{y^2}{2\sigma_n^2}}\, dy \qquad (5.95)$$

where

$$v = \frac{y}{\sqrt{2\varepsilon N_0}} \qquad (5.96)$$

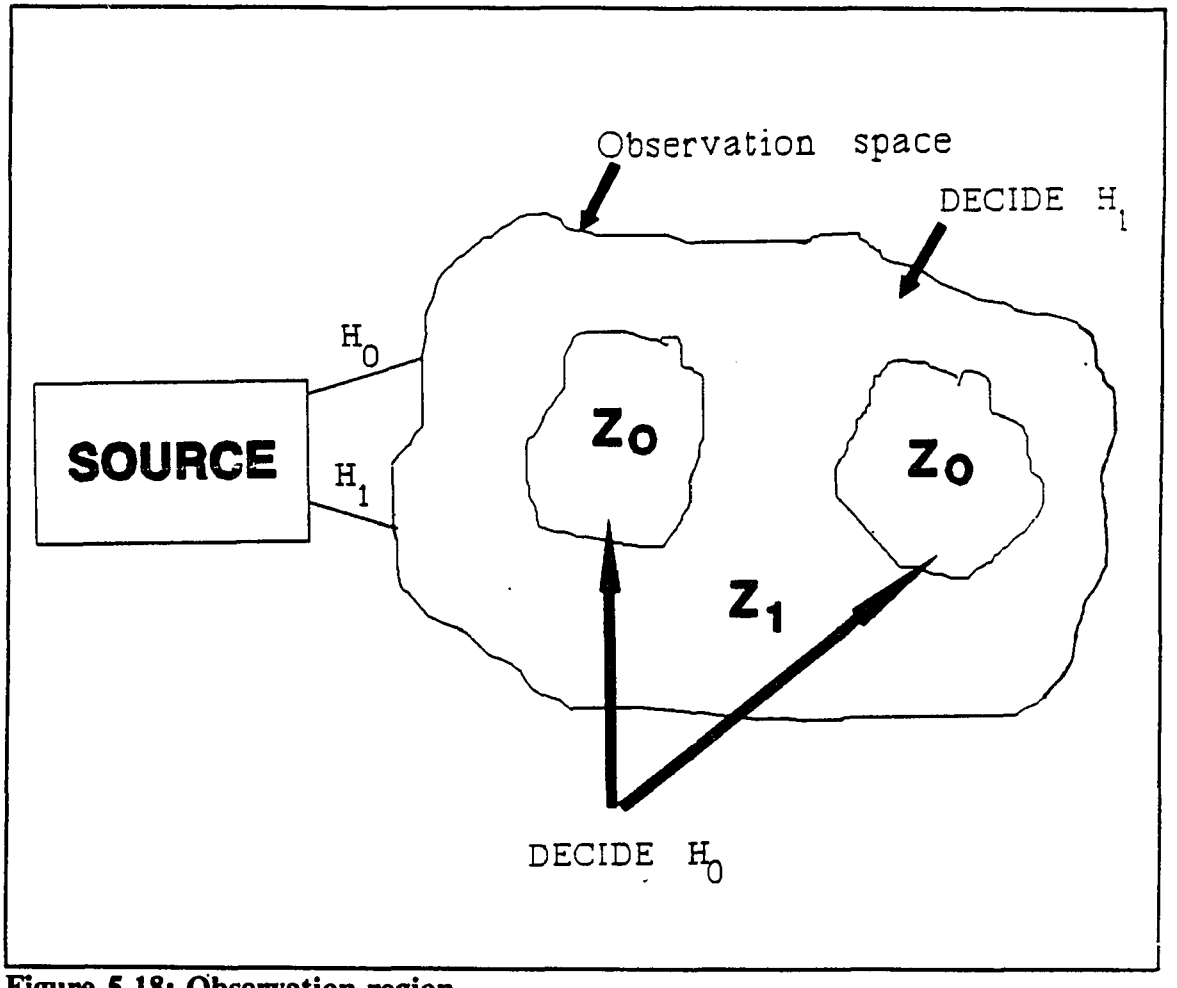

Figure 5.18: Observation region.

Thus, the probability of miss is defined by

$$P_m = 1 - P_D \tag{5.97}$$

From EQ. (5.95) the P_{fa} is given as a function of the noise variance and the threshold *l*. Solving for *l*, we get

$$l = \sqrt{2\sigma_n^2 \log\left[\frac{1}{P_{fa}}\right]} = \sqrt{\frac{N_o T}{2} \log\left[\frac{1}{P_{fa}}\right]} \tag{5.98}$$

Figure 5.19 shows the SNR vs. P_d for various P_{fa}.

5.5 ANTENNAE CONSIDERATION

Antenna is a device that convert electrical power to electromagnetic power, enabling the transmitted signal to traverse the channel. Antennas are a necessary, and often critical, part of any system which employs radio propagation as the means of transmitting information. In some circumstances these purpose may well be served by an antenna of a single element, which may be of various types depending on the specifications. The specification may include some, or all, of the following electrical performance parameters:

Frequency of operation

Radiation pattern

Gain and efficiency

Impedance

Bandwidth

Polarization

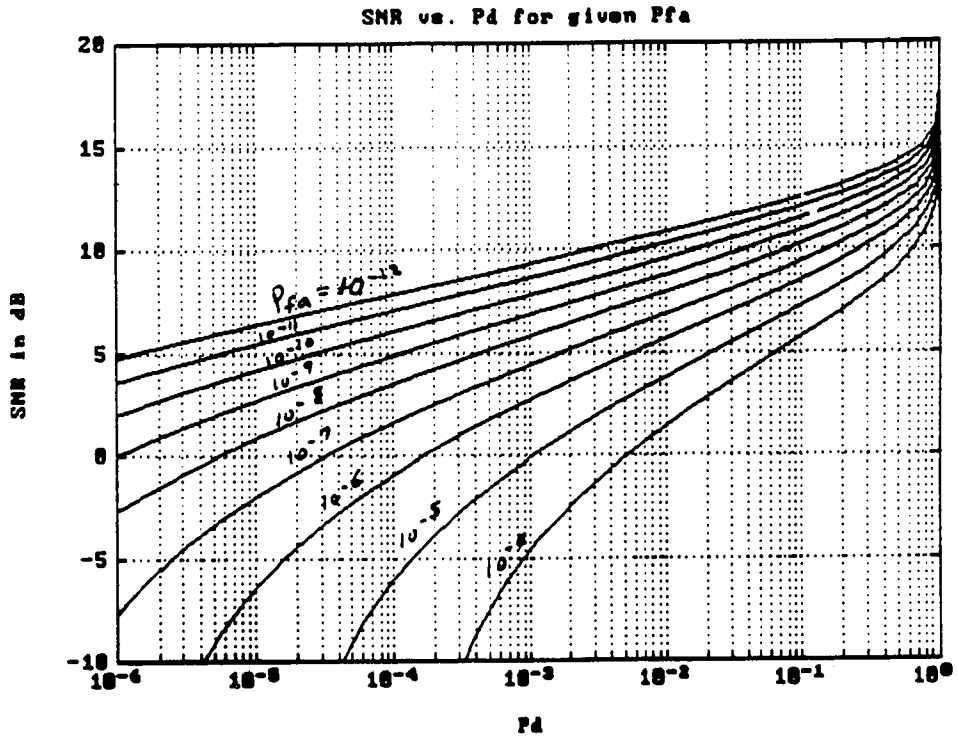

Figure 5.19: SNR vs P_d for various P_{fa}.

In addition there may be the major practical limitation such as dimensional and structural constraints, weight, materials, environmental factors and of course cost.

Antennas can be very broadly classified either by the frequency spectrum or by their basic mode of radiation. For example array antennas, travelling-wave antennas, elemental electric and magnetic currents antennas can be classified by mode of radiation.

For our system, a single isotropic antenna may serve our purposes at particular location of the Space station. However, there might be locations where a more flexible antenna pattern is required, or instance when the overall system gain need to be increased without the need to increase the radiated power.

5.5.1 ANTENNAE GAIN

The power gain is a quantity which define the ability of an antenna to concentrate energy in a particular direction. It is measured at the peak radiation intensity. The power gain of an antenna in a specified direction (θ,ϕ) is

$$G(\theta,\phi) = \frac{4\pi * \text{power radiated per unit solid angle } \epsilon \text{ direction } \theta,\phi}{\text{total power accepted source}} \qquad (5.99)$$

We have a radiator that is radiating energy into space. If the radiator disperse the energy equally in all direction, then the amount of energy collected over an area A is simply the ratio of area A to the area of the entire sphere.

Now let us suppose that at the center of the sphere we have a transmitter that is radiating

a power, P_t, through an antenna that scatters this power isotopically. The amount of power being collected at the receiving end with a device of area A is

$$P_r = \frac{P_t A}{4\pi R^2} \tag{5.100}$$

where R is the radius of the sphere. The power density radiated by an isotropic antenna at distance R per unit area is

$$S = \frac{P_t}{4\pi R^2} \tag{5.101}$$

The gain of a antenna increases the power in the direction of the peak radiation. In general, gain is defined as the gain biased pattern of the antenna. Hence, Power density, $S(\theta,\phi)$, is

$$S(\theta,\phi) = \frac{P_t G(\theta,\phi)}{4\pi R^2} \tag{5.102}$$

The ratio of power gain to directivity is termed the radiation efficiency, η, of the antenna. The surface integral of the radiation intensity over the radiation sphere divided by the input power is the antenna efficiency. Thus,

$$\eta = \int_0^{2\pi}\int_0^{2\pi} \frac{G(\theta,\phi)}{4\pi} \sin\theta \, d\theta \, d\phi \tag{5.103}$$

5.5.2 POLARIZATION

The polarization of an electromagnetic wave, E, at a single frequency describes the shape and arrentation of the locus of the extremities of the field vectors as a function of time. Hence, if the wave is travelling in the z direction, the electric field components in the x and y direction are

$$E_x = E_1 \sin(\omega t - \beta z) \tag{5.104}$$

$$E_y = E_2 \sin(\omega t - \beta z + \delta) \tag{5.105}$$

where E_1 and E_2 are the amplitude of wave linearly polarized in x and y direction respectively and δ is time-phase angle by which E_y lead E_x. Sum of E_x and E_y is the instantaneous total vector field E:

$$E = \alpha_x E_x + \alpha_y E_y \tag{5.106}$$

where α_x and α_y are the unit vector in the direction of x and y. We can also express the spherical wave in the far field in terms of θ and ϕ components of the electric field E.

$$E = E_\theta d\theta + E_\phi d\phi \tag{5.107}$$

Where E_θ and E_ϕ are phaser components in the direction of the unit vectors α_θ and α_ϕ.

Equation (5.106) and (5.107) can be rewritten as

$$E = E_x(\alpha_x + \hat{\rho}_L \alpha_y)$$
$$\hat{\rho}_L = \frac{E_y}{E_x} \tag{5.108}$$

$$E = E_\theta(\alpha_\theta + \hat{\rho}_L \alpha_\phi)$$
$$\hat{\rho}_L = \frac{E_\phi}{E_\theta} \tag{5.109}$$

where ρ_L is the linear polarization, a complex constant. For $E_1 = E_2$ and $\delta = \pm 90°$ or $\rho_L = e^{\pm j\pi/2}$, the wave is circularly polarized. The electric field in the polarization plane can be written as

$$E = \frac{E_L}{\sqrt{2}}(\alpha_\theta + j\alpha_\phi) + \frac{E_R}{\sqrt{2}}(\alpha_\theta - j\alpha_\phi) \tag{5.110}$$

Therefore, the circular polarization can be defined by

$$E = E_L(\alpha_L + \hat{\rho}_c \alpha_R) \tag{5.111}$$

where

$$\hat{\rho}_c = \frac{E_R}{E_L} = \rho_c e^{j\delta_c}$$
$$\alpha_R = \frac{1}{\sqrt{2}}(\alpha_\theta - j\alpha_\phi) \tag{5.112}$$
$$\alpha_L = \frac{1}{\sqrt{2}}(\alpha_\theta + j\alpha_\phi)$$

5.5.3 POLARIZATION RESPONSE

When the antenna polarization dose not match that of the incident radiation, the effective receiving cross section is reduced. In addition polarization mismatch adds an extra loss to the path loss formulas. Under transmitting conditions the radiated field in the z direction is expressed in the form

$$E_a = E_1(\alpha_x + \hat{\rho}_{L1}\alpha_y) \tag{5.113}$$

and the incident wave on the antenna is given by

$$E_i = E_2(\alpha_x + \hat{\rho}_{L2}\alpha_y) \tag{5.114}$$

The response of the antenna to the incident wave can be express as

$$E_a \cdot E_i(1 + \hat{\rho}_{L_1}\hat{\rho}_{L_2}^*) \tag{5.115}$$

If we normalize the incident wave and antenna response, then the loss due to polarization mismatch is found.

$$E_i^* = \frac{\alpha_x + \hat{\rho}_{L_2}^*\alpha_y}{\sqrt{1 + \hat{\rho}_{L_2}\hat{\rho}_{L_2}^*}}$$
$$E_a^* = \frac{\alpha_x + \hat{\rho}_{L_1}^*\alpha_y}{\sqrt{1 + \hat{\rho}_{L_1}\hat{\rho}_{L_1}^*}} \tag{5.116}$$

The normalized voltage response is

$$V = \frac{1 + \hat{\rho}_{L_1}\hat{\rho}_{L_2}^*}{\sqrt{1 + \hat{\rho}_{L_1}\hat{\rho}_{L_1}^*}\sqrt{1 + \hat{\rho}_{L_2}\hat{\rho}_{L_2}^*}} \tag{5.117}$$

When we express it as a power response, we obtain the polarization efficiency Γ:

$$\Gamma = \frac{1 + |\hat{\rho}_{L_2}|^2|\hat{\rho}_{L_1}|^2 + 2|\hat{\rho}_{L_1}||\hat{\rho}_{L_2}|\cos(\delta_1 - \delta_2)}{(1 + |\hat{\rho}_{L_1}|^2)(1 + |\hat{\rho}_{L_2}|^2)} \tag{5.118}$$

Where δ_1 and δ_2 are the phases of the polarization ratio. For Γ=0 the two polarization are orthogonal only if

$$|\hat{\rho}_{L_1}| = \frac{1}{|\hat{\rho}_{L_2}|} \tag{5.119}$$

and

$$\delta_1 - \delta_2 = \pm 180^\circ \tag{5.120}$$

This can be expressed vectorially by the orthonormal generalized vector for polarization. Thus,

$$\alpha_m \cdot \alpha_n = 0 \tag{5.121}$$

We can define in terms of this basis with a polarization ratio ρ. By paralleling the above analysis for linear polarization, we obtain the polarization efficiency for an arbitrary polarization basis.

$$\Gamma = \frac{1 + |\hat{\rho}_2|^2|\hat{\rho}_1|^2 + 2|\hat{\rho}_1||\hat{\rho}_2|\cos(\delta_1 - \delta_2)}{(1 + |\hat{\rho}_1|^2)(1 + |\hat{\rho}_2|^2)} \tag{5.122}$$

For $\delta_1 - \delta_2 = 0$ maximum polarization efficiency Γ_{max} will occur.

$$\Gamma_{max} = \frac{(1 + |\hat{\rho}_1||\hat{\rho}_2|)}{(1 + |\hat{\rho}_1|^2)(1 + |\hat{\rho}_2|^2)} \qquad (5.123)$$

The minimum polarization efficiency Γ_{min} occur when $\delta_1 - \delta_2 = 180°$.

$$\Gamma_{min} = \frac{(1 - |\hat{\rho}_1||\hat{\rho}_2|)}{(1 + |\hat{\rho}_1|^2)(1 + |\hat{\rho}_2|^2)} \qquad (5.124)$$

5.6 ANTENNAE LOCATIONS

Figure 5.20 shows approximate design of the space station. The system under consideration must be able to determine the location of the robot anywhere around the space station, within a few feet, including the hidden spaces. To achieve this goal, the entire space station is broken into five segments. Each segment is required to have at least one transmitting antenna and a minimum of three receiving antennae. However, we have placed six receiving antennae and one transmitting antenna in each region which can provide us with the location of the robots at all times. Therefore, we estimated that a minimum of five transmitting and thirty receiving antennae are required. The number of antennae can be reduced if we need to locate the robots at some distance from the space station. In order to determine the location of the antennae we have followed the following guidelines.

1) At least three receiving antennae must have direct line of sight with the robot.

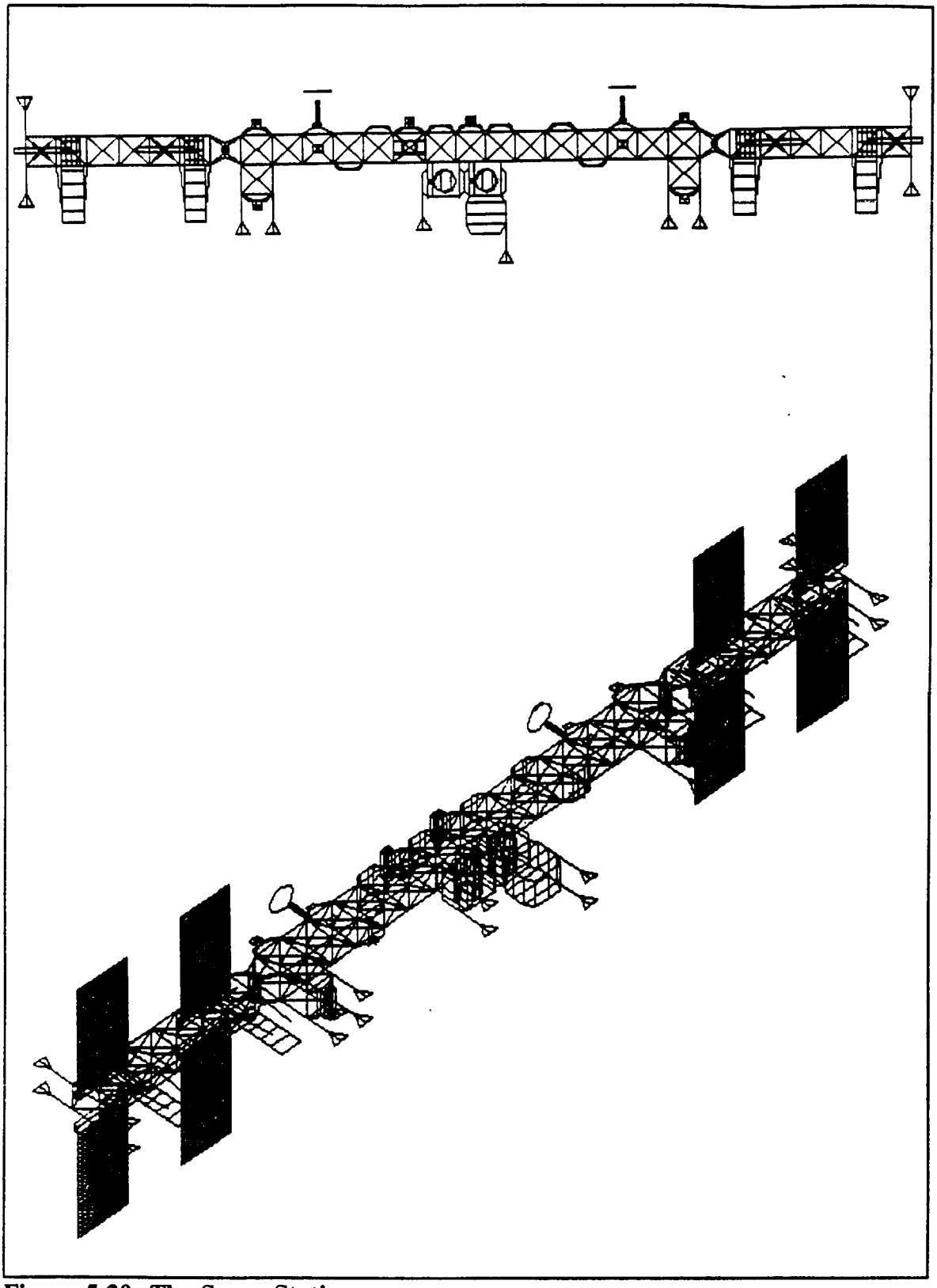

Figure 5.20: The Space Station.

2) Field of view for each antenna must be maximized.

3) Every point around the place station must be inside the common view of at least three antennae.

4) The three receiving antennae working at the same time should not lie on the same line.

5.7 SPACE LINK

Flux density Φ_0 at the robot receiving antenna can be written as

$$\Phi_0 = \frac{P_{TS}}{4\pi R^2} \qquad (5.125)$$

where P_{TS} is power radiated by the transmitting space station antenna and R is the distance of transmission. If the transmitting antenna gain is G_{TS}, the flux density at the robot receiving antenna will be:

$$\Phi_r = \frac{G_{TS}P_{TS}}{4\pi R^2} \qquad (5.126)$$

Hence, total power received by the robot antenna is:

$$P_{RR} = \frac{G_{TS}P_{TS}G_{RR}}{L_U}\left(\frac{\lambda}{4\pi R}\right)^2 \qquad (5.127)$$

where

G_{TS} P_{TS} = Effective isotropic radiated power

G_{RR} = Robot receiving antenna gain

A_R =Effective aperture

L_U = Total power loss in the transmission path

λ = Wavelength of the radiated wave

$(4\pi R/\lambda)^2$ = Free space loss

If the effective noise temperature of the robot receiver is T_{RR}, then the noise power at the robot receiver input will be N_o, and if we replace P_{RR} by C, where C is the carrier

power, uplink carrier-to-noise density ratio can be written as

$$\left[\frac{C}{N_o}\right]_U = \frac{P_{TS}G_{TS}G_{RR}}{T_{RR}L_U\ K}\left[\frac{\lambda}{4\pi R_U}\right]^2 \qquad (5.128)$$

and

$$N_o = KT_{RR} \qquad (5.129)$$

where

$(C/N_o)_U$ = uplink carrier-to-noise density ratio

$P_{TS}G_{TS}$ = Space Station Effective Isotropic Radiated Power (EIRT)

G_{RR}/T_{RR} = Robot receiving sensitivity

$(4\pi R_U/\lambda)^2$ = Free-space loss

L_U = Uplink transmission medium loss

K = Boltzmann's constant.

The downlink carrier-to-noise density ratio can be find by simply replacing the subscript S with R, R with S and U with D in EQ. (5.128). Thus,

$$\left[\frac{C}{N_o}\right]_D = \frac{P_{TR}G_{TR}G_{RS}}{T_{RS}L_D\ K}\left[\frac{\lambda}{4\pi R_D}\right]^2 \qquad (5.130)$$

where

$(C/N_o)_D$ = Downlink carrier-to-noise density ratio

$P_{TR}G_{TR}$ = Space Station Effective Isotropic Radiated Power (EIRT)

G_{RS}/T_{RS} = Robot receiving sensitivity

$(4\pi R_D/\lambda)^2$ = Free-space loss

L_D = Uplink transmission medium loss

K = Boltzmann's constant.

Total carrier power at the Space Station receiver input (C_{RS}), the carrier power at the robot receiver input (C_{RR}), and the carrier power at the robot transmitter output (C_{RT}) can be written respectively as follows:

$$C_{RS} = C_{RT} G_D \tag{5.131}$$

$$C_{RR} = G_U P_{TS} \tag{5.132}$$

$$C_{RT} = C_{RR} G \tag{5.133}$$

where G_U and G_D are

$$G_U = \frac{G_{TS} G_{RR}}{L_U} \left(\frac{\lambda}{4 \pi R_U} \right)^2 \tag{5.134}$$

$$G_D = \frac{G_{TR} G_{RS}}{L_D} \left(\frac{\lambda}{4 \pi R_D} \right)^2 \tag{5.135}$$

and G is the repeater gain.

Consequently, the total link carrier power at the end of the space link (C_T) can be defined as

$$C_T = \frac{N_T C_{RT} G_D}{N_{RS} BW + K T_S BW} \tag{5.136}$$

where N_T, N_{RT}, and N_{RS} are the total space-link noise, noise at the robot transmitter output, noise power at the Space Station receiver input due to robot-generated noise

respectively. Thus,

$$N_T = N_{RS}BW + KT_SBW \tag{5.137}$$

$$N_{RT} = GKT_R \tag{5.138}$$

$$N_{RS} = G_D N_{RT} \tag{5.139}$$

where KT_R is the total noise power at the robot receiver input per unit bandwidth and KT_S is the additional noise power generated at the Space Station input.

Therefore, the uplink carrier-to-noise ratio, downlink carrier-to-noise ratio, and total carrier-to-noise ratio can be written respectively as follows:

$$\left(\frac{C}{N}\right)_U = \frac{C_{RR}}{KT_RBW} \tag{5.140}$$

$$\left(\frac{C}{N}\right)_D = \frac{C_{RS}}{KT_SBW} \tag{5.141}$$

$$\left(\frac{C}{N}\right)_T = \frac{C_{RT}G_D}{N_{RS}BW + KT_SBW} \tag{5.142}$$

5.8 SYSTEM PERFORMANCE

In this section we will analyze the system's performance. The performance of the system can be evaluated by determining:

1. Probability of detection P_D
2. Probability of false alarm P_{fa}

Detection is associated with the case where one of the FFT output crosses the set threshold. However, if the detection is solely due to presence of noise, then it is called a false alarm. We begin by making the following assumptions about the measurements.

1. The receiver should find which direct path signal occupies which frequency bin.

2. Since signals which undergo smaller propagation delay give rise to lower frequency components, the receiver has to identify the components(due to the direct path signal and it's multipath and select the one with the lower frequency.

3. The frequencies obtained by the direct path and the multipath signals are orthogonal to each other.

4. If a measurement is below the threshold, it will be assumed to as due to noise.

5. If a measurement is above the threshold, it will be assumed to as due to signal.

The signal is said to be present, detected, if one of the FFT output crosses the threshold. Obviously by varying the threshold setting, both P_D and P_{fa} can be effected. If the threshold setting is lowered more of the signals is going to be detected. But, at the same time a larger percentage of these signals could be false, since more of the FFT's outputs exceeding the threshold is solely due to noise.

In general, it is desirable to keep P_{fa} low, since it avoids the space station to waste time taking actions. Thus, degrading the performance as far as P_D is concerned. Fortunately, once the noise background is known as in the case here, the system can perform optimally. The receiver can estimate the received signal energy and use that to set threshold for detection purposes. Thus, by setting the P_{fa} and knowing the noise power, the threshold can be computed as follows:

P_{fa} = Pr [at least one noise term above threshold]

= 1 - Pr [all noise terms below threshold]

Denoting l the threshold level, and assuming that M and N antennas receive the direct and multipath signal components, then there are N-M statistically independent noise term, taking on a Rayleigh distribution.

Thus,

$$
\begin{aligned}
P_{fa} &= 1 - Pr[n_1 < l,\ n_2 < l,\ \ldots,\ n_{N-M} < l\ ] \\
&= 1 - (Pr\,[n_1 < l\ ])^{N-M} \\
&= 1 - \left[1 - \int_0^{l} \frac{n_1}{2\varepsilon N_o} e^{-\left(\frac{n_1^2}{4\varepsilon N_o}\right)}\, dn_1\right]^{N-M} \\
&= 1 - \left[1 - e^{-\left(\frac{l^2}{4\varepsilon N_o}\right)}\right]^{N-M}
\end{aligned}
\qquad (5.143)
$$

Once the noise power has been computed the value of l can easily be determined for a given P_{fa}. The value of noise power is simply $(N_oBW)/N$, where BW is the bandwidth at the input of the FFT, N_o is the power spectral density of the noise and N is the number of antenna. Assuming that the system oscillators are perfectly accurate, the probability that the direct path signal will cross the threshold will be

$$
P_D = \int_l^{\infty} \frac{y}{2\varepsilon N_o} e^{\left(-\frac{y^2 + 4\varepsilon^2}{4\varepsilon N_o}\right)} I_o\left(\frac{y}{N_o}\right) dy \qquad (5.144)
$$

Figure 5.21 and 5.22 shows the P_m vs. SNR for various P_{fa} respectively. In addition, probability of false alarm vs. the threshold having SNR as the parameter, as well as the probability of false alarm vs. SNR with threshold as the parameter for various values of N-M, are shown in appendix A.

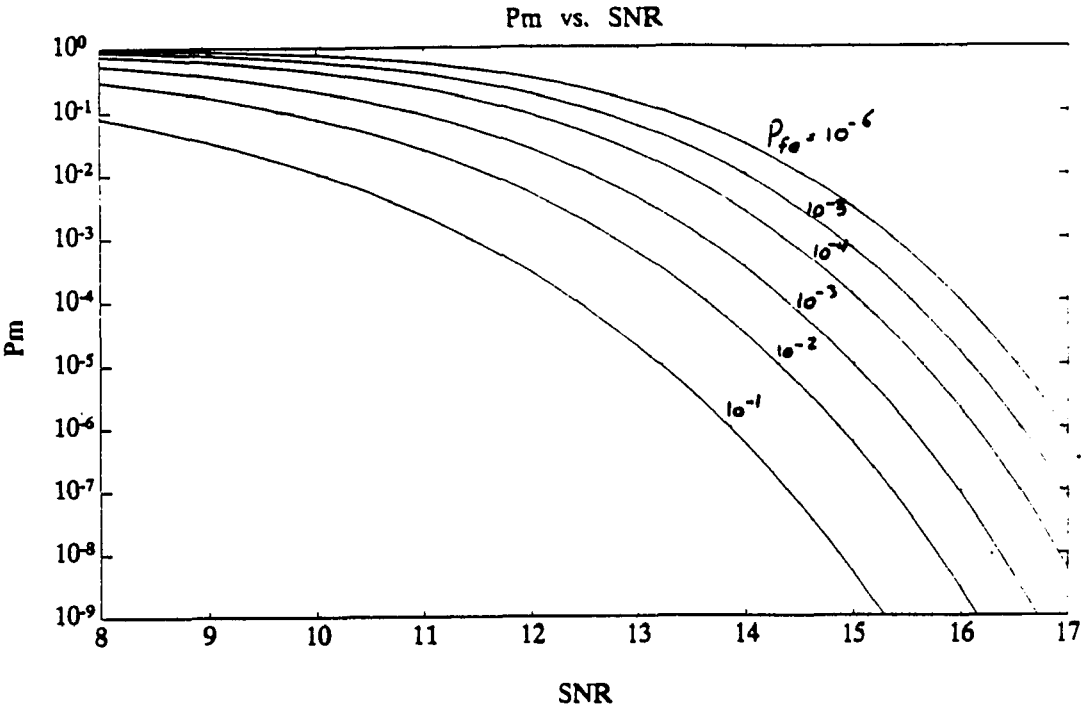

Figure 5.21: P_m vs SNR for different P_{fa}.

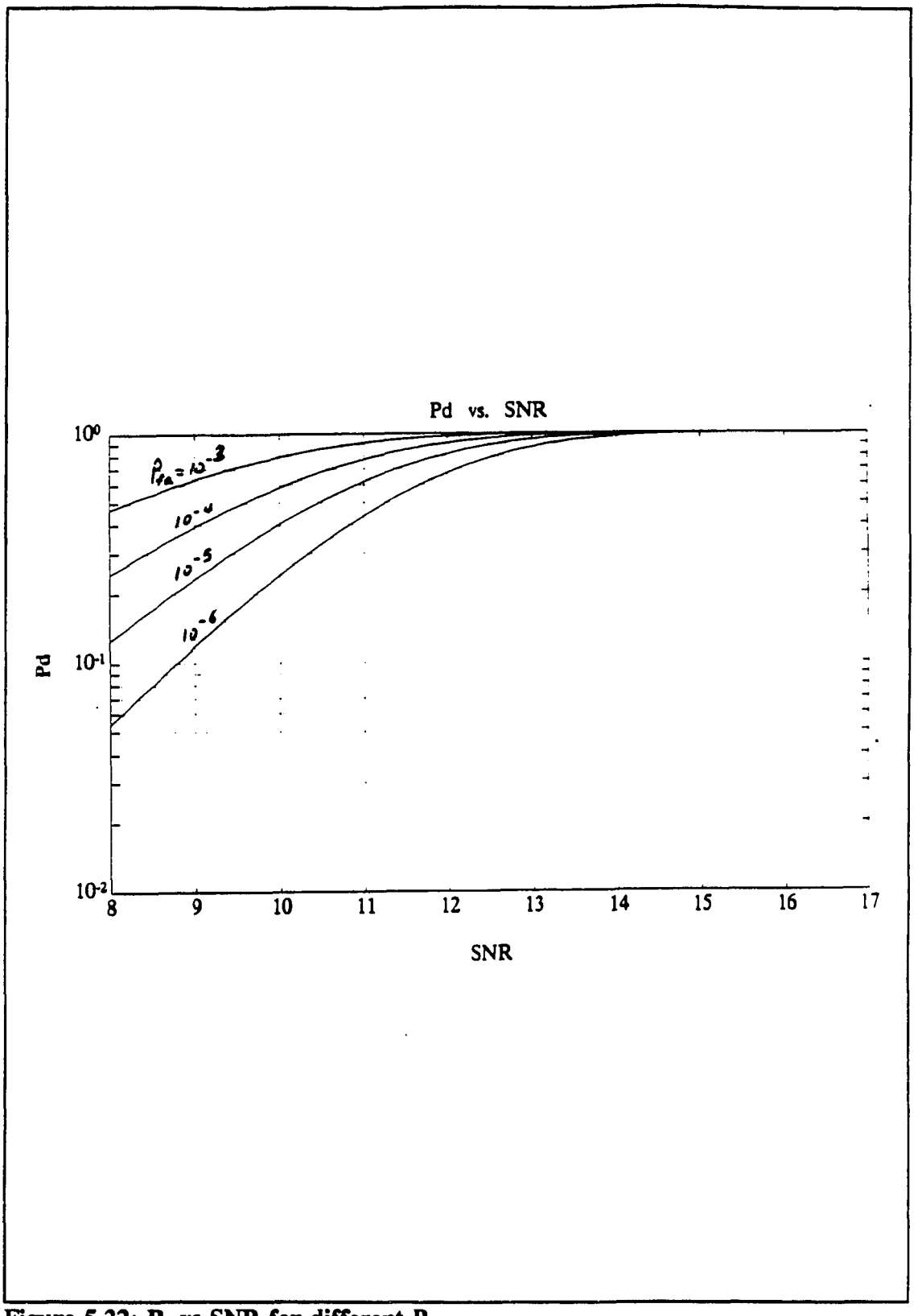

Figure 5.22: P_d vs SNR for different P_{fa}.

5.9 ROBOT LOCATION

The distance between the robot and at least three receiving antennae is measured by determining the signal travel time from the transmitting antenna to the robot and back to the receiving antennae located on the Space Station. Since the distance from antennae to the robot is constant, say r_i , the robot is bound to be located on the surface of a sphere centered on antenna i and having a radius r_i . Knowing the distance r_0 from the robot to receiving antenna A_0, r_1 from the robot to receiving antenna A_1, and r_2 from the robot to receiving antenna A_2, then the location of robot can be found by determining the common intersection of the three spheres. Thus,

$$x_{A_0}^2 + y_{A_0}^2 + z_{A_0}^2 = r_0^2 \tag{5.145}$$

$$(x_{A_0} - x_1)^2 + y_{A_0}^2 + z_{A_0}^2 = r_1^2 \tag{5.146}$$

$$(x_{A_0} - x_2)^2 + (y_{A_0} - y_2)^2 + z_{A_0}^2 = r_2^2 \tag{5.147}$$

where (x_{A0}, y_{A0}, z_{A0}), $((x_{A0}-x_1), y_{A0}, z_{A0})$, and $((x_{A0}-x_2), (y_{A0}-y_2), z_{A0})$ are the location of three receiving antennae respectively. The point (x_R, y_R, z_R) which satisfies all three equation above will be the location of the robot. Thus,

$$x_R = \frac{1}{2x_1}(x_1^2 + r_0^2 - r_1^2) \tag{5.148}$$

$$y_r = \frac{1}{2y_2}(x_2^2 + y_2^2 + r_0^2 - r_2^2 - 2x_2x_R) \tag{5.149}$$

$$z_R = \sqrt{r_0^2 - x_R^2 - y_R^2} \tag{5.150}$$

CHAPTER SIX

SUMMARY & CONCLUSION

6.0 SUMMARY AND CONCLUSION

In this thesis, we have designed and analyzed a new signal processing technique to implement a Space Station robotic tracking system. The system overcomes the existing technical limitations by utilization of a wideband chirp signal in combination with a polling procedure that identifies the presence of a particular robot. The wideband chirp signal is well suited for this system since it easily provides the large time-bandwidth product needed, this signal allows the system to discriminate between multipath signals components and precisely find the location of each robot. In addition, the location of an individual robot can be achieved to within a few meters in a fraction of a second (approximately 400 μsec.). Therefore, the system will be capable of searching the

whole, or part of, the space outside the Space Station in order to continuously locate and track a large number of robots in a fraction of a second.

The overall performance of the system depends on the performance of the tone detector; total power measurement circuit, which provides the system with an estimate of the received noise power at the input of each receiving antennae; as well as the number of antennae.

The P_d of the tone detector, as shown in Figure 5.19, approaches unity as the SNR or the P_{fa} increases. For instance, for $P_{fa}=10^{-6}$, the SNR must be kept above 14 dB for a good performance of the tone detector.

The overall system performance was considered when the power of noise floors are known. This enables one to control the system's overall P_{fa}. As shown in Figure 5.21 for a constant P_{fa} as SNR is increased the P_m is decreased. For example to attain a $P_m < 10^{-3}$ SNR must be kept greater than 14 dB and $P_{fa}=10^{-3}$. In addition, further example of system performance can be observed in appendix A.

To determine the location of the robot anywhere around the space station, within a few feet including the hidden spaces, the entire space station is broken into five segments. Each segment is required to have at least one transmitting antenna and a minimum of three receiving antennae. However, we have placed six receiving antennae and one transmitting antenna in each region which can provide us with the location of the robots at all times. Therefore, we estimated that a minimum of five transmitting and thirty receiving antennae are required. The number of antennae can be reduced if we need to locate the robots at some distance from the space station. Figure 5.20 shows the approximate design of the space station and the location of the antennae.

APPENDIX A

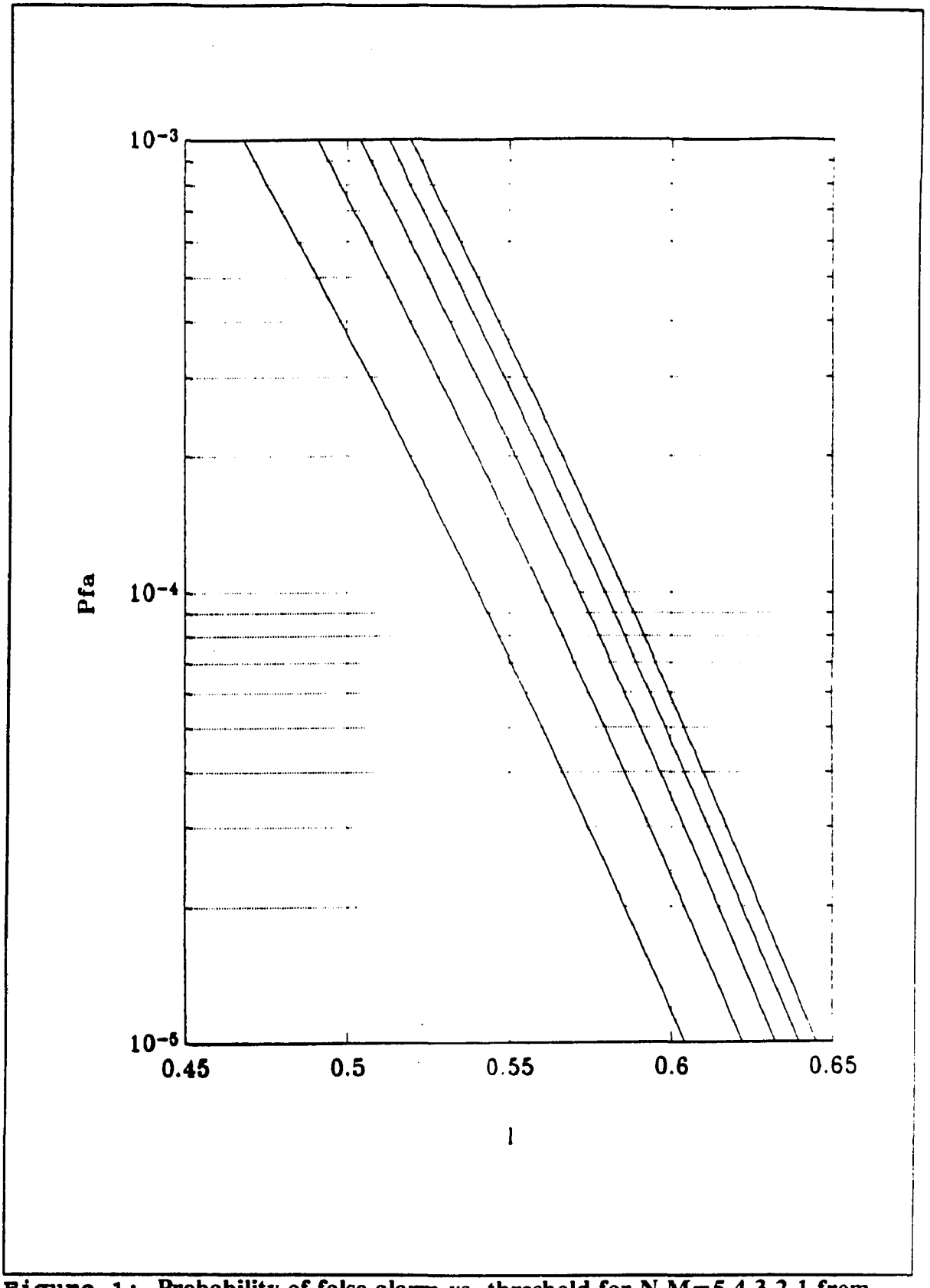

Figure 1: Probability of false alarm vs. threshold for N-M=5,4,3,2,1 from top to bottom and SNR=18.

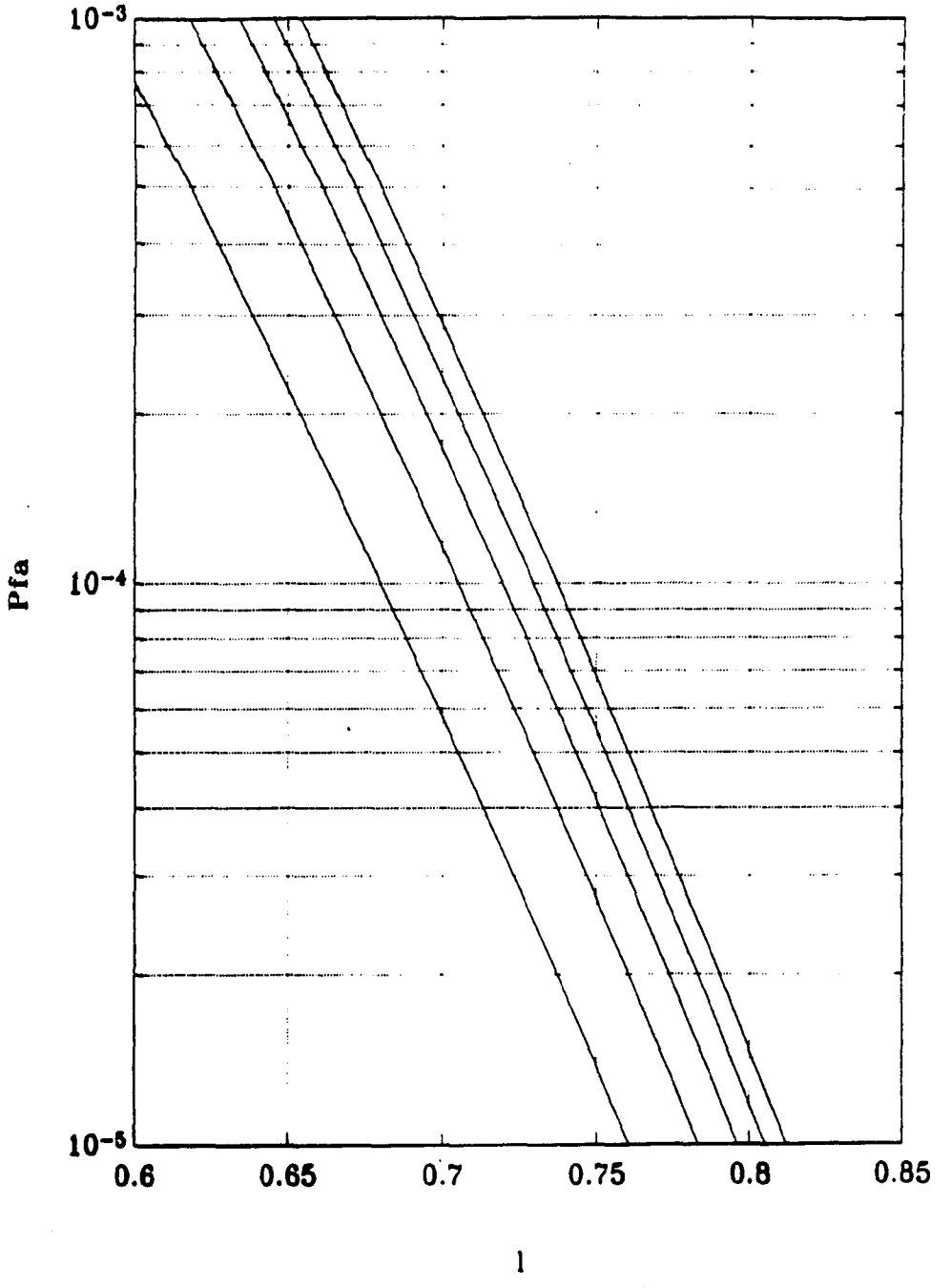

Figure 2: Probability of false alarm vs. threshold for N-M=5,4,3,2,1 from top to bottom and SNR=16.

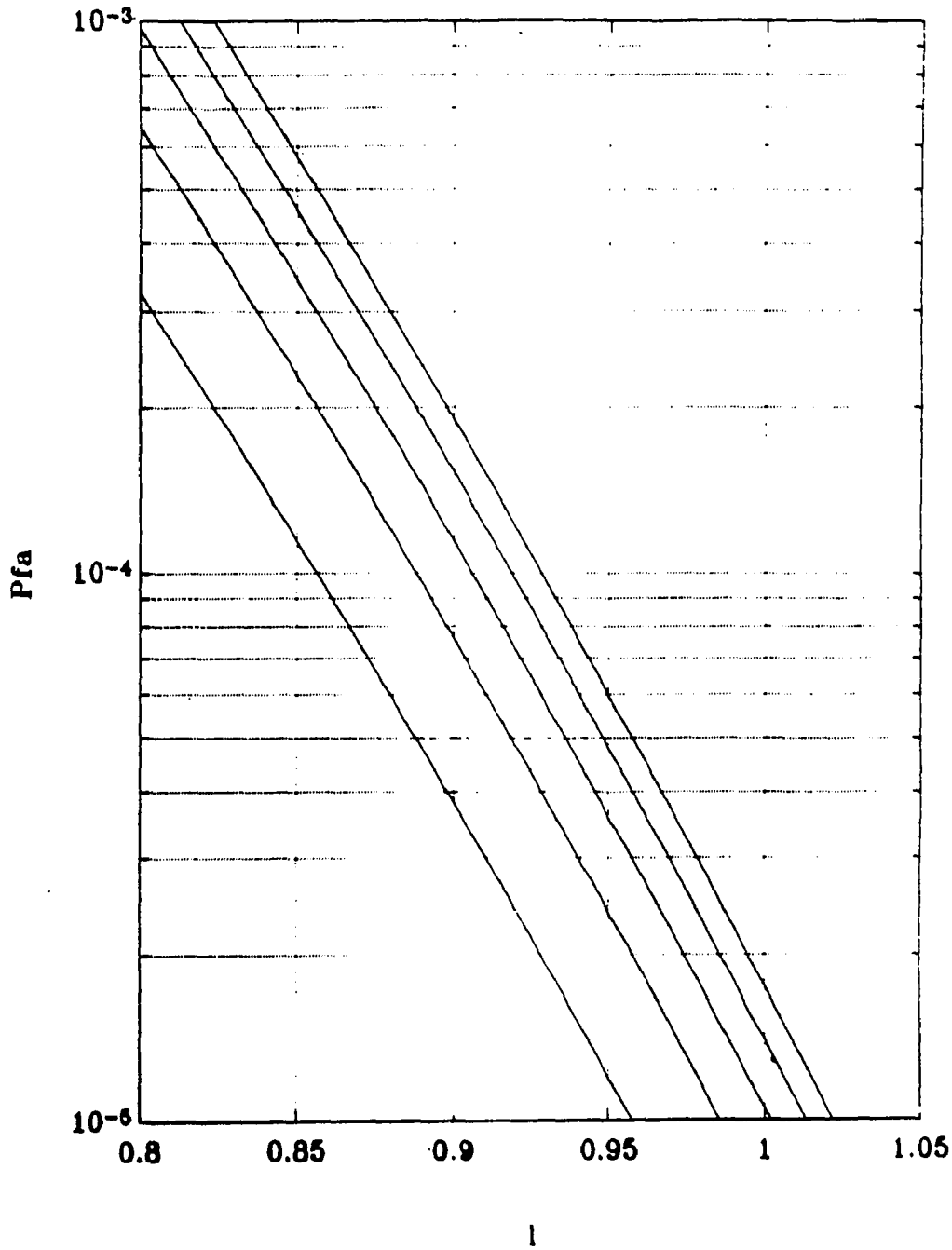

Figure 3: Probability of false alarm vs. threshold for N-M=5,4,3,2,1 from top to bottom and SNR=14.

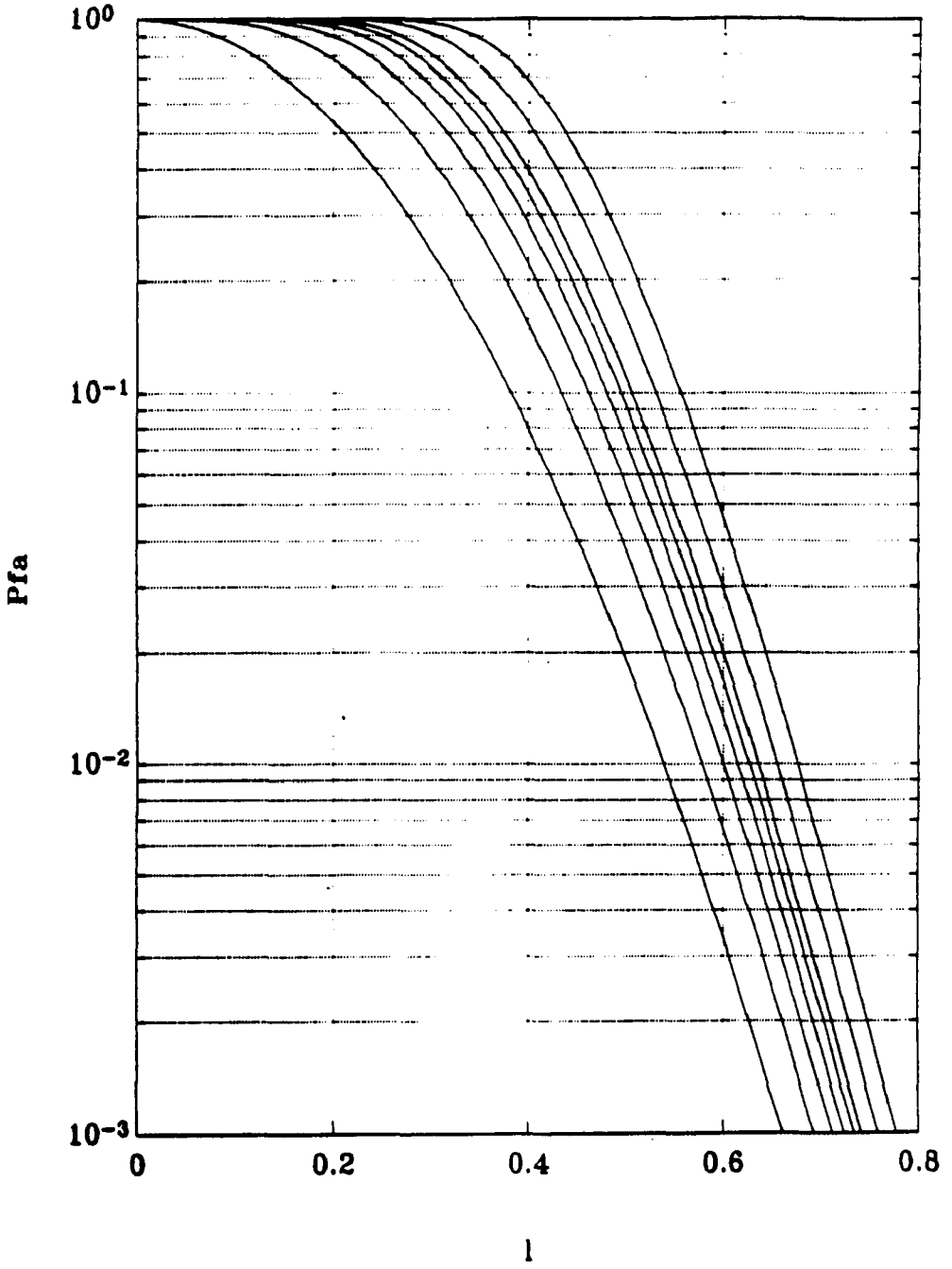

Figure 4: Probability of false alarm vs. threshold for N-M=14,9,6,5,4,3,2,1 from top to bottom and SNR=15.

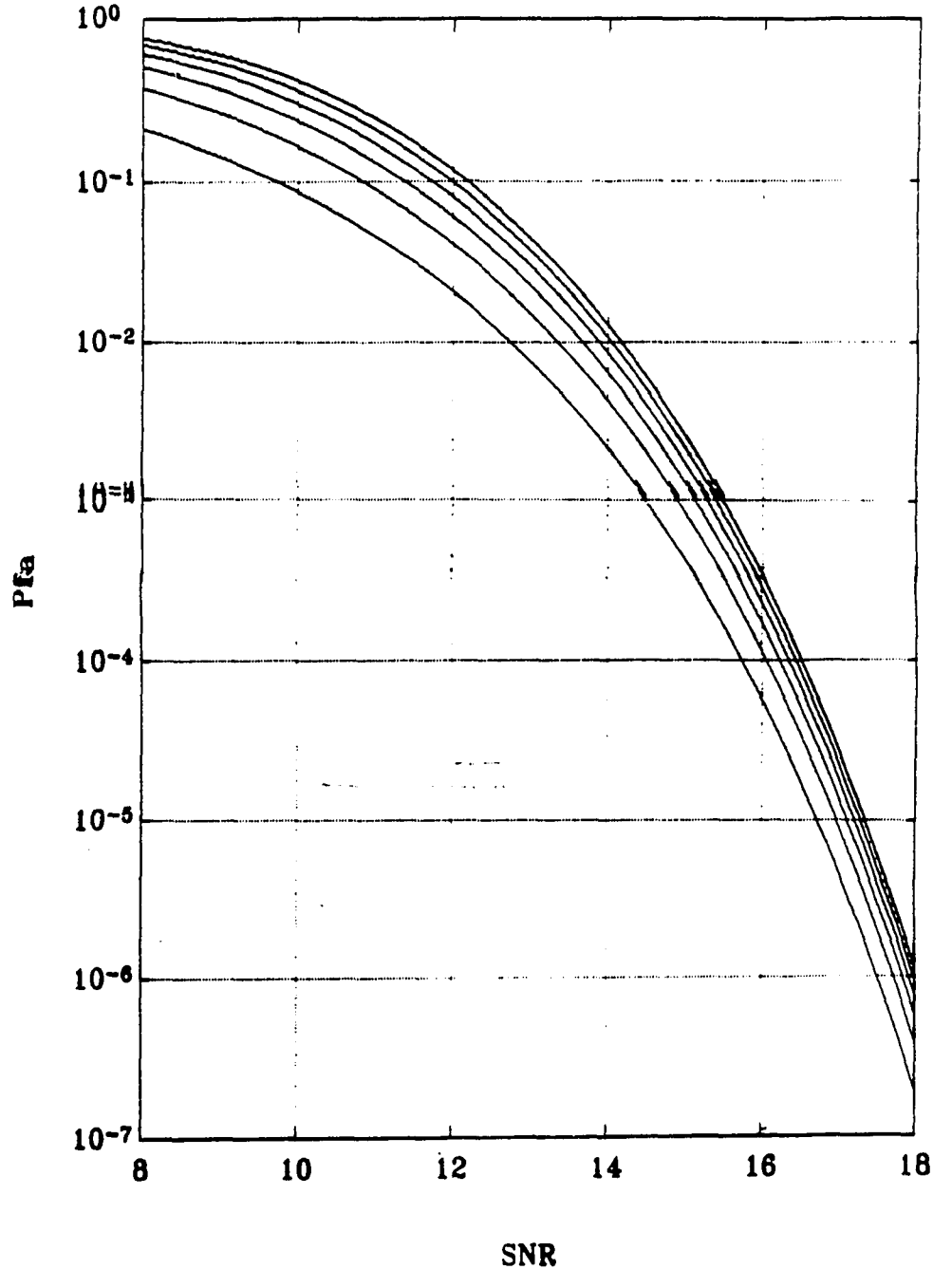

Figure 5: Probability of false alarm vs. SNR for N-M=6,5,4,3,2,1 and l=0.7 from top to bottom .

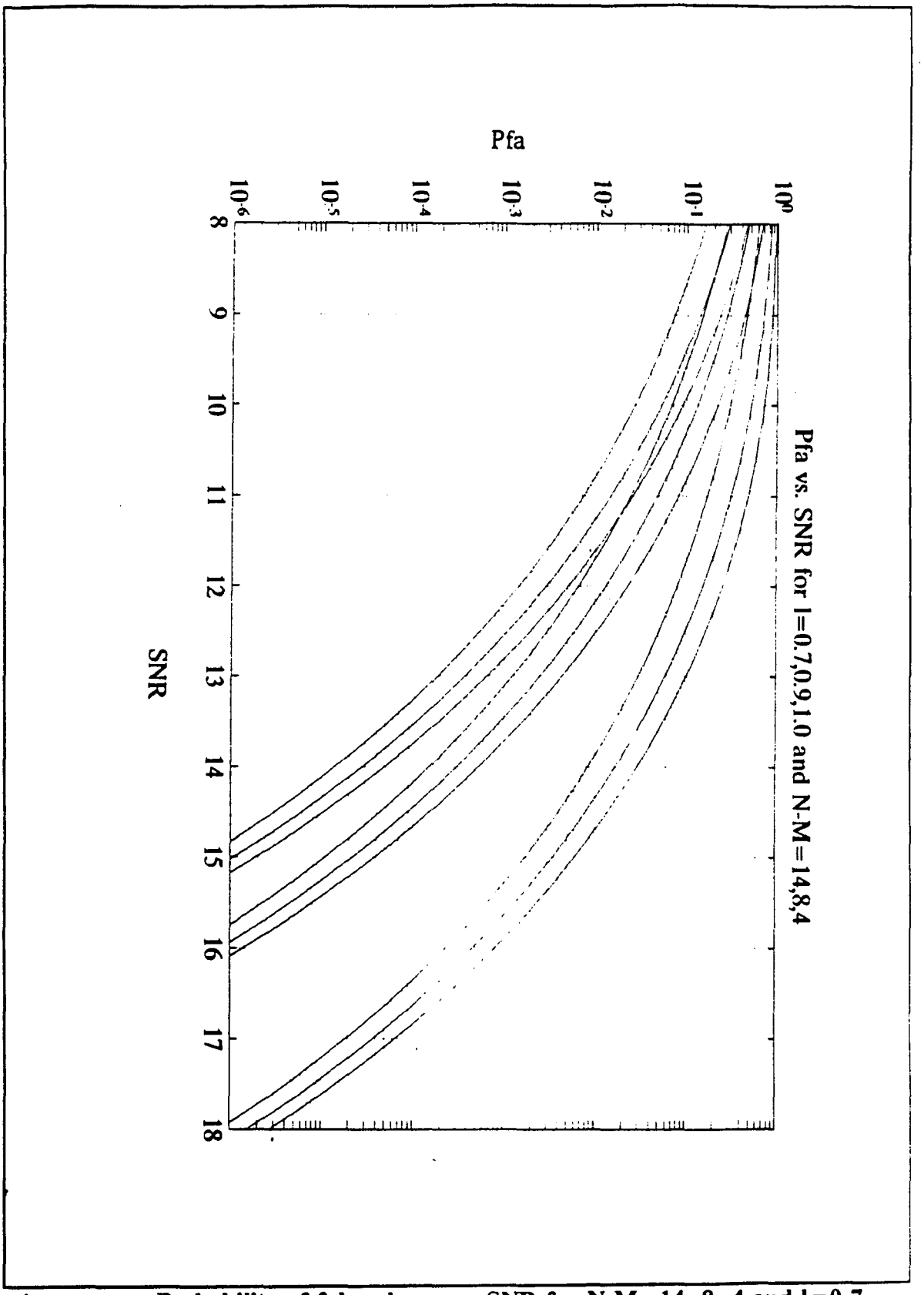

Figure 6: Probability of false alarm vs. SNR for N-M=14, 8, 4 and l=0.7, 0.9, 1 from top to bottom .

REFERENCES

[1] Barkat, M., *Signal Detection and Estimation*, Artech House, Norwood, MA, 1991.

[2] Cook, C. E., " Pulse Compression - Key to More Efficient Radar Transmission," Proceedings of the IRE, pp. 310-316, March 1960.

[3] Davenport, Jr. , W. B., and W. L. Root, *An Introduction to the Theory of Random Signals and Noise,* McGraw-Hill, New York, 1958.

[4] Dillard, R. A., "Detectability of Spread- Spectrum Signals," IEEE Trans. Aerosp. Electron. Syst., Vol. 15, p. 526, July 1979.

[5] Djuric, P., and S. Kay, "Parameter Estimation of Chirp Signals," IEEE Trans. Acoust., Speech, Signal Processing, Vol. 38, pp. 2118-2126, Dec. 1990.

[6] Dudewicz, E. J., *Introduction to Statistics and Probability*, Holt, Rinehart and Winston, New York, 1976.

[7] Edell, J. D., "Wideband, Non-Coherent, Frequency- Hopped Waveforms and Their Hybrids in Low-Probability-of-Intercept Communication," NRL Report, Washington, D.C., November 8, 1976.

[8] Frank, L. E., *Signal Theory,* Prentice-Hall, Englewood Cliffs, NJ, 1969.

[9] Fthenakis, E., *Manual of Satellite Communications,* McGraw-Hill, New York, 1984.

[10] Haykin, S., *Communication Systems,* John Wiley and Sons, New York, 1983.

[11] Haykin, S., *Digital Communication ,* John Wiley and Sons, New York, 1988.

[10] Kay, S. M., *Modern Spectral Estimation Theory and Application,* Prentice-Hall, Englewood Cliffs, NJ, 1988.

[12] Kay, S. M., "The Effects of Noise on the Autoregressive Spectral Estimator," IEEE Trans. Acoust. Speech Signal Process., Vol. ASSP27, pp. 478-485, Oct. 1979.

[13] Lee, Y. W., *Statistical Theory of Communication,* John Wiley and Sons, New York, 1960.

[14] Lezniak, R. , W. Lewis, and R. A. McMillen, "A Dead Reckoning Map/Correlation system for Automatic Vehicle Tracking," IEEE Trans. Vec. Technol., Vol. 22, pp. 47-60, Aug. 1973.

[15] Melsa, J. L., and D. L. Cohn. *Decision and Estimation Theory,* McGraw-Hill, New York, 1978.

[16] Milligan, T. A., *Modern Antenna Design,* McGraw-Hill, New York, 1985.

[17] Mohanty, N., *Signal Processing: Signals, Filtering, and Detection,* Van Nostrand Reinhold, New York, 1987.

[18] Nahi, N. E., *Estimation Theory and Application,* John Wiley and Sons, New York, 1969.

[19] Oppenheim, A. V. and R. W. Schafer, *Digital Signal Processing,* Prentice-Hall, Englewood Cliffs, NJ, 1975.

[20] Papoulis, A., *Probability, Random Variables, and Stochastic Processes,* McGraw-Hill, New York, 1985.

[21] Papoulis, A., *Signal Analysis,* McGraw-Hill, New York, 1977.

[22] Proakis, J. G., *Digital Communication,* McGraw-Hill, New York, 1983.

[23] Rino, C. L., "Factorization of Spectra by Discrete Fourier Transforms," IEEE Inf. Theory, Vol. IT16, pp. 484-485, July 1970.

[24] Riter, S., and J. McCoy, "Automatic Vehicle Location - An Overview," IEEE Trans. Vec. Technol., Vol. 26, pp. 7-11, February 1977.

[25] Riter, S., "The Effect of Background Noise on Phase Ranging Measurements in Urban Vehicle monitoring systems," IEEE Trans. Vec. Technol., Vol. 22, pp. 81-85, Aug. 1973.

[26] Robert, J. B. G., G. L. Moule, and G. Parry, "Design and Application of Real-Time Spectrum Analyzer System," IEEE Proc. 127, Pt. F., April 1980.

[27] Sage, A. P., and J. L. Melsa, *Estimation Theory with Applications to Communication and Control,* McGraw-Hill, New York, 1971.

[29] Schell, S. V. , "High Resolution Direction Finding," IEEE Proc. in press.

[30] Agee, B. G. , S. V. Schell, and W. A. Gardner, "Spectral Self-Coherenc Restoral: A New Approach to Blind Adaptive Signal Extraction Using Antenna Arrays," IEEE Proc. Vol. 78, No. 4, April 1990.

[31] Schmidt, R. U. , "A Signal Subspace Approach to Multiple Emitter Location," Ph.D. Thesis, Stanford, 1982.

[32] Shanmugan, K. S., and A. M. Breipohl, *Random Signals: Detection, Estimation and Data Analysis,* John Wiley and Sons, New York, 1979.

[33] Skolnik, M. I., *Introduction to Radar System,* Second Edition, McGraw-Hill, New York, 1980.

[34] Sorenson, H. W., *Parameter Estimation: Principles and Problems,* Marcel Dekker, New York, 1980.

[35] Srinath, M. D., and P. K. Rajasekaran, *An Introduction to Statistical Signal Processing with Application,* John Wiley and Sons, New York, 1979.

[36] Stark, H., and J. W. Woods, *Probability, Random Processes, and Estimation Theory for Engineers,* Printice-Hall, Englewood Cliffs, NJ, 1986.

[37] Torrieri, D. J., "Adaptive Thresholding System," IEEE Trans. Aerosp. Syst., Vol. 13, p 273, May 1977.

[38] Urkowitz, H., *Signal Theory and Random Processes,* Arech House, Norwood, MA, 1983.

[39] Urkowitz, H., "Energy Detection of Unknown Deterministic Signals," Proc. IEEE Vol. 55, p. 523, April 1967.

[40] Van Trees, H. L., *Detection, Estimation, and Modulation Theory,* Part I, John Wiley and Sons, New York, 1968.

[41] Van Trees, H. L., *Detection, Estimation, and Modulation Theory,* Part III, John Wiley and Sons, New York, 1971.

[42] Whalen, A. D., *Detection of Signals in Noise,* Academic Press, New York, 1971.

[43] Wozencraft, J. M., and I. M. Jacobs, *Principles of Communication Engineering,* John Wiley and Sons, New York, 1965.